THE USE OF STROMAL CELL DERIVED GROWTH FACTOR 1 – ELASTIN LIKE PEPTIDE FUSION PROTEIN NANOPARTICLES TO IMPROVE CHRONIC SKIN WOUNDS

By

AGNES YEBOAH

A dissertation submitted to the

Graduate School – New Brunswick

In partial fulfillment of the requirements

For the degree of

Doctor of Philosophy

Graduate Program in Chemical and Biochemical Engineering

Written under the direction of

François Berthiaume, PhD and Martin L. Yarmush, MD, PhD

And approved by

_____

_____

_____

_____

_____

New Brunswick, New Jersey

May 2016

ABSTRACT OF THE DISSERTATION

The Use of Stromal Cell Derived Growth Factor 1 – Elastin Like Peptide Fusion Protein Nanoparticles to Improve Chronic Skin Wounds

By AGNES YEBOAH

Dissertation Directors:

François Berthiaume, PhD

Martin L. Yarmush, MD, PhD

Chronic skin wounds are characterized by poor re-epithelialization, angiogenesis and granulation. Previous work demonstrated that topical stromal cell-derived growth factor-1 (SDF1) promotes neovascularization, resulting in faster re-epithelialization of skin wounds in diabetic mice. However, the clinical usefulness of such bioactive peptides is limited because they are rapidly degraded in the wound environment due to high levels of proteases. The goal of this project was to develop a novel fusion protein comprising of SDF1 and an elastin like peptide (ELP), which could be used as a therapeutic alternative to recombinant SDF1, for the treatment of chronic skin wounds. ELPs are derivatives of tropoelastin with repeats of VPGXG, where X can be any natural amino acid except Proline. The dissertation aimed to characterize the physical properties of the SDF1-ELP fusion protein, demonstrate its in vitro and in vivo bioactivity and understand its mechanism of action. We showed that SDF1-ELP conferred the ability to self-assemble

into nanoparticles. The fusion protein showed binding characteristics similar to that reported for free SDF1 to the CXCR4 receptor. The biological activity of SDF1-ELP, as measured by intracellular calcium release in HL60 cells was dose dependent, and very similar to that of free SDF1. SDF1-ELP monomers promoted the migration of cells similar to SDF1, and the fusion protein promoted tube formation and capillary-like networks similar to SDF1. In contrast, SDF1-ELP was found to be more stable in elastase and in wound fluid than SDF1. Likewise, the biological activity of SDF1-ELP in vivo was significantly superior to that of free SDF1. When applied to full thickness skin wounds in diabetic mice, wounds treated with SDF1-ELP nanoparticles were 95% closed by day 21, and fully closed by day 28, while wounds treated with free SDF1 and other controls took 42 days to fully close. In addition, the SDF1-ELP nanoparticles increased the amount of vascular endothelial cells, and the epidermal and dermal layer of the healed wound, as compared to the other groups. SDF1-ELP is a promising agent for the treatment of chronic skin wounds.

DEDICATION

To my dear Camille. Thank you for asking about my experiments every day.

ACKNOWLEDGEMENTS

I will like to take this opportunity to thank several people who have contributed to making the completion of my doctorate degree a possibility. My sincere thanks go to my advisors, Dr. Martin Yarmush and Dr. Francois Berthiaume. Dr. Yarmush, thank you for the opportunity to work in your lab, for believing in me all these years, and for your relentless support. Thank you also for the opportunity to be part of the Biotechnology Training Program. Dr. Berthiaume, thank you for helping me to design my experiments and interpret my data appropriately. Thank you for reading and providing comments on all my manuscripts. I also want to thank my committee members, Dr. Stavroula Sofou and Dr. Charles Roth for providing expertise and guidance throughout this project. Though not officially on my committee, Dr. Rene Schloss has been an invaluable advisor to me throughout my time in the doctoral program. Thank you, Dr. Schloss, for providing feedback on my work during lab meetings, and for being a mentor to me throughout my time here.

Outside my committee several people have also contributed to this work. Thank you Dr. Rick Cohen for your significant help with the cloning of SDF1-ELP, for sharing your expertise in protein expression, purification and characterization, for being generous with your lab supplies, your undergraduate students, and for the very useful discussions on my project. Thank you Dr. Xiao-Ping Li for helping me with my Biacore experiments, Dr. Jafar Al-Sharab for helping with the TEM measurements and Dr. Laura Fabris for allowing your graduate students to help me with the Zetasizer and Zeta potential experiments. Thanks to the Center for Advanced Biotechnology and Medicine, Dr. Vikas Nanda and his lab for allowing me to use their Circular Dichroism equipment.

My sincere thanks go to Luke Fritzky from the Digital Imaging and Histology Core at Rutgers-NJMS Cancer Center for his expertise and help in histological sectioning and staining.

Outside my research support network, several people have helped make my stay at Rutgers an enjoyable one. I will like to thank all past and present members of the Yarmush and Berthiaume labs for being great lab mates. I especially want to thank Dr. Renea Faulknor for being a great friend and for showing me the ropes when I joined the lab. I thank the administration of the Chemical Engineering and Biomedical Engineering departments, as well as members of the external grant office for helping me with the administrative aspects of my fellowship.

My sincere thanks go to all my family and friends who have been amazingly supportive of me. Cliff, thank you for encouraging me through the very difficult decision of taking time off from work to finish my doctoral studies full time. Thank you for encouraging me to persevere during difficult times when experiments did not work and for celebrating with me when my manuscripts were submitted and accepted. My dear Cami, you have been a trooper these past years. I am so proud of you. Thank you for all your inquisitive questions about my proteins and for asking about my mice every day! To my parents, who have been my backbone all these years, I couldn't have done this without you. Ma, thank you for your support, for your encouragement and for all your prayers. To Da, who is no longer here with us, I know you are smiling down from heaven at me. I have to also thank all my other family members, my siblings, aunts, uncles, cousins, nephews and nieces. Thank you for your support and encouragement. Lastly, my sincere appreciation goes to all my friends. Thanks for cheering me on!

TABLE OF CONTENTS

LIST OF TABLES

LIST OF ILLUSTRATIONS

1. CHAPTER 1: INTRODUCTION – Therapeutic Delivery of Stromal Cell-Derived Factor-1 for Injury Repair

Note: This chapter is reproduced from the following publication, **written by Agnes Yeboah**:

Agnes Yeboah, Martin L. Yarmush, Francois Berthiaume. Therapeutic Delivery of Stromal Cell-Derived Factor-1 for Injury Repair. Nano LIFE (Accepted, 2015)

1.1 INTRODUCTION

Stromal cell-derived growth factor 1 (SDF1) is a chemokine encoded by the CXCL12 gene, and which is so far known to exist in six different isoforms, SDF1α to ϕ, by alternate splicing of the same gene [1]. SDF1α, shown in Figure 1.1 below, is the predominant isoform found in all tissues. It consists of 89 amino acids. The first 21 amino acids make up the signal peptide, while the mature protein spans Lysine 22 to Lysine 89. SDF1α is comprised of a three β-strands, an α-helix, and is bordered by disordered N and C- terminal ends. It is believed that the N-terminus (residues one to nine) is responsible for SDF1's binding to its receptors [2]. Other isoforms of SDF1 share the same N-terminal amino acid sequence, but have different C-termini.

Figure 1.1 Image of SDF1α by Ryu et al [3]. (RSCB Protein Data Bank ID: 2J7Z). SDF1α monomer was obtained using Pymol. N-terminus is colored blue and C-terminus colored red.

As shown in Table 1.1 below, SDF1α has a net positive charge which is attributed its numerous basic amino acids. It has a molecular weight of about ten kilodaltons.

Table 1.1: General Properties of SDF1α (obtained using the ExPASy Server [4])

Molecular Formula	$C_{453}H_{753}N_{129}O_{119}S_6$
Molecular weight/size	~ 10 kilodaltons
Total number of negatively charged residues (Asp + Glu)	5
Total number of positively charged residues (Arg + Lys)	14
Net charge on protein	Positive (+9)
Theoretical Isoelectric point	9.72
Theoretical Extinction coefficient	8730 M^{-1} cm^{-1}

There are at least two known receptors for SDF1, C-X-C chemokine receptor type four (CXCR4) and type seven (CXCR7)[5]. The binding of SDF1 to CXCR4 results in intracellular signaling via guanine nucleotide-binding proteins (G-proteins), which triggers the activation of the MAPK, PI3K and IP3 pathways, as well as intracellular calcium release, resulting in increases in target cell survival, proliferation, and chemotaxis [6]. CXCR4 is expressed by several cell types such as hematopoietic stem

cells, endothelial and epithelial cells [7], as well as cells in the immune and central nervous systems [8].

SDF1 was originally identified as the factor that promotes the retention of hematopoietic stem cells in the bone marrow [9]. One of the first therapeutic interventions targeting the SDF1 pathway involved blocking SDF1 binding to its receptor to induce the release of bone marrow stem cells, thus increasing their numbers in the circulation. The blood enriched in stem cells could then be used for bone marrow transplantation procedures [10]. SDF1, as other angiogenic factors, is also known to perpetuate cancer tumor growth and progression; therefore, several studies have also evaluated the benefit of blocking this pathway as a potential cancer therapy [7]. Through its binding to CXCR4, SDF1 may also be an endogenous inhibitor of CXCR4-trophic HIV-1 strains [11].

SDF1 is also known to been implicated in the endogenous response to tissue damage and subsequent tissue repair. For example, SDF1 may be expressed in the local injury area to promote the recruitment of stem cells from the bone marrow to injured tissues/organs [12]. It is believed that SDF1, upon entering the bone marrow environment, induces the release of soluble kit-ligand (sKitL), which induces the release of more SDF1, enhancing mobilization of the CXCR4+ and c-Kit+ cells to the circulation [13]. Once the progenitor cells reach the injury site, it is thought that they participate in the regeneration of damaged blood vessels. Thus, exogenous SDF1 has been explored as a therapeutic molecule to enhance these processes in several acute and chronic injury types that otherwise tend to heal poorly, such as injuries related to the central nervous system, including spinal cord [14, 15], multiple sclerosis[16], stroke[17] and myocardial

infarction [18-20]. It is also being explored for treatment of chronic skin wounds [12, 21] and acute burn wounds [22].

A major limitation in the use of SDF1 as a therapeutic molecule, like many other similar peptides, is its short in vivo half-life due to rapid degradation by proteases. Providing a sustained supply of SDF1 in the first two to three weeks of injury healing (proliferative phase) would be clinically beneficial.

Different strategies are being explored to increase the stability of SDF1 in vivo in the context of different injury types and disease situations. Some researchers have focused attention on designing derivatives of SDF1 with increased in vivo stability [19], [23], [24], [25], [26, 27]. Other researchers have explored incorporating SDF1 into biomaterials such as hydrogels and scaffolds in order to prolong its release profile and protect it from degradation. Nanoparticle-based delivery is especially advantageous because the delivery system can be administered in a variety of ways, and can be easily incorporated into biomaterials that are already used to enhance tissue repair.

Therefore, here we review the various stabilization and delivery methods available for SDF1, some of which have been already used, as well as others that have been used with other bioactive peptides, but would be potentially applicable to SDF1.

1.2 CHALLENGES WITH DELIVERING SDF1

SDF1 has a short half-life in vivo as it is readily degraded by multiple proteases, including dipeptidyl peptidase IV, a serine exopeptidase, matrix metalloproteinases [28, 29], cathepsin G [30] and neutrophil elastase [31] which are activated at the sites of injury and typically attack the chemokine at the N-terminus. Cleavage of the N-terminus

of SDF1 results in a loss of binding to its receptor CXCR4, and as such a loss of its chemoattractant activity.

In addition to potential N-terminus cleavage, SDF1α can also be cleaved at the C-terminus by carboxypeptidase N (CPN), which also results in attenuated chemoattractant activity [32], [33]. The in vivo half-life of SDF1α is known to be about 25.8 minutes [34]. Due to the presence of additional exons on the C-terminus, the other isoforms of SDF1 are not susceptible to proteolysis by carboxypeptidase N.

Since exogenous recombinant SDF1 is susceptible to the same proteolytic mechanisms as the endogenous one, in the absence of any engineered delivery system, high and repeated doses of the peptide may be needed for therapeutic activity. For example, in studying the effect of SDF1α on model wounds in mice, Sarkar et al [35] demonstrated that a repeated dosing regimen of four daily applications of 1 μg SDF1α was needed to allow for faster reepithelialiization of an excisional wound made on wild-type mice.

Repeated application of SDF1 is costly and impractical. Thus, protein engineering technologies and delivery methods that will allow for a stabilization of the growth factor in vivo are essential. Below we first discuss some of the protein engineering approaches being used to alter the structure of the peptide itself, and then the delivery systems used to protect the peptide (either native or modified) to allow sustained delivery in vivo.

1.3 STABILIZATION OF SDF1 USING PROTEIN ENGINEERING

1.3.1 Fusion Proteins and Derivatives of SDF1 with Longer Half Lives

One way to increase the stability of SDF1 is to construct a fusion protein comprised of the SDF1 gene juxtaposed to another protein or peptide at either the N or C-terminus (for

SDF1α only). As shown in Figure 1.2 below, both the terminal ends of SDF1α are susceptible to degradation. Since the N-terminus is involved in binding to the CXCR4 receptor, fusions are typically made at the C-terminus. "Capping" the C-terminus of SDF1α with a peptide or protein should help reduce its degradation. For example, SDF1β, which only differs from SDF1α by having a fourth exon at the C-terminus, has a longer half-life in vivo and as a result is known to be twice as potent [1].

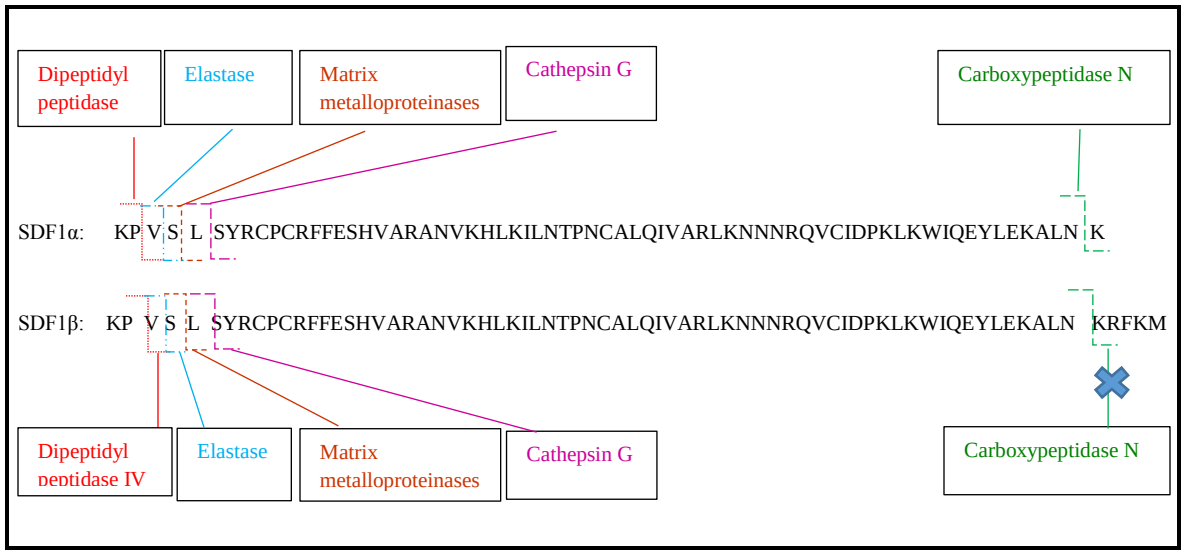

Figure 1.2 SDF1α and SDF1β degradation by different proteases. Dipeptidyl peptidase IV cleaves off Lys22 and Pro23 (KP); Elastase cleaves off Lys22, Pro23 and Val24 (KPV); Matrix metalloproteinases cleave off Lys22, Pro23, Val 24, Serine 25 (KPVS); Cathepsin G cleaves off Lys22, Pro23, Val24, Ser25, Leu26 (KPVSL).Carboxypeptidase N cleaves off the Lysine at the C-terminus of SDF1α. Due to the presence of an additional exon at the C-terminus, SDF1β is not subjected to degradation by Carboxypeptidase N

Ziegler et al [19] explored this concept with their design of a bispecific SDF1-GPVI fusion protein, consisting of SDF1α and the platelet collagen receptor GPVI. GPVI was

fused to the C-terminus of SDF1α (SDF1α-GPVI), as well as the N-terminus of SDF1α (GPVI-SDF1α). This work was done on the assumption that the binding of GPVI to the collagen triple helix in the sub-endothelial matrix would allow for an increased concentration of SDF1 at the site of injury (in this case injured myocardium), allowing for SDF1α to be persist longer and recruit bone marrow cells to the damaged area, thus resulting in a better healing process. As expected, the activity of GPVI-SDF1α was greatly diminished, while SDF1α-GPVI fusion protein showed a higher binding activity to the CXCR4 receptor, triggered chemotaxis, increased cell survival and enhanced endothelial differentiation. In-vivo, SDF1α-GPV1, which was injected intravenously, allowed for the recruitment of significantly more bone marrow cells after tissue damage, as compared with recombinant SDF1α.

Other researchers have designed derivatives of SDF1 with "minor" mutations to the N-terminus region in an attempt to change recognizable cleavage sequences for the proteases, while trying to maintain the integrity of the binding region of the chemokine

Segers et al [23] developed a new version of SDF1α consisting of a modification to the N-terminus region to reduce susceptibility to common proteases (matrix metalloproteinase-2 and dipeptyl peptidase IV). As opposed to SDF1α, whose N-terminus region is comprised of is KPVSLSYR, S-SDF1α (S4V) has a few modifications shown in red: SKPVVLSYR. An additional serine was added in front of the N-terminal lysine, while the serine in the fourth position was changed to valine as shown in Figure 1.3 below.

N-terminus region of native SDF1α:	KPVSLSYR
S-SDF1:	SKPVSLSYR
S-SDF1 (S4V):	SKPVVLSYR

Figure 1.3 Amino acid modifications made to SDF1 by Segars et al [23].

The team noted that the S-SDF1(S4V) variant of SDF1 was bioactive but resistant to cleavage by DPPIV and MMPs, as compared to native SDF1. S-SDF1 (S4V), the protease-resistant variant of SDF1, was then fused at the C-terminus to RAD16-II (RAD), which has sequence RARADADARARADADA, and self-assembles into nanofibers. S-SDF-1(S4V) improved cardiac function after myocardial infarction when it was tethered to the self-assembling peptide RAD for controlled delivery [23].

Similarly, Baumann et al [24] engineered another derivative of SDF1α (AAV-[S4V]-SDF1α) to have a better stability than recombinant SDF1α. As shown in Figure 1.4 below, two alanines and one valine were inserted in front of the N-terminal lysine, and the 4th serine was changed to a valine, similar to the approach taken by Segers et al. These changes prevented the degradation of the engineered SDF1α derivative by DPPIV and MMP. The engineered protein was delivered using starPEG heparin hydrogels. The hydrogel delivery results are discussed in 1.3.2.2 Biomaterials.

N-terminus region of native SDF1α:	KPVSLSYR
V-(S4V)-SDF1α:	VKPVVLSYR
AAV-(S4V)-SDF1α:	AAVKPVVLSYR

Figure 1.4 Amino acid modifications made to SDF1 by Baumann et al [24].

Likewise, Yang et al [25] demonstrated that inserting a methionine in front of the N-terminal lysine (Lysine 23) of SDF1β as shown in Figure 1.5 below enhanced its functional activity compared to native SDF1β. While they acknowledged that the modification resulted in a slightly lower affinity of the chemokine to its receptor, they highlighted that the Met-SDF1β induced a significantly higher intracellular calcium flux

indicating a much higher bioactivity as compared to native SDF1β. Similar to other researchers, Yang et al. explained that placing a methionine in front of Lysine 23 perturbed the action of DPPIV, allowing the growth factor to be more stable and more bioactive.

N-terminus region of native SDF1β:	KPVSLSYR
Methionine-SDF1β:	MKPVSLSYR

Figure 1.5 Amino acid modifications made to SDF1 by Yang et al [25].

In another effort to stabilize SDF1α when used in vivo, Hiesinger et al [26, 27] engineered an SDF1α polypeptide analog named ESA (Figure 1.6), with comparable to better activity than recombinant SDF1α. Computational molecular modeling and design was used to cleave off the large central β sheets of SDF1α, replacing them with proline residues, to connect the N-terminus responsible for receptor binding with the C-terminus, so that ESA would have a similar conformation as native SDF1α.

ESA was able to induce EPC migration and improve ventricular performance as compared to the recombinant SDF1α used as a control. The team believes that compared to native SDF1α, the relatively small size of ESA provides enhanced stability and function, allows for easier and cheaper synthesis, and perhaps more importantly enhances the diffusion potential and the speed at which the chemotactic signal is deployed [26].

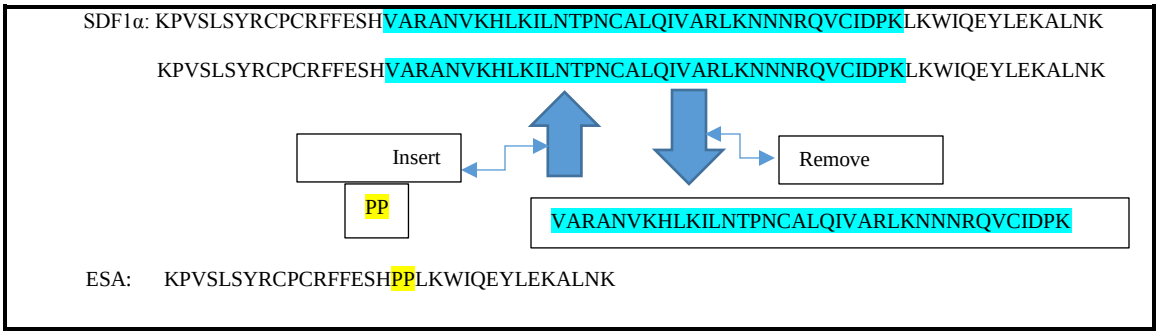

Figure 1.6 Amino acid modifications made to SDF1 by Hiesinger et al. ESA is a derivative of SDF1 without the large central β sheets of SDF1 but instead 2 proline residues which connects the N-terminus to the C-terminus [26, 27].

1.3.2 Stabilization of SDF1 using Various Delivery Mechanisms

1.3.2.1 Gene Therapy

Using viral or non-viral constructs encoding for the SDF1 gene can result in an overexpression of SDF1 allowing for a longer protein presence at the injury site.

To this end, Badillo et al [36] made full thickness excisional wounds on diabetic mice and treated them with lentiviral construct containing SDF1 gene fused to green fluorescent protein (GFP) to induce the overexpression of SDF1 in wounds. The viral plasmid with GFP alone was used as a control. The production of SDF1 by transduced cells was confirmed by a measuring the total wound mRNA isolated from wounds treated with the SDF1-GFP lentiviral plasmid or the control alone. The research team confirmed that the lentiviral SDF1 treated wound showed an increased production of SDF1 mRNA seven days post injection of the viral plasmid in the wound area. This corresponded to a decrease in wound surface area and an increased granulation tissue seven days post wounding.

Similarly, Sundararaman et al [37] injected different luciferase plasmid DNA (non-viral) encoding human SDF1 into rat heart 1 month after myocardial infarction. Expression of the gene ranged from five to 32 days. Heart function and immunohistochemistry of the heart tissue was assessed after plasmid injection. Increase in cardiac function was noticed four weeks after injection, attributed to increase in blood

vessel density. The degree of functional improvement positively correlated with level of vector expression.

1.3.2.2 Biomaterials

Biomaterials have been used for the controlled release, for the prolongation of half-life and enhancement of the therapeutic efficacy of bioactive molecules, including growth factors. Biomaterials have been used to deliver growth factors in a matrix-bound manner, as the biomaterial surface allows for the growth factor to be concentrated and delivered locally [38].

Biomaterials such as alginate scaffolds and hydrogels, degradable poly (lactide ethylene oxide fumarate) (PLEOF) hydrogels, poly(L-lysine) and hyaluronan, and starPEG-heparin hydrogels have been used to deliver SDF1.

Rabbany et al [39] and Henderson et al [40] demonstrated the sustained release of SDF1 from alginate hydrogels for wound healing. Rabbany et al. loaded alginate hydrogel patches with recombinant human SDF1 proteins and monitored the in vitro and in vivo release profile. The hydrogels released about 50% of the protein within the first day and minimally released the rest of the protein over the remaining five day monitoring period. Wounds treated with SDF1 protein delivered in the hydrogel patch healed faster and showed a significantly faster wound closure as compared to non-treated wounds.

Henderson et al. also monitored the release of the SDF1 chemokine from an alginate hydrogel scaffold which was applied on directly unto a wound bed made on the dorsum of wild type mice. The scaffold was designed to allow for a slow release of the growth factor over 18 to 24 hours. The team showed that the SDF1 treated wounds closed rapidly between one to three days after application to the wound bed, and much less between

three to seven days as compared to the saline control potentially because the SDF1 had been depleted from the scaffold by day three.

In addition to alginate hydrogels, degradable poly (lactide ethylene oxide fumarate) (PLEOF) hydrogels, poly(L-lysine) and hyaluronan, and starPEG-heparin hydrogels have been used to deliver SDF1 in a controlled manner.

He et al [41] developed a macromer made of PLEOF that was cross-linked with different initiators to produce biodegradable hydrogels. Three different hydrogels with different levels of hydrophobicity were evaluated for their SDF1 release profile and its effect on the migration of bone marrow stem cells. The team noted that the hydrogels that were designed to be more hydrophilic had an initial burst release of SDF1 followed by a period of controlled delivery for 21 days. The hydrophobic hydrogels had a less pronounced burst release and displayed a slow but constant release between days one to nine, followed by a fast release from days nine to 18. The migration of bone marrow stem cells closely followed the SDF1 release kinetics out of the hydrogels. That is, the more hydrophilic hydrogels had a higher extent of cell migration initially but finished with the lowest extent of cell migration while the more hydrophobic hydrogels had a lower extent of initial cell migration but finished off with the highest extend of cell migration.

Dalonneau et al [38] loaded SDF1 into polyelectrolyte multilayer films which was made of poly(L-lysine) and hyaluronan (PLL/HA), to allow for the growth factor to be delivered in a matrix bound manner to myoblast cells. The PLL/HA films exhibited an initial burst release during the first hour, after which the growth factor release was steady. The matrix bound SDF1 enhanced myoblast spreading and considerably promoted cell migration.

Prokoph et al [42] and Baumann et al [24] demonstrated the delivery of SDF1 and its derivative, AAV-[S4V]-SDF-1 (discussed above) using a starPEG-heparin hydrogels. The release profile of native SDF1 from the starPEG hydrogel was highly similar to that of the SDF1 derivative. Both of them were released at a high level (high initial burst) initially, followed by a sustained release. However, the relative migration of endothelial progenitor cells (EPCs) was significantly higher using the engineered derivative of SDF1 delivered via the hydrogel compared with the native SDF1.

1.4 OVERALL LIMITATIONS WITH EXISTING STRATEGIES FOR THERAPEUTIC SDF1 USE

While the above strategies and delivery options address some of the challenges in using SDF1 therapeutically, some overall limitations still exist, as highlighted below:

1.4.1 Fusion Proteins and Derivatives of SDF1 with Longer Half Lives

- Potential for decrease or loss of activity of growth factor,
- High cost for producing and purifying material.

1.4.2 Gene Therapy

- Toxicity and immunogenicity of some of the vectors used not well understood,
- Concerns about the potential random integration of viral genes into host genome,
- Possibility of sustained transgene expression, which could have detrimental (e.g. cancer-causing) effects,
- Low transfection efficiency of some of the vectors, resulting in low levels of gene expression.

1.4.3 Biomaterials

- High initial burst release from some hydrogels/scaffolds,
- High amount of SDF1 needed for loading into hydrogels due to low loading efficiency of some hydrogels,
- Total fraction of SDF1 released from hydrogels over a period of time relatively low compared to how much was loaded,
- Material of construction for some hydrogels could result in unwanted byproducts when degraded.

1.5 THE IDEAL DELIVERY SYSTEM FOR SDF1

The “perfect” delivery system for therapeutic SDF1 use would therefore be one that encompasses all or a majority of the following characteristics:

- Gradually release SDF1 for about two to three weeks (that is, throughout the proliferative phase of healing after an injury,
- Protect SDF1 from degradation,
- Have minimal to no impact on the bioactivity of the chemokine,
- Can be manufactured less expensively, thus reducing the overall cost of the therapy,
- Allow the right dose of the growth factor to be delivered (typically in the nanogram range),
- Should not be toxic, non-immunogenic and biocompatible,
- Allow for the growth factor to be readily assessable to its receptor (easy bioavailability).

1.6 FUTURE PERSPECTIVES

1.6.1 Nanoparticle technologies for SDF1

A more versatile delivery system would make it easier to translate SDF1-based therapies into reality. Nanoparticles seem to be a viable option to address the shortcomings of the other delivery strategies described above, and also encompasses several of the desired characteristics of the ideal delivery system.

The use of nanoparticles to deliver SDF1 offers several advantages. First, formulating SDF1 into nanoparticles will allow the chemokine to be delivered in the same size range as proteins and other macromolecular structures found inside living cells. This is expected to result in improved bioavailability and rapid therapeutic action. Second, it is believed that highly efficient drug delivery system based on nanomaterials could potentially reduce the drug dose needed to achieve therapeutic benefit, which, in turn, would lower the cost and/or reduce the side effects associated with particular drugs. In addition, drugs delivered as nanoparticles have been shown to have prolonged circulation time in vivo [43] Formulating SDF1 as nanoparticles could allow the growth factor not only to be injected as a suspension but also incorporated as appropriate to topical creams or into existing skin substitutes which have pores in the 10-100 μm range.

Lim et al [44], Huang et al [45], Yin et al [46] all incorporated SDF1 into chitosan/chitosan-based nanoparticles. Lim et al. noted that their nanoparticle released about eight percent of the SDF1 over a period of seven days implying that the delivery system would be suitable for sustained release of the growth factor. The SDF1 enclosed in the nanoparticle delivery system allowed for chemotactic recruitment of adult neuronal progenitor cells (aNPC) by three to 45-fold relative to hydrogels that lacked SDF1.

Similarly, Huang et al [45] highlighted that their chitosan based nanoparticles protected SDF1 against proteolysis and allowed for a sustained control release up to seven days. Up to 23 ng/ml of SDF1 was released, which retained mitogenic activity, enhanced the migration of mesenchymal stem cells and promoted PI3K expression. Yin et al [46] delivered SDF1 as 700nm particles in order for the growth factor to reach the alveolus/alveolar duct which is reported to be 25 – 100 μm in diameter. The incorporated SDF1 in the nanoparticles was slowly released (three percent was released over seven days) and was able to cause full chemotactic activity and receptor activation as compared to the native free SDF1. When aerosolized in the lungs, the SDF1 nanoparticles showed a greater retention time than that of free SDF1.

Olekson et al [47] demonstrated the delivery of SDF1 using liposome nanoparticles. Liposome nanoparticles were used to extend the half-life of the growth factor by serving as a local reserve of the chemokine. The SDF1α lipid nanoparticles were tested for chemotactic activity using HL-60 cells (HL60 cells express the CXCR4 receptor). The nanoparticles exhibited similar functional response as free SDF1. When used on an excisional wound created on diabetic mouse, the SDF1 liposomes increased the fractional area of closed tissue by about 15% as compared to free SDF1. This was attributed to the persistence of the SDF1 nanoparticles at the wound area.

1.6.2 Nanoparticle technologies for other growth factors

Thus, despite the potential benefits, few nanotechnology-based delivery approaches have been implemented for SDF1. On the other hand, when considering other growth factors and chemokines, several different nanosystems are potentially available that would

exhibit the desirable characteristics for delivering SDF1, some of which are discussed below.

1.6.2.1 Release kinetics and protection from degradation

As shown in Table 1.2, nanoparticles made of materials such as silica, elastin and lipids have been successfully designed and used to deliver different types of growth factors. The nanoparticles were only slowly degraded in vivo thus enabling the release of growth factors over an extended period of time. For example, the porous silica nanoparticles designed by Zhang et al [48] allowed for basic fibroblast growth factor (bFGF) to be released for at least three weeks. Similarly, the heparin and ε-poly-L-lysine (PL) nanoparticles designed by LuZhong et al [49] for delivery of nerve growth factor (NGF) and basic fibroblast growth factor (bFGF) had a sustained and slow release profile; 43% of bFGF and 60% of NGF was released from the particles within 20 days of use in treatment of peripheral nerve injury.

1.6.2.2 Biocompatibility

All the nanoparticle systems described in Table 1.2 were designed for eventual use in vivo. For example, multiple studies have shown that elastin like peptide (ELP) used to deliver keratinocyte growth factor [48] are nonimmunogenic, non-pyrogenic and are biologically compatible [49] Likewise, the lipid nanoparticles used to deliver epidermal growth factor are biodegradable and no adverse reactions were reported by Gainza et al [50] when the nanoparticles were used on mice. Zhang et al [51] demonstrated that the porous silica nanoparticles used to deliver bFGF were not cytoxic. Some studies have described the use of porous silica nanoparticles in vivo and reported no adverse events [52]. One concern with the porous silica system, however, is that it is not biodegradable,

and therefore further in vitro and in vivo biocompatibility studies may need to be performed if it is to be used in a clinical setting.

1.6.2.3 Ease of manufacturing

Eventual translation of the nanoparticle-based delivery system to the clinic will require large-scale production. For example, the PEG-PLGA nanoparticles used to deliver bFGF for Alzheimer's treatment are well-established nanocarriers for nanomedicine applications, and are relatively simple to manufacture [53]. It is noteworthy that all of the systems described above

require the bioactive peptide to be produced on a large scale using traditional methods for expressing and purifying the product. The bioactive peptide-ELP approach has the unique feature that, while the methods to express the fusion protein in bacterial production systems are not fundamentally different from any other peptide, purification can be accomplished through repeated temperature cycles to precipitate the final product by centrifugation, thus avoiding the use of expensive chromatography-based methods [54] The main challenge in using ELP fusion proteins is that care must be taken to preserve biological activity of the bioactive peptide, and as suggested by Hassouneh et al [55], the specific properties of the bioactive peptide (in this case the size and charge of SDF1) can be factored into the design of the ELP chain length, and sequence, as well as the type and length of the linker used for the fusion protein, so that aggregation temperature is in a desirable range (usually between 30°C and 40°C).

Table 1.2: Examples of nanoparticles which have been used for other growth factors

Growth Factor	Disease Area / Application	Type of Nanoparticle Used/Authors	Reasons for Using Nanoparticle Approach
Basic Fibroblast Growth Factor (bFGF)	Wound Healing	Porous Silica Nanoparticles Zhang et al [51].	Porous silica nanoparticles were used to achieve a prolonged release of bFGF for at least 3 weeks.
Keratinocyte Growth Factor (KGF)	Wound Healing	Elastin-like peptide (ELP) nanoparticles Koria et al [48].	Designed nanoparticles comprised of the fusion of KGF to elastin-like peptides which allowed for topical administration of the growth factor to the wound area and also improved the growth factor's bioavailability to the injury site.
Nerve Growth Factor (NGF) and Basic Fibroblast Growth Factor (bFGF).	Axonal Regeneration	Polymeric nanoparticle delivery system composed of heparin and ε-poly-L-lysine (PL) LuZhong et al [56].	Nanoparticles were prepared for controlled and slow release of nerve growth factor (NGF) and basic fibroblast growth factor (bFGF) for the treatment of peripheral nerve injury. A sustained and no initial burst in vitro release profile of growth factors (NGF and bFGF) from the particles was observed For the bFGF, about 43% of the loaded growth factor was released from particles within 20 days. For NGF, about 60% of the loaded growth factor was released from particles within 20 days for the NGF.
Epidermal Growth Factor (EGF)	Wound Healing	Lipid nanoparticles Gainza et al [50].	Lipid nanoparticles were used to allow for topical and sustained delivery of recombinant human EGF to chronic wounds.
Basic Fibroblast Growth Factor (bFGF)	Alzheimer's	Lectins modified polyethylene glycol-polylactide-polyglycolide (PEG-PLGA) nanoparticles Zhang et al [57].	The lectin modified PEG-PLGA nanoparticles were used to deliver basic fibroblast growth factor to the central nervous system via intranasal administration for treatment of Alzheimer's disease. The growth factor was formulated into nanoparticles to protect it from being from degradation within the lumen of the nasal cavity or during passage across the epithelial barrier. The nanoparticle conjugation with lectin allowed for selective binding to N-acetyl glucosamine on the nasal epithelial membrane for its brain delivery

1.7 REFERENCES

[1] M. Janowski, Functional diversity of SDF-1 splicing variants, Cell Adhesion and Migration, 3 (2009) 243-249.

[2] P. Loetscher, J.H. Gong, B. Dewald, M. Baggiolini, I. Clark-Lewis, N-terminal peptides of stromal cell-derived factor-1 with CXC chemokine receptor 4 agonist and antagonist activities, J Biol Chem, 273 (1998) 22279-22283.

[3] E.K. Ryu, T.G. Kim, T.H. Kwon, I.D. Jung, D. Ryu, Y.M. Park, J. Kim, K.H. Ahn, C. Ban, Crystal structure of recombinant human stromal cell-derived factor-1alpha, Proteins, 67 (2007) 1193-1197.

[4] E. Gasteiger, C. Hoogland, A. Gattiker, S. Duvaud, M.R. Wilkins, R.D. Appel, A. Bairoch, Protein Identification and Analysis Tools on the ExPASy Server, in: J.M. Walker (Ed.) The Proteomics Protocols Handbook, Humana Press, 2005, pp. 571-607.

[5] J.M. Burns, B.C. Summers, Y. Wang, A. Melikian, R. Berahovich, Z. Miao, M.E.T. Penfold, M.J. Sunshine, D.R. Littman, C.J. Kuo, K. wei, B.E. McMaster, K. Wright, M.C. Howard, T.J. Schall, A novel chemokine receptor for SDF-1 and I-TAC involved in cell survival, cell adhesion, and tumor development, The Journal of Experimental Medicine, 203 (2006) 2201-2213.

[6] Y. Doring, L. Pawig, C. Weber, H. Noels, The CXCL12/CXCR4 chemokine ligand/receptor axis in cardiovascular disease, Frontiers in physiology, 5 (2014).

[7] B.A. Teicher, S.P. Fricker, CXCL12 (SDF-1)/CXCR4 Pathway in Cancer, Clinical Cancer Research, 16 (2010) 2927-2931.

[8] Y.R. Zou, A.H. Kottmann, M. Kuroda, I. Taniuchi, D.R. Littman, Function of the chemokine receptor CXCR4 in haematopoiesis and in cerebellar development, Nature, 393 (1998) 595-599.

[9] M.Z. Ratajczak, C.H. KIm, A. Abdel-Latif, G. Schneider, M. Kucia, A.J. Schneider, M.J. Laughlin, J. Ratajczak, A novel perspective on stem cell homing and mobilization: review on bioactive lipids as potent chemoattractants and cationic peptides as underappreciated modulators of responsiveness to SDF-1 gradients, Leukemia, 26 (2012) 63-72.

[10] Y. Kang, B.J. Chen, D. DeOliveira, J. Mito, N.J. Chao, Selective Enhancement of Donor Hematopoietic Cell Engraftment by the CXCR4 Antagonist AMD3100 in a Mouse Transplantation Model, PLoS ONE, 5 (2010).

[11] E.A. Berger, Introduction: HIV co-receptors solve old questions and raise many new ones, Semin Immunol, 10 (1998) 165-168.

[12] X. Xu, F. Zhu, M. Zhang, D. Zeng, D. Luo, G. Liu, W. Cui, S. Wang, W. Guo, W. Xing, H. Liang, L. Li, X. Fu, J. Jiang, H. Huang, Stromal Cell-Derived Factor-1 Enhances Wound Healing through Recruiting Bone Marrow-Derived Mesenchymal Stem Cells to the Wound Area and Promoting Neovascularization, Cells Tissues Organs, 197 (2013) 103-113.

[13] I. Petit, D. Jin, S. Rafii, The SDF-1-CXCR4 signaling pathway: a molecular hub modulating neo-angiogenesis, Trends in Immunology, 28 (2007) 299-307.

[14] A. Jaerve, F. Bosse, H.W. Muller, SDF-1/CXCL12: Its role in spinal cord injury, The International Journal of Biochemistry and Cell Biology, 44 (2012) 452-456.

[15] H. Takeuchi, A. Natsume, T. Wakabayashi, C. Aoshima, S. Shimato, M. Ito, J. Ishii, Y. Maeda, M. Hara, S.U. Kim, J. Yoshida, Intravenously transplanted human neural stem cells migrate to the injured spinal cord in adult mice in an SDF-1 and HGF-dependent manner, Neuroscience Letters, 426 (2007) 69-74.

[16] K.S. Carbajal, C. Schaumburg, R. Strieter, T.E. Lane, Migration of engrafted neural stem cells is mediated by CXCL12 signaling through CXCR4 in a viral model of multiple sclerosis, 107 (2010) 11068-11073.

[17] S. Woei-Cherng, L. Demeral David, L. Shinn-Zong, L. Wen-Wen, S. Ching-Yuan, C. Ying-Chen,
W. Hsiao-Jung, W. Hsing-Won, T. Chang-Hai, L. Hung, Implantation of olfactory ensheathing cells promotes neuroplasticity in murine model of stroke, 118 (2008) 2482-2495.

[18] M. Penn, Importance of the SDF-1:CXCR4 Axis in Myocardial Repair, Circulation Research,
104 (2009) 1133-1135.

[19] M. Ziegler, M. Elvers, Y. Baumer, C. Leder, C. Ochmann, T.J. Schonberger, T. Geisler, B. Schlosshauer, O. Lunov, S. Engelhardt, T. Simmet, M. Gawaz, The Bispecific SDF1-GPVI Fusion Protein Preserves Myocardial Function After Transient Ischemia in Mice, Circulation, 125 (2012) 685-696.

[20] S.K. Ghadge, S. Muhlstedt, C. Ozcelik, M. Bader, SDF-1α as a therapeutic stem cell homing factor in myocardial infarction, Pharmacology and Therapeutics, 129 (2011) 97-108.

[21] S. Rabbany, J. Pastore, M. Yamamoto, T. Miller, S. Rafii, R. Aras, M. Penn, Continuous Delivery of Stromal Cell-Derived Factor-1 From Alginate Scaffolds Accelerates Wound Healing, Cell Transplantation, 19 (2010) 399-408.

[22] J. Ding, K. Hori, R. Zhang, Y. Marcoux, D. Honardoust, H.A. Shankowsky, E.E. Tredget, Stromal cell-derived factor 1 (SDF-1) and its receptor CXCR4 in the formation of postburn hypertrophic scar (HTS), Wound Repair and Regeneration, 19 (2011) 568-578.

[23] V.F.M. Segers, T. Tokunou, L.J. Higgins, C. MacGillivray, J. Gannon, R.T. Lee, Local Delivery of Protease-Resistant Stromal Cell Derived Factor-1 for Stem Cell Recruitment after Myocardial Infarction, Circulation, 116 (2007) 1683-1692.

[24] L. Baumann, S. Prokoph, C. Gabriel, U. Freudenberg, C. Werner, A.G. Beck-Sickinger, A novel, based-like SDF1 derivative acts synergestically with starPEG-based heparin hydrogels and improves eEPC migration in vitro, Journal of controlled release, 162 (2012) 68-75.

[25] O.O. Yang, S. Swanberg, L. , Z. Lu, M. Dziejman, J. McCoy, A.D. Luster, B.D. Walker, S.H. Hermann, Enhanced Inhibition of Human Immunodeficiency Virus Type 1 by Met-Stromal-Derived Factor 1b Correlates with Down-Modulation of CXCR4, Journal of Virology, 73 (1999) 4582-4589.

[26] W. Hiesinger, A. Goldstone, J. Woo, Re-Engineered Stromal Cell-Derived Factor-1α (SDF) and the Future of Translatable Angiogenic Polypeptide Design, Trends in Cardiovascular Medicine, 22 (2012) 139-144.

[27] W. Hiesinger, J.M. Perez-Aguilar, P. Atluri, N. Marotta, J. Frederick, J.R. Fitzpatrick III, R.C. McCormick, J.R. Muenzer, E.C. Yang, R.D. Levit, L.-J. Yuan, J.W. MacArthur, J.G. Saven, Y.J. Woo, Computational Protein Design to Re-Engineer Stromal Cell-Derived Factor-1alpha (SDF) Generates an Effective and Translatable Angiogenic Polypeptide Analog, Circulation, 124 (2011) S18-S26.

[28] C. Durinx, A.M. Lambeir, E. Bosmans, J.B. Falmagne, R. Berghmans, A. Haemers, S. Scharpe, I. De Meester, Molecular characterization of dipeptidyl peptidase activity in serum: soluble CD26/dipeptidyl peptidase IV is responsible for the release of X-Pro dipeptides, Eur J Biochem, 267 (2000) 5608-5613.

[29] G.A. McQuibban, G. Butler, J.-H. Gong, L. Bendall, C. Power, I. Clark-Lewis, C. Overall, Matrix Metalloproteinase Activity Inactivates the CXC Chemokine Stromal Cell-Derived Factor-1, 276 (2001) 43503-43508.

[30] M.B. Delgado, I. Clark-Lewis, P. Loetscher, H. Langen, M. Thelen, M. Baggiolini, M. Wolf, Rapid inactivation of stromal cell-derived factor-1 by cathepsin G associated with lymphocytes, Eur J Immunol, 31 (2001) 699-707.

[31] A. Valenzuela-Fernández, T. Planchenault, F. Baleux, I. Staropoli, K. Le-Barillec, D. Leduc, T. Delaunay, F. Lazarini, J. Virelizier, M. Chignard, D. Pidard, F. Arenzana-Seisdedos, Leukocyte elastase negatively regulates stromal cell-derived factor-1 (SDF-1)/CXCR4 binding and functions by amino-terminal processing of SDF-1 and CXCR4, J Biol Chem, 277 (2002) 15677-15689.

[32] D.A. Davis, K.E. Singer, M. De La Luz Sierra, M. Narazaki, F. Yang, H.M. Fales, R. Yarchoan, G. Tosato, Identification of carboxypeptidase N as an enzyme responsible for C-terminal cleavage of stromal cell-derived factor-1α in the circulation, Blood, 105 (2005) 4561-4568.

[33] L. Marquez-Curtis, A. Jalili, K. Deiteren, N. Shirvaikar, A.-M. Lambeir, A. Janowska-Wieczorek, Carboxypeptidase M Expressed by Human Bone Marrow Cells Cleaves the C-Terminal Lysine of Stromal Cell-Derived Factor-1alpha: Another Player in Hematopoietic Stem/Progenitor Cell Mobilization, Stem Cells, 26 (2008) 1211-1220.

[34] P. Misra, D. Lebeche, H. Ly, M. Schwarzkopf, G. Diaz, R. Hajjar, A. Schecter, J. Frangioni Quantitation of CXCR4 Expression in Myocardial Infarction Using 99mTc-Labeled SDF-1α, The Journal of Nuclear Medicine, 49 (2008) 963-969.

[35] A. Sarkar, S. Tatildede, S.S. Scherer, D.P. Orgill, F. Berthiaume, Combination of stromal cell derived factor-1 and collagen-glycosaminoglycan scaffold delays contraction and accelerates reepithilization of dermal wounds in wild-type mice, Wound Repair Regen., 19 (2011) 71-79.

[36] A.T. Badillo, S. Chung, L. Zhang, P. Zoltick, K. Liechty, Lentiviral Gene Transfer of SDF-1 to Wounds Improves Diabetic Wound Healing, Journal of Surgical Research, 143 (2007) 35-42.

[37] S. Sundararaman, T. Miller, J. Pastore, M. Kiedrowski, R. Aras, M. Penn, Plasmid-based transient human stromal cell-derived factor-1 gene transfer improves cardiac function in chronic heart failure, 18 (2011) 867-873.

[38] D. Fabien, Q.L. Xi, S. Rabia, A. Jorge, C.M. Hichem, B. Franz, A.-R. Corinne, W. Marianne, L.-J. Hugues, P. Catherine, The effect of delivering the chemokine SDF-1a in a matrix-bound manner on myogenesis, Biomaterials, 35 (2014) 4525-4535.

[39] S.Y. Rabbany, J. Pastore, M. Yamamoto, T. Miller, S. Rafii, R. Aras, M. Penn, Continuous Delivery of Stromal Cell-Derived Factor-1 From Alginate Scaffolds Accelerates Wound Healing, Cell Transplanation, 19 (2010) 399 - 408.

[40] P.W. Henderson, S.P. Singh, D.D. Krijgh, M. Yamamoto, D.C. Rafii, J.J. Sung, S. Rafii, S.Y. Rabbany, J.A. Spector, Stromal-derived factor-1 delivered via hydrogel drug-delivery vehicle accelerates wound healing in vivo, Wound Repair and Regeneration, 19 (2011) 420 - 425.

[41] X. He, J. Ma, E. Jabbari, Migration of Marrow Stromal Cells in Response to Sustained Release of Stromal-Derived Factor-1α from Poly(lactide ethylene oxide fumarate) Hydrogels, International Journal of Pharmaceutics, 390 (2010) 107-116.

[42] S. Prokoph, E. Chavakis, K.R. Levental, A. Zieris, U. Freudenberg, S. Dimmeler, C. Werner, Sustained delivery of SDF-1a from heparin-based hydrogels to attract circulating pro-angiogenic cells, Biomaterials, 33 (2012) 4792 - 4800.

[43] R. Gref, Y. Minamitake, M.T. Peracchia, V. Trubetskoy, V. Torchilin, R. Langer, Biodegradabe Long-Circulating Polymeric Nanospheres, Science, 263 (1994) 1600-1603.

[44] T.C. Lim, S. Rokkappanavar, W.S. Toh, L.-S. Wang, M. Kurisawa, M. Spector, Chemotactic recruitment of adult neural progenitor cells into multifunctional hydrogels providing sustained SDF-1 release and compatible structural support, The FASEB journal, 27 (2013) 1023 - 1033.

[45] Y.-C. Huang, T.-J. Liu, Mobilization of mesenchymal stem cells by stromal cell-derived factor-1 released from chitosan/tripolyphosphate/fucoidan nanoparticles, Acta Biomater, 8 (2011) 1048 - 1056.

[46] T. Yin, A.R. Bader, T.K. Hou, B.A. Maron, D.D. Kao, R. Qian, D.S. Kohane, D.E. Handy, J. Loscalzo, Y.-Y. Zhang, SDF-1α in Glycan Nanoparticles Exhibits Full Activity and Reduces Pulomanry Hypertension in Rats, Biomacromolecules, 14 (2013) 4009-4020.

[47] M. Olekson, R. Faulknor, A. Bandekar, M. Sempkowski, H. Hsia, S. Sofou, A. Schmidt, F. Berthiaume, Strategies for improving growth factor function in diabetic wounds, Presented at the Annual Wound Healing Society Meeting, Orlando, FL (April 23-27, 2014), Abstract published in WOUND REPAIR AND REGENERATION, 22 (2014) A54-A55.

[48] P. Koria, H. Yagi, Y. Kitagawa, Z. Megeed, Y. Nahmias, R. Sheridan, M.L. Yarmush, Self-assembling elastin-like peptides growth factor chimeric nanoparticles for the treatment of chronic wounds, Publication of the National Academy of Sciences, 108 (2011) 1034-1039.

[49] D. Urry, T. Parker, M. Reid, D. Gowda, Biocompatibility of the bioelastic materials, Poly(GVGVP) and its gamma-irradiation crosslinked matrix: summary of generic biological test results., Journal of Bioactive and Compatible Polymers, 6 (1991) 263-282.

[50] G. Gainza, M. Pastor, J.J. Aguirre, S. Villullas, J.L. Pedraz, R.M. Hernandez, M. Igartua, A novel strategy for the treatment of chronic wounds based on the topical administration of rhEGF-loaded lipid nanoparticles: In vitro bioactivity and in vivo effectiveness in healing-impaired db/db mice, Journal of controlled release, 185 (2014) 51-61.

[51] J. Zhang, L.-M. Postovit, D. Wang, R.B. Gardiner, R. Harris, M.M. Abdul, A.A. Thomas, In Situ Loading of Basic Fibroblast Growth Factor Within Porous Silica Nanoparticles for a Prolonged Release, Nanoscale Research Letters, 4 (2009) 1297-1302.

[52] J.M. Rosenholm, C. Sahlgren, Towards multifunctional, targeted drug delivery systems using mesoporous silica nanoparticles - opportunities & challenges, Nanoscale, 2 (2010) 1870-1883.

[53] E. Locatelli, M.C. Franchini, Biodegradable PLGA-b-PEG polymeric nanoparticles: synthesis, properties, and nanomedical applications as drug delivery system, Journal Of Nanoparticle Research, 14 (2012).

[54] S. MacEwan, W. Hassouneh, A. Chilkoti, Non-chromatographic Purification of Recombinant Elastin-like Polypeptides and their Fusions with peptides and proteins from Ecoli, Journal of
Visual Experiments, 88 (2014).

[55] W. Hassouneh, T. Christensen, A. Chilkoti, Elastin-like Polypeptides as a Purification Tag for Recombinant Proteins, Current Protocols in Protein Science, (2010).

[56] Z. LuZhong, Z. YouLang, L. GuiCai, Z. YaHong, G. XiaoSong, Y. YuMin, Nanoparticle mediated controlled delivery of dual growth factors, Science China Life Sciences, 57 (2014) 256-262.

[57] C. Zhang, J. Chen, C. Feng, X. Shao, Q. Liu, Q. Zhang, Z. Pang, X. Jiang, Intranasal nanoparticles of basic fibroblast growth factor for brain delivery to treat Alzheimer's disease, International Journal of Pharmaceutics, 461 (2014) 192-202.

2. CHAPTER 2: Elastin-like polypeptides: A strategic fusion partner for biologics

Note: This chapter is reproduced from the following publication **written by Agnes Yeboah**:

Agnes Yeboah, Rick I. Cohen, Charles Rabolli, Martin L. Yarmush, Francois Berthiaume. Elastin-like polypeptides: A strategic fusion partner for biologics. Biotechnology and Bioengineering (Submitted, 2015)

2.1 INTRODUCTION

Elastin is an extracellular matrix protein that gives elasticity to many vertebrate tissues such as the skin, heart, and blood vessels. In humans, it is encoded by the ELN gene. Tropoelastin, a soluble 70 kilodalton precursor of elastin, is comprised of two domains; hydrophobic - rich in Valine, Proline, Alanine and Glycine; and hydrophilic - comprised of Lysine and Alanine residues [1].

Elastin-like peptides (ELPs) are derived from the hydrophobic region of tropoelastin having repeat sequence motifs of Valine-Proline-Glycine-Xaa-Glycine (VPGXG), where Xaa can be any amino acid except Proline. ELPs have a unique property, inverse temperature phase transition, which allows a temperature dependent reversible change from soluble monomer to insoluble aggregate. The reversible inverse transition temperature is a function of the ELP chain length (the number of repeats of the VPGXG sequence motif in an ELP peptide), Xaa, the guest residue in the VPGXG sequence and the salt concentration used during the purification of the ELP peptide [2], [3]. ELPs are known to be nonimmunogenic, non-pyrogenic and biologically compatible [2].

The fusion of ELP at the N or C terminus of a target protein at the genetic level, also known as “ELPylation”, has been exploited for several applications, such as, for the targeted delivery of therapeutic drugs [4], and for prolonging the half-life of drugs in vivo [5]. However, the most remarkable benefit of using an ELP as a fusion partner is that it allows the target protein to be purified using the thermally driven, phase transition property of the ELP [6].

Using ELPylation for purification of therapeutic proteins should be particularly interesting to biopharmaceutical and biotechnology companies, who spend vast amounts of money and resources on the purification of their biologic drugs, which typically involves a series of chromatography and filtration steps. For example Vimizim (elosulfase alfa, RhGALNS) from Biomarin Pharmaceutical is purified in a sequence of chromatography, viral inactivation and filtration, and ultrafiltration/diafiltration steps (European Medicines Agency Assessment Report 2014). Similarly, Sylvant (Siltuximab active substance) from Jansenn Biotech is purified by several purification steps (protein A, cation exchange and anion exchange chromatography (European Medicines Agency 2014 Assessment Report)). It is believed that the downstream processing of proteins (including purification) represent between 50 to 90% of the total cost of manufacture of a recombinant protein [7].

Despite its potential appeal for reducing manufacturing costs, ELPylation has not yet been used as a purification step in a commercially supplied therapeutic, although PhaseBio Pharmaceuticals, Inc.’s Vasomera^{TM}, which uses the ELP technology, has successfully completed some early phase clinical trials. Accordingly, here we review the

concept of ELPylation, its applications and benefits and provide some considerations for translating the ELPylation purification strategy to biopharmaceutical protein purification.

2.2 PART I: INVERSE TRANSITION PROPERTY OF ELASTIN-LIKE-PEPTIDES

2.2.1 Single ELP chains form aggregates via a "twisted filament" intermediate

The most commonly used ELP has the pentapeptide sequence $(VPGXG)_n$ where "X" is seen as a guest residue that can be occupied by any amino acid except proline and "n" indicates the number of repeats of the pentapeptide needed to achieve the desired ELP chain length. The choice of the guest residue is known to directly impact the inverse transition temperature property of the ELP. Hydrophilic guest residues increase the inverse transition temperature while hydrophobic residues lower it. Proline cannot be used as the guest residue because it destroys the inverse phase transition property of the ELP [8]. "X" can be a single amino acid, or a combination of amino acids. For example, the expanded sequence of ELP $[Val_5Ala_2Gly_3\text{-}90]$, which is the most widely used ELP fusion construct [9] is $[[VPGVG]_5[VPGAG]_2[VPGGG]_3]_9$. In this case, "X" is a combination of Valines, Alanines and Glycines in a ratio 5:2:3. Single ELP chains exist as random coils below their transition temperature, but form insoluble aggregates above their transition temperature. The mechanism of aggregate formation is by random coiling of single chain ELPs, which was first proposed by Urry et al [3], and is illustrated in Figure 2.1. Random single ELP chains begin to assume a β-turn conformation, followed by a β-spiral conformation and then stack up against each other to form "twisted filaments" as they reach their transition temperature. Above their transition temperature, the twisted filaments associate with each other to form insoluble aggregates.

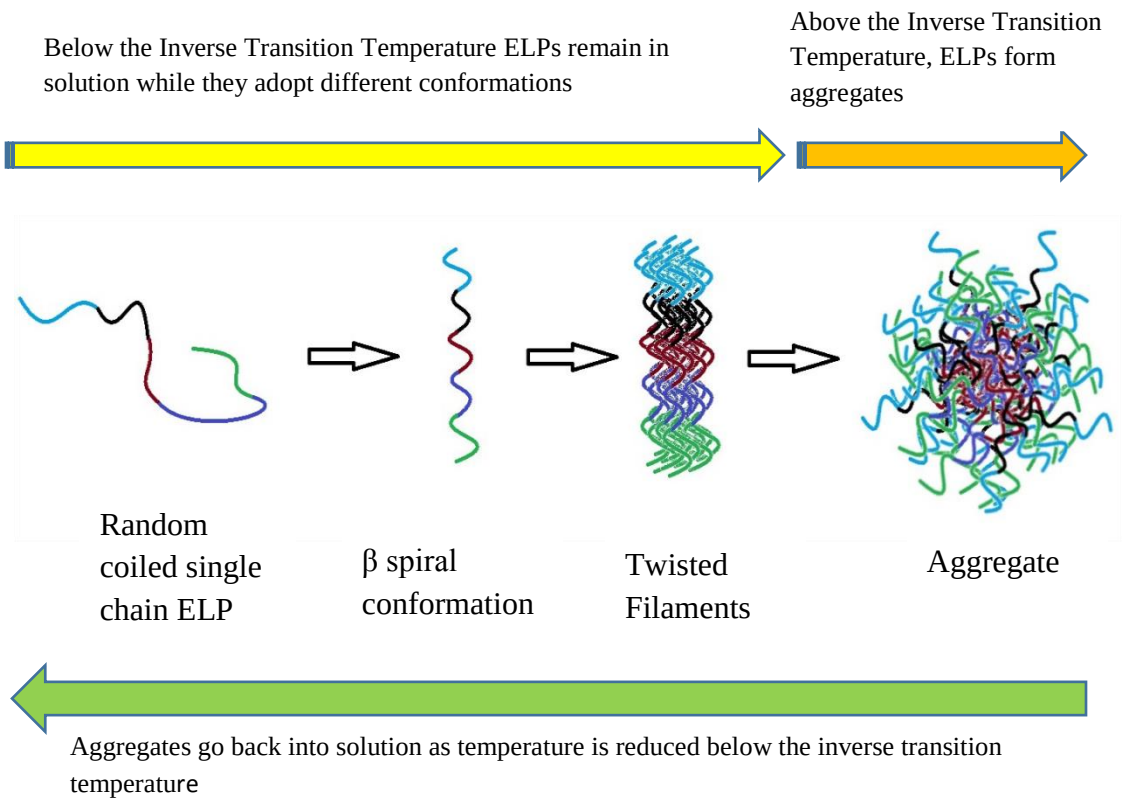

Figure 2.1 Formation of aggregates by single chain ELPs, as originally proposed by Urry et al [3]. Figure is a modified version of that drawn by Kowalczyk et al [10].

2.2.2 ELP coblock polymers form aggregates via a "micelle" intermediate

An amphiphilic ELP chain which was designed to have a hydrophobic domain and a hydrophilic domain was first reported by Lee et al [11]. The hydrophobic sequence was designed as follows: $[Val\text{-}Pro\text{-}Gly\text{-}Glu\text{-}Gly(Ile\text{-}Pro\text{-}Gly\text{-}Ala\text{-}Gly)_4]_{14}$ while the hydrophilic sequence was designed as follows: $[Val\text{-}Pro\text{-}Gly\text{-}Phe\text{-}Gly(Ile\text{-}Pro\text{-}Gly\text{-}Val\text{-}Gly)_4]_{16}$. The difference in polarity of the guest residues results in a drastic difference in phase behavior between the domains which causes the ELP chain to form micelles in aqueous solutions above the inverse temperature of the hydrophobic block, but below the

inverse temperature of the hydrophilic block. When the temperature rises above the transition temperature of the hydrophilic block, the amphiphilic ELP chains collapse into an aggregate, as shown in Figure 2.2

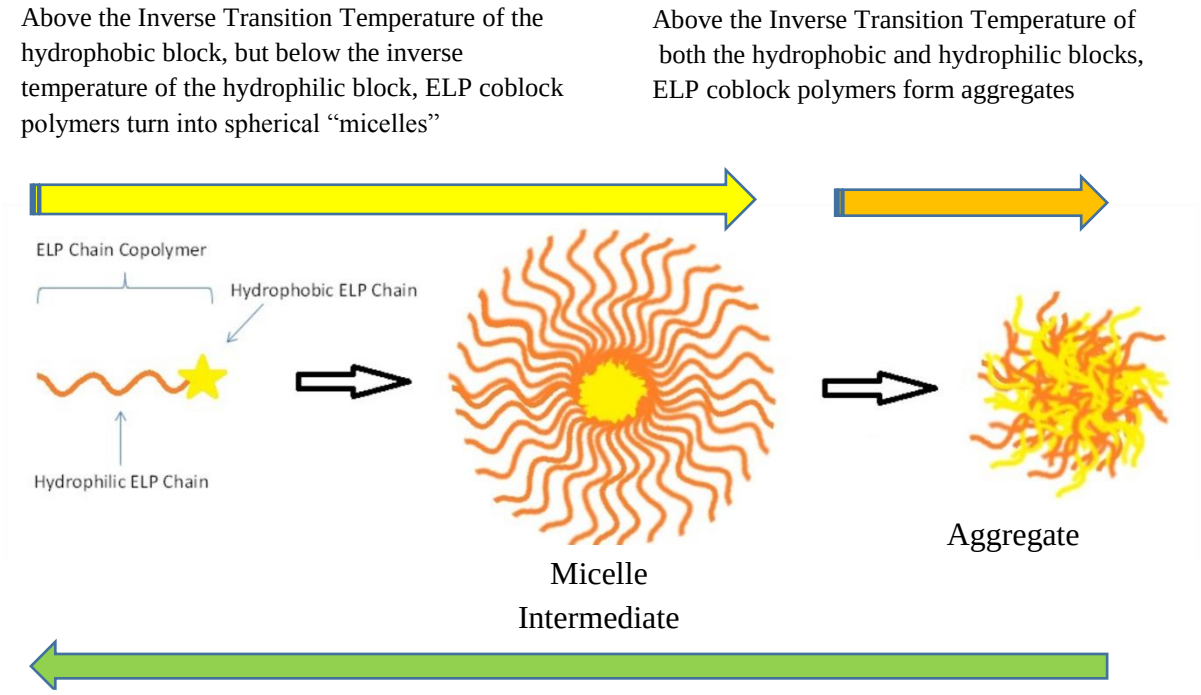

Figure 2.2. Formation of aggregates by ELP coblock polymers. Figure is a modified version of that drawn by Hassouneh et al [12]. Reprinted (adapted) with permission from [12] . Copyright (2015) American Chemical Society.

2.3 PART 2: ELASTIN-LIKE PEPTIDES AS FUSION PARTNERS IN DIFFERENT APPLICATIONS

In 1999, Chilkoti and coworkers discovered that the inverse transition property of an ELP is maintained when the ELP motif is fused to another protein [6]. Since then, the use of

ELPs as fusion partners has been reported for several purposes such as protein purification, improvement of the half-life of target proteins, increase in expression level/yields of desired proteins, as macromolecular carriers for the delivery of proteins, and for thermal targeting for cancer treatments. Below, we review some of the existing ELP fusion proteins to date, grouped by the host cell system used to express the protein and the purpose for using ELP as a fusion partner.

2.3.1 Elastin-Like Peptide Fusion Proteins Expressed in Escherichia coli

In 2005, Massodi et al [13] showed that cell penetrating peptides can be fused to elastin like peptides, and the fusion protein can be used as potential vehicles for delivering drugs to cells. Different cell penetrating peptides (penatratin peptide (Antp)), Tat peptide and MTS, a hydrophobic peptide) were fused to the N-terminus of an ELP sequence and manufactured using E. coli. The team successfully demonstrated the cellular uptake of the fluorescein labelled CPP-ELP in HeLA cervical carcinoma cells indicating that CPP-ELPs have the potential of delivering therapeutics to cells, especially cancerous cells. To prove this, the team fused a kinase inhibitor, p21, known to be toxic to SKOV-3 cells, to the C-terminus of Antp-ELP (Antp-ELP-p21) and monitored its uptake in the SKOV-3 cells. The fusion protein successfully inhibited proliferation of the SKOV-3 cells.

In 2007, Kang et al [14] demonstrated the use of different chain lengths of ELP to purify levansucrase, an enzyme that catalyzes the synthesis of levan from sucrose. (Levan is a natural homopolymer of fructose). Levansucrase-ELP fusion gene was constructed in a pUC19 vector and expressed using E. coli DH5α. The team successfully purified the

fusion protein and showed that the activity of the levansucrase was maintained despite the fusion to ELP. In the same year, Kim et al [15] reported the fusion ELP to interleukin-1 receptor antagonist (IL-1ra) to allow for the cytokine to be immobilized on self-assembled monolayers and to determine whether the immobilized IL-1ra would induce changes in the inflammatory profile of target cells. The team showed that IL-1ra – ELP caused monocytes stimulated with lipopolysaccharide (LPS) to decrease their expression of pro-inflammatory cytokines and to increase the secretion of anti-inflammatory cytokines.

In 2010, Hu et al [16] described the fusion of an antimicrobial peptide, Halocidin18 (Hal18), to an ELP in an attempt to improve the expression level and simplify the purification process of the antimicrobial peptide. The team designed different ELP sequences using Valine, Alanine and Glycine as guest residues in a 5:2:3 ratio and fused that to Halocidin18 (Hal18), an 18 amino acid antimicrobial peptide. The team reported that by using ELP as a purification tag, it allowed about 69 mg of Hal18 to be produced from a 1 liter E.coli culture, which is much higher than the 29 mg of protein obtained when polyhistidine was used as a purification tag. The final Hal18 product was cleaved off of the ELP using hydroxylamine, and exhibited antimicrobial activity towards Micrococcus luteus and antifungal activity against Pichia pastoris.

In 2011, Koria et al [17] demonstrated the fabrication of a fusion protein comprised of elastin-like peptide and keratinocyte growth factor (KGF) for use in skin wound healing. When tested in vitro, the fusion protein, which was expressed in E. coli retained the performance characteristics of both KGF and ELP. The team showed that KGF-ELP fusion protein nanoparticles enhanced reepithelialization and granulation of an excisional

wound made on a diabetic mice. In the same year, Simnick et al [18] reported the fusion of an NGR ligand to an ELP diblock copolymer with composition ELP $[V_1A_8G_7]_{64}$/ELP $[V]_{90}$ that self assembles into monodisperse micelles. NGRs are peptides containing Asparagine-Glycine-Arginine motifs that are known to target CD13 isoforms in tumor vessels [19]. By fusing the NGR ligand to an ampiphilic diblock copolymer, and subsequently inducing micelle formation, multiple NGR ligands would be presented to the CD13 receptor. Multivalent binding of NGR to CD13 proceeds with much higher affinity compared to monovalent binding. Using fluorescent reporters, the team showed that NGR fused to the diblock copolymer resulted in greater accumulation in tumors generated in nude mice compared to the low affinity which had been previously reported for the NGR peptide in linear form [20]

In 2012, Moktan et al [21] fused the KLAKLAKKLAKLAK peptide (KLAK) to the C-terminus of an ELP, which was attached to a cell penetrating peptide, SynB1 at its N-Terminus (SynB1-ELP-KLAK). KLAK is known to induce apoptosis by disrupting the mitochondria of cells, and as such is a promising molecule for cancer treatment. Based on previous work (described above) which showed that fusing cancer cell penetrating peptides to ELPs led to an improvement in cancer cell inhibition in response to hyperthermia, the group monitored the cytotoxic effect of SynB1-ELP-KLAK on human breast cancer cell lines. The team noted that the fusion protein was cytotoxic against the cancer cells, and the potency was enhanced with hyperthermia.

In 2013, Amiram et al [22] showed that fusion of an ELP to glucagon-like peptide-1 (GLP1), a type-2 diabetes drug, enhanced its stability profile. Although GLP1 is potentially useful as a treatment against diabetes, its therapeutic benefit is severely

limited by its short in vivo half-life. The team demonstrated that GLP1-ELP was more stable in neutral endopeptidase, a protease that is known to degrade GLP-1 in vivo, as compared to free GLP1. When used in mice, the group reported that a single injection of the GLP1-ELP fusion protein was able to reduce blood glucose levels in mice for 5 days, which is about 120 times longer than what was observed with free GLP1.

2.3.2 Elastin-Like Peptide Fusion Proteins Expressed in Mammalian and Plant Cells

In 2006, Lin et al [23] reported the fusion of mini-glycoprotein130 to 100 ELP repeats, and its expression in tobacco leafs. Glycoprotein 130 blocks interleukin-6 (IL-6) signaling which is known to promote the pathology of autoimmune diseases such as Crohn and rheumatoid arthritis in murine models Mini gp130 comprises the first three (cytokine binding) domains of full-length gp130. Because its manufacture is expensive, ELP tagging was specifically used to decrease manufacturing costs. Furthermore, tobacco plant leafs are 10-50 times cheaper than E.coli as a production system. The team noted that fusing mini gp130 to ELP allowed 141 μg of purified protein per gram of tobacco leaf weight to be produced.

In 2008, Floss et al [24] reported the fusion of an ELP to an anti-HIV-1 monoclonal antibody 2F5. The 2F5 antibody, which is being evaluated for the treatment of HIV, has been expressed in both transgenic tobacco plants and Chinese hamster ovary cells; the proteins expressed from both culture systems were determined to have similar quality attributes and functionality. However, the team notes that the accumulation and yield of 2F5 produced in the plant cells were significantly lower than in mammalian cells. As such they tagged ELP to 2F5 to evaluate the potential increase in accumulation of the 2F5

antibody and more importantly to investigate if the post translational modifications of 2F5 (glycosylation) typically seen from mammalian cells will be maintained when it is tagged with the ELP, and produced in plant cells. The team observed that attaching ELP to 2F5 significantly increased the amount of the antibody produced from the tobacco leaf cells compared to the antibody that lacked the ELP, an observation which has also been reported by several researchers, including Scheller et al [25] and Patel et al [26], and is attributed to the ability of the ELP tag to protect the target protein from hydrolysis and from proteolytic enzymes, thereby increasing the protein yield [27]. They also demonstrated that the fusion of 2F5 antibody's light and heavy chains to ELP did not impact the attachment of oligosaccharides to its glycosylation site, and that the glycosylation patterns as well as the binding kinetics of 2F5-ELP made in plants was similar to 2F5 antibody made in both Chinese hamster ovary (CHO) cells and plant cells.

In 2009, Floss et al [28] showed that the anti-HIV-1 antibody 2G12 can be successfully fused to ELP, produced using tobacco cells, and that the final product shows similar activity and glycosylation profile to native 2G12 which is normally produced in CHO cells. Again in 2010, [29] published their work on the fusion of mycobacterial antigens (TBAg) against tuberculosis (Ag85B and ESAT-6) to ELP and subsequent expression in transgenic tobacco plants. ELP was tagged to TBAg and expressed with a plant based system in an attempt to reduce the vaccine's production cost. When the fusion protein was used in both mice and pig models, the team noted that the fusion protein was able to trigger antibodies and T-cells recognizing the Ag85B and ESAT-6 in the fusion protein.

In 2011, Phan et al [30] demonstrated the successful fusion of ELP to two avian flu H5N1 antigens and their successful expression using transgenic tobacco plants. They used a fluorescence-based assay to confirm the activity of the antigens. In subsequent work published in 2013 [31], the team also demonstrated that the H5-ELP fusion proteins provided effective protection against infection.

2.4 PART 3: ELPS AS TAGS FOR PROTEIN PURIFICATION VERSUS EXISTING PURIFICATION TAGS

As shown in Table 2.1, several different fusion tags are commercially available to standardize purification methods for recombinant proteins. Among several disadvantages highlighted in Table 2.1, one common drawback with the existing purification tags is the fact that most of them rely on affinity chromatography, which is costly, especially when performed on a large scale.

In contrast, ELPs used as purification tags rely on a simpler and straightforward purification procedure, and as a result can significantly reduce the production costs of recombinant proteins. The purification of ELP fusion proteins involves a warm up step to induce ELP-mediated aggregation and precipitation, a centrifugation step, and a re-dissolution of the precipitated protein in a desired buffer as shown in Figure 2.3. Two to three rounds of the warming-centrifugation-resolubilization steps are generally sufficient to purify the desired protein. ELPylation eliminates the need for expensive chromatography equipment, resins and reagents, and as such represents a very cost effective and an easy to scale up purification process.

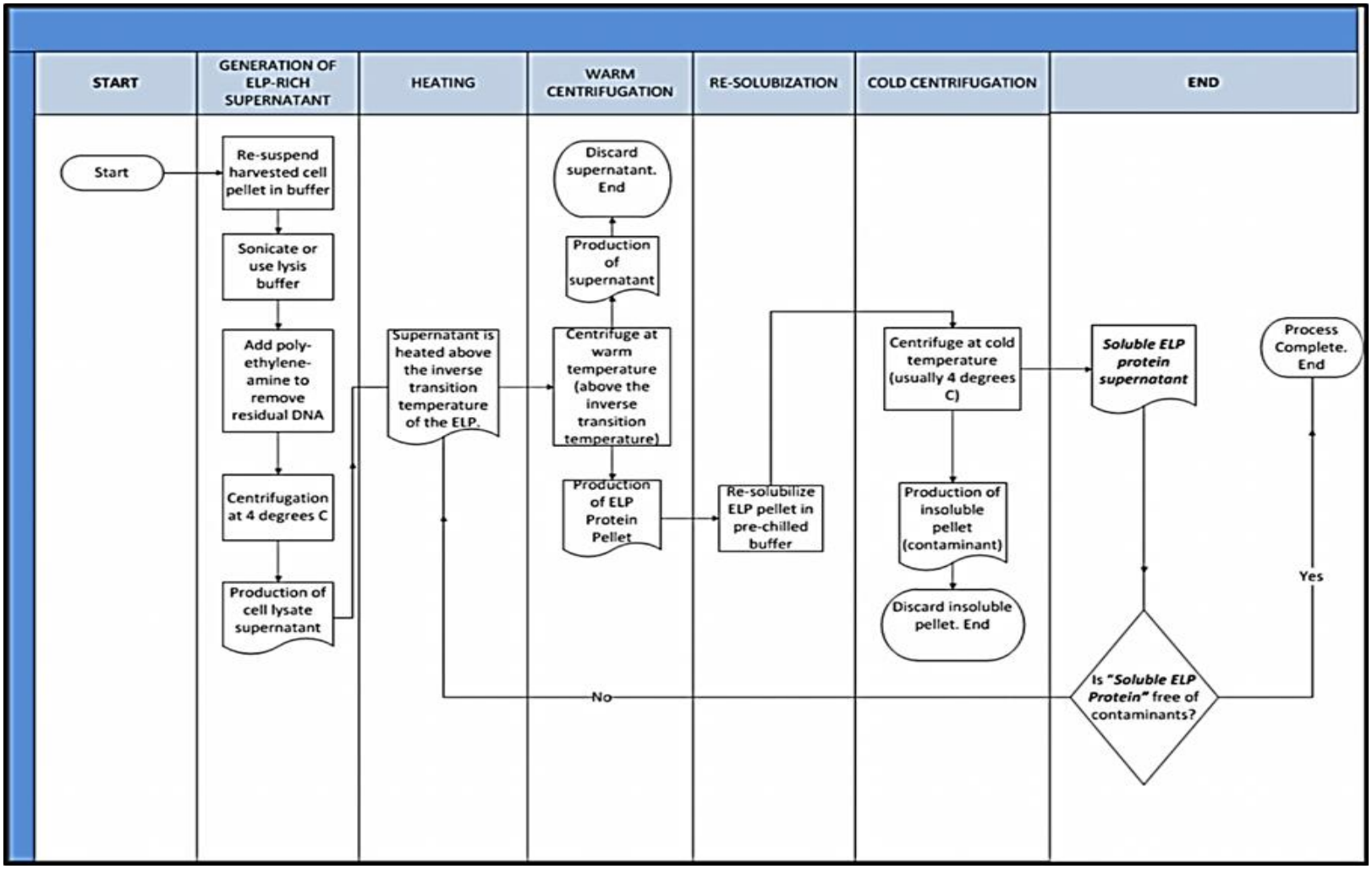

Figure 2.3. Purification of ELP proteins using its inverse phase transition property

Table 2.1: Some Pitfalls of Existing Tags Used for Biopharmaceutical Purification

Purification Tag	Mechanism of action	Disadvantages	References
Maltose Binding Protein (MBP)	Affinity chromatography The maltose binding protein has affinity for immobilized amylose resin in a column	• Resin is **expensive** • Chromatography using MBP tag **doesn't yield samples with high purity** and additional purification techniques need to be employed	[32], [33]
Poly histidine tag (HIS)	Affinity chromatography The histidine moiety of the protein binds to immobilized metals such as nickel or cobalt in a column.	• There is potential for a **protein with his tag to form dimers or trimers** due to the existence of metal ions • There is potential for the **co-elution of his-tagged protein of interest with other naturally existing proteins** that have the histidine group	[34], [35]
Poly arginine tag	Cation exchange chromatography /affinity chromatography Proteins with the arginine tag are purified using a cation exchange resin SP-Sephadex. The arginine residues can subsequently be removed using carboxypeptidase B	• Poly arginine tags might have an **impact on the tertiary structure of proteins with hydrophobic C-terminal regions**. • **Cleavage of the tag** by carboxypeptidase is usually **poor and not specific**	[36]
Glutathione S-transferase (GST)	Affinity chromatography The GST tag has an affinity for immobilized glutathione	• GST has **poor solubility** and when fused to proteins usually causes the fusion protein to go into inclusion bodies	[37]
FLAG tag	Affinity chromatography Chromatography column is filled with Anti-FLAG resin. The FLAG tag binds to the antibody	• **Low binding capacity** of the FLAG tag, resulting in **expensive scale up costs**.	[38]
Strep-tag	Affinity chromatography The Strep tag on the fusion protein binds to Strep-Tacin which is immobilized on a column	• Resin is **expensive**	[39]

2.5 PART 4: CONSIDERATIONS FOR TRANSLATING ELPYLATION TO BIOPHARMACEUTICAL PROTEIN PURIFICATION

Despite its potential to significantly reduce the production costs of proteins, translating ELPylation to biopharmaceutical manufacturing still remains a challenge for several reasons, some of which we highlight below

2.5.1 Choice of Host Cell

As discussed above, E.coli has been the primary expression system for most ELP fusion proteins which can be expressed in high yield by these cells [40]; however, these cells lack eukaryotic post-translational systems, bacterial cell walls contain pro-inflammatory compounds (i.e. endotoxin) that must be removed from the product, and the expressed protein may sometimes lead to the formation of inclusion bodies which increases processing needed for extraction of the protein from the bacteria [41]. For these reasons, the preferred host cell expression system for biopharmaceutical protein manufacturing is mammalian cells. In particular, Chinese hamster ovary (CHO) cells are especially popular because of their ability to produce more human-compatible post-translational modifications [42]. The CHO cell is a well-established and accepted cell line by regulatory bodies for the production of therapeutic glycoproteins [42]. Table 2.2 is a summary of all the biologic products that have been approved by the United States Food and Drug Administration Center for Drug Evaluation and Research for the period from 2010 to 2014. As shown in the table, about 70% of the approved biologics were made in mammalian host cell expression systems. While one abstract has been published on the attempted production of an ELP fusion protein expressed in CHO cells (Wu and Wood, AIChE 2008 Annual Meeting), limited information was provided, although the authors

acknowledged that the ELP was found to be genetically unstable after incorporation into the CHO cell genome. Indeed there could be potential challenges in incorporating the tandem repeats of ELP into a CHO cell genome or into a mammalian expression system due to the higher possibility for homologous recombination, which is deficient in most E.coli strains used for protein expression [40, 41]. A breakthrough in this research area could potentially open up this ELPylation technology to a wide range of biopharmaceutical products. One potential solution to address this genetic instability could be transient transfection of the ELP fusion protein into the CHO cell host system. This could allow for a fully post-translationally modified fusion protein without the need to develop a stable cell line. However, this is far from perfect since inherent variability in the efficiency of transfection will likely increase batch-to-batch variation

Table 2.2: Summary of biologics approved by the US FDA Center for Drug Evaluation and Research from 2010 to 2014

Trade name	Company	Approval date	Expression cell	Trade name	Company	Approval date	Expression cell
Blincyto	Amgen	12//2014	**CHO cells**	Zaltrap	Sanofi-Aventis U.S. LLC	08/2012	**CHO cells**
Opdivo	Bristol-Myers Squibb	12//2014	**CHO cells**	Granix (Former Neutroval)	Sicor Biotech UAB (Teva Pharmaceuticals Industries Ltd.	08/2012	E.coli
Keytruda	Merck Sharpe & Dohme Corp	09/2014	**CHO cells**	Perjeta	Genentech Inc.	06/2012	**CHO cells**
Trulicity	Eli Lilly & Company	09/2014	**CHO cells**	Voraxaze	BTG International Inc.	01/2012	E.coli
Plegridy	Bioden Idec	08/2014	**CHO cells**	Erwinaze	Eusa Pharma (USA) Inc.	11/2011	Erwinia chrysanthemi
Entyvio	Takeda Pharmaceuticals	05/2014	**CHO cells**	Eylea	Regeneron Pharmaceuticals Inc.	11/2011	**CHO cells**
Tanzeum	GlaxoSmithKline	04/2014	Yeast	Adcetris	Seattle Genetics, Inc.	08/2011	**NS0 cell**
Cyramza	Eli Lilly and Company	04/2014	**NS0 cells**	Nulojix	Bristol-Myers Squibb Company	06/2011	**CHO Cells**
Sylvant	Janssen Biotech	04/2014	**CHO cells**	Yervoy	Bristol-Myers Squibb Company	03/2011	**CHO cells**
Vimizim	Biomarin Pharmaceutical	02/2014	**CHO cells**	Benlytsa	Human Genome Sciences Inc.	03/2011	**NS0 cell**
Myalept	Amylin Pharmaceuticals	02/2014	E.coli	Krystexxa	Savient Pharmaceuticals, Inc.	09/2010	E.coli
Gazyva	Genentech	11/2013	**CHO cells**	Xeomin	Merz Pharmaceuticals GMBH	07/2010	Clostridium botulinum serotype A
Simponi	Janssen Biotech	07/2013	**Murine hybridoma cells**	Prolia	Amgen, Inc	06/2010	**CHO cells**
Kadcyla	Genentech	02/2013	**CHO cells**	Lumizyme	Genzyme Corporation	05/2010	**CHO cells**
Abthraxtm	Human Genome Sciences Inc.	12/2012	**Murine cells**	Xiaflex	Auxilium Pharmaceuticals, Inc.	02/2010	Clostridium histolyticum

2.5.2 Potential Impact to Post Translational Modifications

Biopharmaceutical proteins often carry several post translational modifications. For example, Advate® (octocog alfa) from Baxter is known to be heavily glycosylated, with 25 N-linked and 12 O-linked glycosylation sites [43]. Interrupting the post translational modification of such proteins typically leads to improperly folded proteins, with little to no activity and a potential for safety and immunogenicity problems [44].Therefore, it is important to demonstrate that post-translational modifications of the target/desired proteins are not impeded or altered when fused to ELP. This concern was addressed in plant cells by Floss et al [24] who expressed an anti-human HIV-1 monoclonal antibody to ELP in tobacco leaf cells. The goal of their work was to find out what the impact of the fusion of the ELP to a heteromultimeric protein, such as an antibody, would have on post-translational modifications. Mass spectrometry was used to quantify the N-linked glycans attached the glycosylation site (Asparagine 297) on the antibody, and determined that the N-glycan profiles of the anti-HIV-ELP protein were very similar to the free anti-HIV protein, thus demonstrating that there was no interference of the ELP to the attachment of oligosaccharides to Asparagine 297. More generally, studies to assess whether or not the ELP tag can cause steric hindrance to glycan transferase or any other post-translational modification systems would be important to translate the ELP technology to biopharmaceutical proteins.

2.5.3 Considerations for Large Scale Manufacturing

2.5.3.1 Lysis Step

For the ELP proteins expressed using E. coli or plant based host systems, protein products are trapped within the cells and recovering the protein involves using sonication

or chemical-induced lysis. For large scale manufacturing, secreted production of the ELP fusion protein might be desirable because it removes the cumbersome lysis step. It also enables more different means of mass culturing; besides large batch fermenters, hollow fiber systems and continuous culture methods may be used. As such, one consideration for the application of ELPylation to the roughly 30% of biopharmaceutical proteins that are currently manufactured in bacteria or plant cells, is to add a signal peptide to enable secretion, and to design the ELP tag and temperature of the fermenter below the inverse transition temperature of the fusion protein. The latter would ensure that the protein will stay in solution during the expression phase.

2.5.3.2 Temperature Cycling (Precipitation of Target Protein and Resolubilization)

ELP fusion proteins are purified through a temperature dependent reversible cycle where proteins change from soluble monomers to insoluble aggregates. The final purified form of the protein is the soluble monomer which is usually stored at or below refrigeration temperatures similar to other proteins. Setting up two bioreactors to perform the temperature cycling at industrial scale should not be a concern since large scale bioreactors are equipped with chillers/heat exchangers with efficient cooling and heating capacities. However, a potential concern with precipitating the target protein is the possibility for some aggregates to remain even after resolubilization. While considerable work has been done confirming that proteins resolubilize when the temperature of the batch is dropped below its inversion temperature, any residual aggregates will have to be completely removed, as they may trigger undesired immune responses.

2.5.3.3 Recovery of Precipitated Protein

The ELP technology generally relies on batch centrifugation for recovery of the precipitated target protein, which is generally not scalable to manufacturing levels. The batch centrifugation process can be adapted to a continuous flow ultracentrifuge, which can separate a wide range of particles including nanoparticles, and is widely used for cGMP industrial purification of viruses and proteins [45]. For example, two continuous flow ultracentrifuges can be set up consecutively with two bioreactors and the pair preset to two temperatures (one below and one above the inverse transition temperature of the ELP fusion protein) to allow for two rounds of phase transition purification to be performed. Alternatively, a continuous flow membrane filtration system could be used to recover the precipitated protein, in lieu of batch centrifugation.

2.5.3.4 Volume Considerations

For purification by ELPylation to be successful, protein concentrations need to be at least 100 µg of soluble expressed protein per liter of culture [46]. Since the amount of medium used for batch fermentation of mammalian cells is typically large, if the protein is expressed at a very low level, a volume reduction step may be needed to make it feasible to use the temperature phase transition purification strategy. For example, a unidirectional flow system such as tangential flow filtration equipment could be used as an initial concentration step to concentrate the cell culture medium prior to initiation of the temperature phase transition. Alternatively, it has been shown that free ELP will co-aggregate with the ELPylated product; thus by adding excess free ELP it may be possible to precipitate low levels of protein by phase transition [46].

2.5.3.5 Potential Impact to Yield or Activity

Proteins which have been purified using the ELP technology typically have reported yields of up to 500 mg/L [9], which is comparable to the titers obtained for some biopharmaceutical proteins. However, some researchers have highlighted that the yields for ELP fusion proteins were generally higher when the ELP tag was placed at the C-terminus instead of the N-terminus [47]. ELP tags, when fused at the C-terminus of target proteins, resulted in approximately 50 to 90% higher yield of protein than when fused at the N-terminus of the target protein [48]. Yet, the choice of fusing a specific purification tag to either the N- or C- terminus of a target protein will depend on the effect on the biochemical properties of the target protein. For obvious reasons, the purification tag is preferably placed as far as possible from the protein's receptor binding region. If the latter is far from either the N- or C- terminus, either end may be used. This preferred unidirectional positioning of the ELP purification tag could potentially be a limiting factor if the specific biopharmaceutical protein has its binding epitope at or near the C-terminus, and will need to be further investigated. As such, standardization of the positioning of the ELP tag based on the properties of the target protein may need to be further developed to allow for a multitude of biologicals to be purified using this technology.

2.5.3.6 Cleavage of the ELP Fusion Tag – Potential Immunogenicity or Activity Concerns

Similar to other purification tags, ELP tags can be cleaved off from the target protein after purification, if the ELP tag is not desired in the final form of the protein. This is easily achieved by engineering a protease cleavage site between the ELP tag and

the specific target protein. Several researchers have reported the insertion of tobacco etch virus (TEV) or thrombin recognition sites in the fusion protein, which have easily been cleaved off with the relevant proteases along with the ELP tag after the final purification step. In these cases, once the purification process using the ELP phase transition property is completed, the protease manufacturer's step for cleaving off the protease site is followed and an additional temperature cycling step incorporated to remove the ELP-protease cleavage site from the final target protein. While the process is straightforward, residual amino acids from the protease sites could remain on the target protein which could cause immunogenicity issues or could influence activity. As such, the impact of residual amino acids from the typical protease cleavable sites used for ELP fusion proteins needs to be thoroughly understood.

An alternative to using TEV and thrombin recognizable sequences as fusion linkers is to use self-cleaving inteins [49]. The intein (and the ELP tag) can be triggered to split from the purified target protein with a change in pH or an addition of thiol. With this approach, any potential for the pH change or thiol addition to impact the physicochemical properties of the final protein will need to be assessed.

2.5.3.7 Other Considerations – ELP Fusion Scaffolds

As an alternative to using ELP as a fusion partner to the target protein for purification, some researchers have also developed ELP affinity scaffolds such as ELP-Protein G, ELP-Protein L, ELP-z and ELP-zz for potential purification of immunoglobulins by affinity precipitation [50], [51]. This technology has the potential to resolve some of the above mentioned issues of using ELP as a purification tag for biopharmaceutical purification. For example, since the ELP scaffolds are not fused to the

target molecules, concerns about incorporating an ELP fusion protein into mammalian host cells and the potential for the ELP tag to impact post translational modification are eliminated.

2.6 CONCLUSIONS

The thermal responsiveness of elastin like peptides, coupled with their non-toxicity, biocompatibility and non-immunogenicity make them a desirable class of fusion tags for several applications such as targeted drug delivery, enhancing the half-life of drugs and more significantly, for protein purification. Although numerous works have been published showing the effectiveness of ELP fusion tags for protein purification, the technology has not yet been adapted to make it feasible for use in biopharmaceutical protein purification.

Future approaches that seek to adapt the ELP technology to the purification needs of the biotech industry, should include

- tailoring it to proteins manufactured in CHO cells,
- ensuring that the ELP tag does not impact the post translational modification, yield and activity of the target protein ,
- assessing the scalability of the technology to the equipment, volumes and systems used in large scale protein purification,
- removing residual protein aggregates to eliminate the possibility of unwanted immune responses,
- understanding the impact of residual amino acids (which could remain after cleavage of the ELP tag) on the activity and immunogenicity of the target protein.

The above adaptations will allow ELPylation to be attractive to several biopharmaceutical companies who spend immense amounts of money on their protein therapeutics purification.

2.7 REFERENCES

[1] B. Vrhovski, A.S. Weiss, Biochemistry of tropoelastin, Eur J Biochem, 258 (1998) 1-18.

[2] M.F. Shamji, H. Betre, V.B. Kraus, J. Chen, A. Chilkoti, R. Pichika, K. Masuda, L.A. Setton, Development and Characterization of a Fusion Protein Between Thermally Responsive Elastin-like Polypeptide and Interleukin-1 Receptor Anatagonist, Arthritis and Rheumatism, 56 (2007) 3650-3661.

[3] D.W. Urry, T.L. Trapane, K.U. Prasad, Phase-structure transitions of the elastin polypentapeptide-water system within the framework of composition-temperature studies, Biopolymers, 24 (1985) 2345-2356.

[4] J.R. McDaniel, D.J. Callahan, A. Chilkoti, Drug Delivery to solid tumors by elastin-like polypeptides, Advanced Drug Delivery Reviews, 62 (2010) 1456-1467.

[5] S.M. Hearst, Q. Shao, M. Lopez, D. Raucher, P.J.S. Vig, The design and delivery of PKA inhibitory polypeptide to treat SCA1, Journal of Neurochemistry, (2014).

[6] D.E. Meyer, A. Chilkoti, Purification of recombinant proteins by fusion with thermally-responsive polypeptides, Nat Biotechnol, 17 (1999) 1112-1115.

[7] M. Saraswat, L. Musante, A. Ravida, B. Shortt, B. Byrne, H. Holthofer, Preparative purification of recombinant proteins: current status and future trends, Biomed Res Int, 2013 (2013) 312709.

[8] D.W. Urry, Free energy transduction in polypeptides and proteins based on inverse temperature transitions, Prog Biophys Mol Biol, 57 (1992) 23-57.

[9] W. Hassouneh, T. Christensen, A. Chilkoti, Elastin-like polypeptides as a purification tag for recombinant proteins, Curr Protoc Protein Sci, Chapter 6 (2010) Unit 6 11.

[10] T. Kowalczyk, K. Hnatuszko-Konka, A. Gerszberg, A.K. Kononowicz, Elastin-like polypeptides as a promising family of genetically-engineered protein based polymers, World Journal of Microbiology and Biotechnology, 30 (2014) 2141-2152.

[11] T.A.T. Lee, A. Cooper, R.P. Apkarian, V.P. Conticello, Thermo-reversible self-assembly of nanoparticles derived from elastin-mimetic polypeptides, Advanced Materials, 12 (2000) 1105-+.

[12] W. Hassouneh, E.B. Zhulina, A. Chilkoti, M. Rubinstein, Elastin-like Polypeptide Diblock Copolymers Self-Assemble into Weak Micelles, Macromolecules, 48 (2015) 4183-4195.

[13] I. Massodi, G.L. Bidwell, 3rd, D. Raucher, Evaluation of cell penetrating peptides fused to elastin-like polypeptide for drug delivery, J Control Release, 108 (2005) 396-408.

[14] H.J. Kang, J.H. Kim, W.J. Chang, E.S. Kim, Y.M. Koo, Heterologous expression and optimized one-step separation of levansucrase via elastin-like polypeptides tagging system, J Microbiol Biotechnol, 17 (2007) 1751-1757.

[15] D.H. Kim, J.T. Smith, A. Chilkoti, W.M. Reichert, The effect of covalently immobilized rhIL-1ra-ELP fusion protein on the inflammatory profile of LPS-stimulated human monocytes, Biomaterials, 28 (2007) 3369-3377.

[16] F. Hu, T. Ke, X. Li, P.H. Mao, X. Jin, F.L. Hui, X.D. Ma, L.X. Ma, Expression and purification of an antimicrobial peptide by fusion with elastin-like polypeptides in Escherichia coli, Appl Biochem Biotechnol, 160 (2010) 2377-2387.

[17] P. Koria, H. Yagi, Y. Kitagawa, Z. Megeed, Y. Nahmias, R. Sheridan, M.L. Yarmush, Self-assembling elastin-like peptides growth factor chimeric nanoparticles for the treatment of chronic wounds, Proc Natl Acad Sci U S A, 108 (2011) 1034-1039.

[18] A.J. Simnick, M. Amiram, W. Liu, G. Hanna, M.W. Dewhirst, C.D. Kontos, A. Chilkoti, In vivo tumor targeting by a NGR-decorated micelle of a recombinant diblock copolypeptide, J Control Release, 155 (2011) 144-151.

[19] R. Soudy, S. Ahmed, K. Kaur, NGR Peptide Ligands for Targeting CD13/APN Identified through Peptide Array Screening Resemble Fibronectin Sequences, Acs Combinatorial Science, 14 (2012) 590-599.

[20] G. Colombo, F. Curnis, G.M. De Mori, A. Gasparri, C. Longoni, A. Sacchi, R. Longhi, A. Corti, Structure-activity relationships of linear and cyclic peptides containing the NGR tumor-homing motif, J Biol Chem, 277 (2002) 47891-47897.

[21] S. Moktan, D. Raucher, Anticancer Activity of Proapoptotic Peptides is Highly Improved by Thermal Targeting using Elastin-like Polypeptides, International Journal of Peptide Research and Therapeutics, 18 (2012) 227-237.

[22] M. Amiram, K.M. Luginbuhl, X. Li, M.N. Feinglos, A. Chilkoti, A depot-forming glucagon-like peptide-1 fusion protein reduces blood glucose for five days with a single injection, J Control Release, 172 (2013) 144-151.

[23] M. Lin, S. Rose-John, J. Grotzinger, U. Conrad, J. Scheller, Functional expression of a biologically active fragment of soluble gp130 as an ELP-fusion protein in transgenic plants: purification via inverse transition cycling, Biochemical Journal, 398 (2006) 577-583.

[24] D.M. Floss, M. Sack, J. Stadlmann, T. Rademacher, J. Scheller, E. Stoger, R. Fischer, U. Conrad, Biochemical and functional characterization of anti-HIV antibody-ELP fusion proteins from transgenic plants, Plant Biotechnol J, 6 (2008) 379-391.

[25] J. Scheller, M. Leps, U. Conrad, Forcing single-chain variable fragment production in tobacco seeds by fusion to elastin-like polypeptides, Plant Biotechnol J, 4 (2006) 243-249.

[26] J. Patel, H. Zhu, R. Menassa, L. Gyenis, A. Richman, J. Brandle, Elastin-like polypeptide fusions enhance the accumulation of recombinant proteins in tobacco leaves, Transgenic Res, 16 (2007) 239-249.

[27] A.J. Conley, J.J. Joensuu, A.M. Jevnikar, R. Menassa, J.E. Brandle, Optimization of elastin-like polypeptide fusions for expression and purification of recombinant proteins in plants, Biotechnol Bioeng, 103 (2009) 562-573.

[28] D.M. Floss, M. Sack, E. Arcalis, J. Stadlmann, H. Quendler, T. Rademacher, E. Stoger, J. Scheller, R. Fischer, U. Conrad, Influence of elastin-like peptide fusions on the quantity and quality of a tobacco-derived human immunodeficiency virus-neutralizing antibody, Plant Biotechnol J, 7 (2009) 899-913.

[29] D.M. Floss, M. Mockey, G. Zanello, D. Brosson, M. Diogon, R. Frutos, T. Bruel, V. Rodrigues, E. Garzon, C. Chevaleyre, M. Berri, H. Salmon, U. Conrad, L. Dedieu, Expression and Immunogenicity of the Mycobacterial Ag85B / ESAT-6 Antigens Produced in Transgenic Plants by Elastin-Like Peptide Fusion Strategy, Journal of Biomedicine and Biotechnology, 2010 (2010).

[30] H.T. Phan, U. Conrad, Membrane-based inverse transition cycling: an improved means for purifying plant-derived recombinant protein-elastin-like polypeptide fusions, Int J Mol Sci, 12 (2011) 2808-2821.

[31] H.T. Phan, J. Pohl, D.M. Floss, F. Rabenstein, J. Veits, B.T. Le, H.H. Chu, G. Hause, T. Mettenleiter, U. Conrad, ELPylated haemagglutinins produced in tobacco plants induce potentially neutralizing antibodies against H5N1 viruses in mice, Plant Biotechnol J, 11 (2013) 582-593.

[32] B.P. Austin, Nallamsetty, Sreedevi,Waugh, David S., Hexahistidine-Tagged Maltose-Binding Protein as a Fusion Partner for the Production of Soluble Recombinant Proteins in Escherichia coli, in: S.A. Doyle (Ed.) Methods in Molecular Biology: High Throughput Protein Expression and Purification, Humana Press, 2009, pp. 157-172.

[33] S. Raghava, S. Aquil, S. Bhattacharyya, R. Varadarajan, M.N. Gupta, Strategy for purifying maltose binding protein fusion proteins by affinity precipitation, J Chromatogr A, 1194 (2008) 90-95.

[34] S. Magdeldin, A. Moser, Affinity Chromatography: Principles and Applications, InTech, 2012.

[35] J.A. Bornhorst, J.J. Falke, Purification of proteins using polyhistidine affinity tags, Applications of Chimeric Genes and Hybrid Proteins, Pt A, 326 (2000) 245-254.

[36] K. Terpe, Overview of tag protein fusions: from molecular and biochemical fundamentals to commercial systems, Appl Microbiol Biotechnol, 60 (2003) 523-533.

[37] S. Costa, A. Almeida, A. Castro, L. Domingues, Fusion tags for protein solubility, purification and immunogenicity in Escherichia coli: the novel Fh8 system, Front Microbiol, 5 (2014) 63.

[38] A. Einhauer, A. Jungbauer, The FLAG peptide, a versatile fusion tag for the purification of recombinant proteins, J Biochem Biophys Methods, 49 (2001) 455-465.

[39] O. Huber, M. Huber-Wunderlich, Recombinant proteins, in: M. Kastner (Ed.) Protein Liquid Chromatography, Elsevier, Amsterdam, Netherlands, 2000, pp. 557-586.

[40] D.C. Chow, M.R. Dreher, K. Trabbic-Carlson, A. Chilkoti, Ultra-high expression of a thermally responsive recombinant fusion protein in E. coli, Biotechnol Prog, 22 (2006) 638-646.

[41] J.E. Gagner, W. Kim, E.L. Chaikof, Designing protein-based biomaterials for medical applications, Acta Biomater, 10 (2014) 1542-1557.

[42] T. Lai, Y. Yang, S.K. Ng, Advances in Mammalian cell line development technologies for recombinant protein production, Pharmaceuticals (Basel), 6 (2013) 579-603.

[43] G. Walsh, Biopharmaceuticals: Approvals and approval trends in 2004, Biopharm International, 18 (2005) 58-+.

[44] V. Jawa, L.P. Cousens, M. Awwad, E. Wakshull, H. Kropshofer, A.S. De Groot, T-cell dependent immunogenicity of protein therapeutics: Preclinical assessment and mitigation, Clin Immunol, 149 (2013) 534-555.

[45] T. Hahn, D. Courbron, M. Hamer, M. Masoud, J. Wong, K. Taylor, J. Hatch, M. Sowers, E. Shane, M. Nathan, H. Jiang, Z. Wei, J. Higgins, K.-H. Roh, J. Burd, D. Chinchilla-Olszar, M. Malou-Williams, D. Baskind, G. Smith, Rapid Manufacture and Release of a GMP Batch of Avian Influenza A(H7N9) Virus-Like Particle Vaccine Made Using Recombinant Baculovirus-Sf9 Insect Cell Culture Technology, BioProcessing Journal, 12 (2013) 4-17.

[46] T. Christensen, Trabbic-Carlson, Kimberly,Liu, Wenge, Chilkoti, Ashutosh, Purification of recombinant proteins from E. coli at low expression levels by inverse transition cycling, Analytical Biochemistry, 360 (2007) 166-168.

[47] W. Hassouneh, S.R. MacEwan, A. Chilkoti, Fusions of elastin-like polypeptides to pharmaceutical proteins, Methods Enzymol, 502 (2012) 215-237.

[48] T. Christensen, M. Amiram, S. Dagher, K. Trabbic-Carlson, M.F. Shamji, L.A. Setton, A. Chilkoti, Fusion order controls expression level and activity of elastin-like polypeptide fusion proteins, Protein Sci, 18 (2009) 1377-1387.

[49] D.W. Wood, J.A. Camarero, Intein applications: from protein purification and labeling to metabolic control methods, J Biol Chem, 289 (2014) 14512-14519.

[50] J.Y. Kim, A. Mulchandani, W. Chen, Temperature-triggered purification of antibodies, Biotechnol Bioeng, 90 (2005) 373-379.

[51] B. Madan, G. Chaudhary, S.M. Cramer, W. Chen, ELP-z and ELP-zz capturing scaffolds for the purification of immunoglobulins by affinity precipitation, J Biotechnol, 163 (2013) 10-16.

3. CHAPTER 3: The development and characterization of SDF1α-elastin-like-peptide nanoparticles for wound healing

Note: This chapter is reproduced from the following publication **written by Agnes Yeboah**:

Agnes Yeboah, Rick I. Cohen, Renea Faulknor, Rene Schloss, Martin L. Yarmush, Francois Berthiaume. The development and characterization of SDF1α-elastin-like-peptide nanoparticles for wound healing. Journal of Controlled Release (Submitted, 2015)

3.1 INTRODUCTION

In the United States, approximately $25 billion are spent annually on the treatment of chronic skin wounds [1], which are characterized by prolonged and excessive inflammation [2], and are prone to recurrent infections [3]. High levels of proteolytic activity degrade endogenous growth factors [4], resulting in poor angiogenesis, granulation and re-epithelialization [5]. Although this could be remediated by the application of exogenous growth factors at the wound site, potential therapeutic peptides are inactivated by the same proteolytic mechanisms.

Stromal cell-derived factor1 (SDF1), a key mediator of the wound healing response, has been reported by several literature sources to recruit endothelial progenitor cells that proliferate and differentiate into mature vascular endothelium [6, 7], which contributes to the revascularization which is needed to support re-epithelialization [8-10]. Others have suggested that are potentially many different cellular targets for SDF1 [11], making its role in the wound healing process more complicated.

Repeated high doses of topical SDF1, although costly and impractical, can achieve therapeutic efficacy [12]. Methodologies to increase SDF1 stability in vivo include mutating its protease cleavage sites [13-15], engineering derivatives of the molecule with a better stability profile [16, 17], [18] and incorporating it into biomaterials [19-21] or liposomes [22]. Nonetheless, all of these methods require expensive procedures for producing and purifying recombinant proteins.

Elastin-like peptides (ELPs) are nonimmunogenic, non pyrogenenic and biologically compatible [23] derivatives of tropoelastin with pentapeptide repeats of Valine-Proline-Glycine-(Xaa)-Glycine, where Xaa can be any natural amino acid except Proline. ELPs reversibly aggregate into nanoparticles and become insoluble above a transition temperature. ELPs can be also be expressed as fusion proteins together with a wide range of bioactive peptides, in which case they can be used as an inexpensive way to purify the protein [24],[25],[26]. ELP-based fusion proteins, by forming nanoparticles, have been shown to protect biomolecules from proteolysis [27], and can act as "drug depots" that release the biomolecules over an extended period of time [23]. Here, we describe the development and characterization of an SDF1-ELP fusion protein that exhibits in vitro activity similar to that of free SDF, but is much more effective in vivo.

3.2 MATERIALS AND METHODS

3.2.1 Cloning of SDF1-ELP

SDF1-ELP is a fusion protein which consists of the human growth factor SDF1 and an elastin-like peptide (ELP). A pET25B+ plasmid with 50 pentapeptide repeats of ELP as described by Koria et al [28] was used for cloning. The plasmid was obtained from the Center Engineering in Medicine, Massachusetts General Hospital. Sequencing of the

plasmid by Genewiz Inc. indicated the presence of XbaI and NdeI restriction sites at the N-terminus of the ELP in the plasmid. SDF1 was fused to ELP via these 2 restriction sites. The NdeI and XbaI restriction enzymes and DNA ligation kit used for cloning were obtained from Thermo Fisher Scientific. The SDF1 gene string used was designed and ordered from Life Technologies as follows:

GGCACCTCGATTAGTTCTCGTCTAGAATGAATGCGAAAGTCGTTGTCGTGCTG
GTGTTGGTCTTAACTGCACTGTGTTTGTCTGATGGTAAACCGGTGAGTCTTTCG
TACCGTTGCCCGTGCCGTTTCTTCGAATCACATGTTGCTCGCGCGAACGTGAA
ACACCTGAAAATTTTGAATACGCCGAATTGCGCACTGCAGATTGTGGCGCGTC
TGAAAAACAATAACCGCCAGGTATGCATCGACCCTAAACTGAAGTGGATTCAA
GAATATCTTGAAAAAGCACTTAACAAAGGTGGGGGTGGCTCTGGGGGCGGTG
GTTCCGGAGGTGGTGGATCACATATGGAGTTCATGCGCTTCAAGGT

Key

Forward primer sequence added for PCR: GGCACCTCGATTAGTTCTCG
Xba1 site: TCTAGA
SDF1 Gene string™: Underlined sequence
Linker $(G_4S)_3$: GGTGGGGGTGGCTCTGGGGGCGGTGGTTCCGGAGGTGGTGGATCA
NdeI site: CATATG
Reverse primer sequence added for PCR: GAGTTCATGCGCTTCAAGGT

The SDF1 Gene string™ was amplified using Pfu Ultra II (Agilent Technologies) and Kapa Hifi (Kapa Biosystems) polymerases. Sequencing of the final cloned product was performed by Genewiz Inc. Subsequent to the successful cloning, site directed mutagenesis was performed by GenScript on the pET25B+ vector with SDF1-ELP, to bring an out of frame His tag on the plasmid in frame. The final cloned product, SDF1-ELP in pET25B+ vector, with an "in-frame" His tag was confirmed by Genewiz Inc.

3.2.2 Expression of SDF1-ELP Fusion Protein

The pET25B+ vector with SDF1-ELP was retransformed in E. coli (BL21 Star DE3), which was obtained from Invitrogen by Life Technologies. One bacteria colony was picked for an overnight culture in 5 ml LB medium containing 25µg/mL carbenicillin. The overnight culture was used to inoculate 500 mL of terrific broth supplemented with 100 mM of L-proline (Fisher Scientific) and with 25µg/mL carbenicillin. The culture was monitored until it reached an optical density at 600 nm of about 0.6, after which 0.5 mM of IPTG (Sigma) was added to induce the protein. The culture was left overnight. The next day, the culture was centrifuged at 3000 x g, and the pellet diluted with 40 ml of PBS and the suspension sonicated twice on ice for 9 min in cycles of 10 s on and 20 s off. Poly(ethyleneimine) solution (Sigma Aldrich) was added to a final concentration of 0.5% w/v to remove residual DNA, and after centrifuging, SDF1-ELP protein transition to nanoparticles was induced with the addition of 1M NaCl and warming to about 40°C.

3.2.3 Purification of SDF1-ELP Fusion Protein

3.2.3.1 Using ELP Inverse Transition Temperature Cycling

The inversion temperature of SDF1-ELP protein was obtained by warming up a sample of protein from 20°C to 50 °C while observing the change in optical density in a spectrophotometer (Spectramax, Molecular Devices), and was determined to be ~35°C. SDF1-ELP protein was purified by warming the protein to 40°C, thus inducing aggregation, centrifuging at the same temperature, and then resuspending the pellet in PBS at 4°C, thus disaggregating the particles. Two rounds of temperature cycling were

used and the final SDF1-ELP nanoparticles were obtained by warming up the purified protein above its inverse temperature to ~40°C. For control studies, the ELP protein alone, and another fusion protein, KGF-ELP [28] were expressed and purified similarly.

3.2.3.2 Using Nickel NTA Chromatography

We also purified SDF1-ELP using traditional nickel NTA chromatography using the protocol described in the Qiagen® Ni-NTA Spin Kit Handbook. The imidazole used to prepare the different buffers needed for purification was from Thermo Fisher Scientific, while the benzonase endonuclease was obtained from Merck KGaA. Lysosyme was obtained from Thermo Fisher.

3.2.4 Physical Characterization

3.3.3.1 SDS-PAGE

An 8–16% Mini-PROTEAN® TGX™ 10 well, 50 µl Gel from Bio-Rad Laboratories, Inc. was used in a Bio-Rad Mini Protean Tetracell. All relevant reagents for the assay were obtained from Bio-Rad. SDF1-ELP Protein in 1X PBS buffer was diluted with loading buffer and run under native conditions on the gel.

3.3.3.2 Western Blot

SDS-PAGE gels were transferred onto a nitrocellulose membrane (Bio-Rad Laboratories), blocked with blotting-grade blocker (Bio-Rad Laboratories), treated with anti-human SDF1 (Peprotech) and incubated overnight at 4°C. After thorough washing with TBST, goat anti-rabbit IgG HRP (Abcam) was added. The blots were rinsed, exposed to ECL substrate and exposed to film to detect the positive SDF1 bands.

3.3.3.3 Circular Dichroism

A Circular dichroism spectrometer (Model 420SF) was used to obtain secondary structure information on SDF1-ELP. The equipment was run at 4°C, and a CD signal obtained for wavelengths between 190 and 260 nm. In separate experiments, CD signals were also obtained for ELP and for SDF1. The raw CD signal was corrected for concentration of the individual proteins (SDF1-ELP: 15µM; SDF: 25µM; ELP: 4µM) and path length of the cuvette.

3.3.3.4 Particle Size and Charge

SDF1-ELP in PBS (~50 µM) was used to measure particle size in a Zetasizer Nano series (Malvern, Piscataway, NJ) set to 37°C. Gold nanoparticles (100 nm; Sigma Aldrich) was used for calibration. Particles were put on a 200 mesh Lacey Carbon Copper TEM Grid (SPI Supplies/Structure Probe Inc.) and transmission electron micrographs (TEM) images were obtained on a Topcon (Piscataway, NJ) microscope. SDF1-ELP in PBS (~20 µM) was used to measure nanoparticle charge in a Zetasizer Nano-ZS (Malvern).

3.2.5 Binding Activity

A Biacore™ T200 was used to measure binding affinity of SDF1-ELP to CXCR4. SDF1-ELP, free SDF1 (Peprotech) and ELP were mobilized on different channels on a Series S Sensor Chip CM4 (General Electric). The first channel on the sensor chip was left blank and used as a reference**.** The chip temperature was set to 37°C. Kinetic experiments were done with 5 different concentrations of recombinant human CXCR4 (Creative Biomart) diluted in PBS (0.74nM to 60nM). Sensograms obtained for SDF1-ELP and SDF1 were

subtracted from the reference channel signal and the curves were fitted to a one-site interaction model using the Biacore T200 software.

3.2.6 Biological Activity - Calcium Flux Assay

The bottom of 12-well plates was coated with 125µL of fibronectin solution (200µg/mL in PBS and 1000X Pluronic® F-68; Sigma) each. HL-60 cells were washed in Hanks buffered saline solution supplemented with calcium and magnesium (HBSS+; Life Technologies). The cells were then suspended to 10^6 cells/mL in HBSS+, incubated with 4µM fluo-4 acetoxymethylester (AM) for 45 min at 37°C, washed again in HBSS+, and plated at a density of $5x10^5$ cells/well on the fibronectin-coated wells. Cell were allowed to attach to the plates for 15 min at 37°C, unattached cells were aspirated, and 250 µL HBSS+ added. Background images were taken using an Olympus IX81® microscope, the HBSS+ was removed, and replaced with 250 µL of SDF1-ELP, free SDF1, ELP alone, or KGF-ELP. Images were taken for the next 3.5 min, the test solutions removed and replaced with 1µg/mL ionomycin (EMD Millipore), and imaged again for 3.5 min. Fluorescence intensity was quantified on the digital images by ImageJ software (NIH) after background was subtracted.

3.2.7 Nanoparticle versus Monomeric Activity of SDF1-ELP

To investigate whether biological activity resides in the nanoparticle vs. the monomeric form of SDF1-ELP, SDF1-ELP at a concentration of 8µM in 500 µL PBS was warmed up to 40°C to initiate nanoparticle formation and pipetted into a 1.5mL Nanosep® and Nanosep MF centrifuge tube with a 10nm nominal pore size (Pall Corporation). The tube was centrifuged at 5000 x g for 5 min at 40°C to separate monomers (which end up in the filtrate) from nanoparticles (which remain on top of the membrane). 600 µL of the

filtered SDF1-ELP monomer, or SDF1-ELP nanoparticles, made to a concentration of 100nM in HBSS+ were used as the test solutions, with a control group using unfiltered SDF1-ELP (100nM).

3.2.8 Stability studies in Elastase

SDF1-ELP and SDF1 (both at 10 μM) were incubated with ~1 μM of elastase (197 units / mg protein; Sigma) at 37°C for 12 days. Samples were taken on day 0, 4, 8 and 12 and subjected to western blot analysis as explained in Section 2.4.2

3.2.9 Animal Studies

3.2.9.1 Diabetic mice wound assay

Animal studies were conducted in accordance with a protocol approved by the Rutgers University Institutional Animal Care and Use Committee (IACUC). Genetically modified diabetic mice (BKS.Cg-Dock7^{m} +/+ Lepr^{db}/J) were ordered from Jackson Laboratory and were used at the age of 10 weeks. On the day before surgery, the back of mice was shaved and depilated using clippers and Nair™ cream, followed by thorough rinsing with water. On the day of surgery (the next day), the mice were put under isoflurane anesthesia and betadine scrub (Purdue Products) and 70% ethanol were applied alternatively to prepare the dorsal skin area for surgery. Wounds were created by excising a 1 cm x 1 cm square of full thickness skin on the back the mice, using a pre-made template. Test solutions (SDF1-ELP, SDF, ELP and plain PBS) were prepared in fibrin gels to prevent them from leaking away when pipetted on the wound area. Fibrin gels were prepared as previously described [28]. Briefly, SDF1-ELP, SDF1, ELP, and plain PBS were mixed with 6.25 mg/mL of fibrinogen (Sigma Aldrich). The SDF1-ELP

and ELP were incubated at 37°C for 1 hour to initiate particle formation. Prior to application to the wound, 120 µL of the individual fibrinogen with treatment solution was mixed with 30 µl of thrombin (12.5 U/mL, Sigma Aldrich). The mixture was immediately applied to the wound and allowed to gel for up to 2 min, after which the wounds were covered with Tegarderm™ (3M) and secured using sutures (Henry Schein). The wound was monitored over a period of 42 days. Digital photographs were captured weekly, and compared to the initial photographs using Image J (NIH). The wound closure percentage was calculated as $\left(1 - \frac{\text{remaining wound area}}{\text{initial wound area}}\right) \text{x } 100$.

3.2.9.2 Wound tissue histology

On post-wounding day 42, all the animals were sacrificed and the wound area excised. The tissues were placed in a surgical casket and fixed in 10% formalin (VWR) for 24 hours after which they were transferred to a jar with 70% ethanol and stored at 4°C. For histology, tissues were embedded in paraffin and thin sections were stained with picosirius red to visualize collagen deposition as well as morphological features of the skin. Image J was used to determine the epidermal and dermal thickness. Values shown are averages of two different tissue sections per group, with three 4x magnification fields evaluated per section.

3.2.10 Statistical Analysis

Statistical comparisons were performed using KaleidaGraph software. The Fisher Least Significant Difference was used to analyze the data from two independent groups, after performing a one way ANOVA. A p-value <0.05 is considered statistically significant. A p-value of <0.05 is represented by a star (*) on the graphs while a p-value of < 0.01 is

represented by two stars (**) or by two plusses (++) on the graphs; both are considered statistically significant.

3.3 RESULTS

3.3.1 Cloning of SDF1-ELP

ELP was fused to the C-terminus of SDF1 via a linker sequence motif comprising of three repeats of four glycines and 1 serine $(G_4S)_3$ as shown in Figure 3.1A. This relatively long linker (total of 15 amino acids) allows for a wide separation between the ELP chain and the binding region of SDF1, which is located on residues 1-9 at the N-terminus [29]. The pET25B+ expression plasmid used for the SDF1-ELP cloning is shown in Figure 3.1B. After cloning, the plasmid and SDF1-ELP were mutated to bring a 6X Histidine tag in frame, to allow it to be used for epitope detection and as a purification tag.

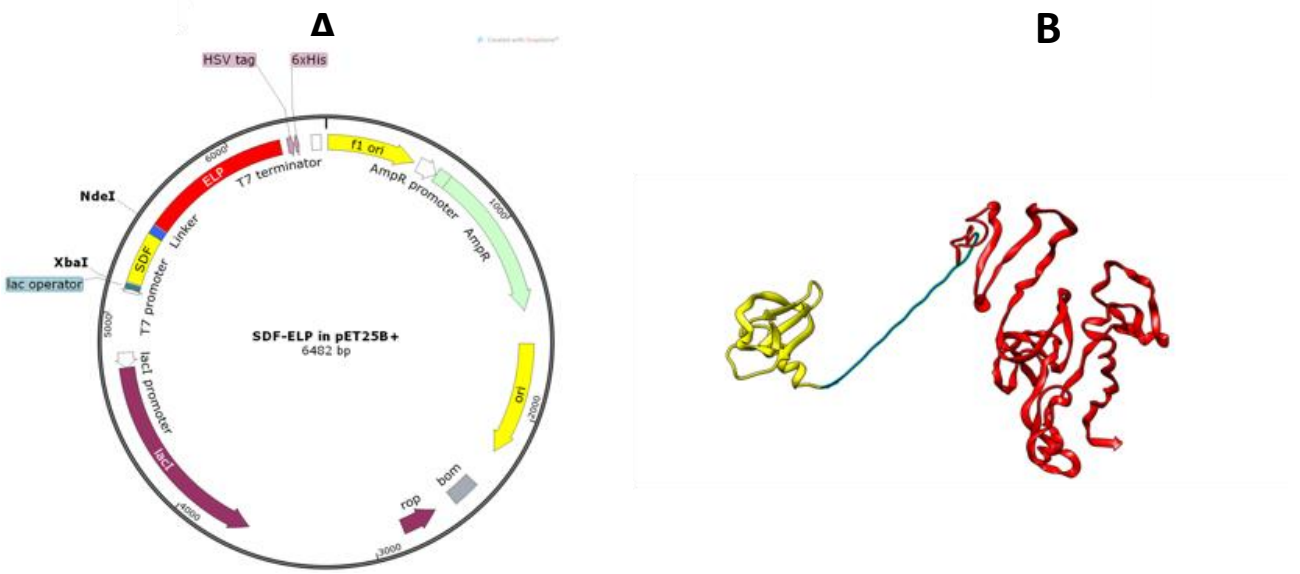

Figure. 3.1: Design and cloning of SDF1-ELP. (A) Cloning of SDF-ELP was done using a peT25B+ expression vector. SDF1 was fused to ELP using the XbaI and NdeI restriction sites. The plasmid with SDF1-ELP was mutated to put a 6X Histidine tag in frame with the protein sequence. The plasmid diagram was obtained using SnapGene®

software (from GSL Biotech; available at snapgene.com). (B) Pymol rendition of SDF1-ELP**.** SDF1 (in yellow) is separated from ELP (red) by a linker (in blue) comprising 3 repeats of 4 glycines and 1 serine**.** SDF1 monomer sequence was extracted from Ryu et al.[30] (RSCB Protein Data Bank ID: 2J7Z). The ELP portion was modeled using I-TASSER software [31],[32],[33].

3.3.2 Purification and Characterization of SDF1-ELP

3.3.2.1 SDS-PAGE and Western Blot

The bacterial lysate containing the SDF1-ELP product was initially separated using the histidine-tag (6-His) on a nickel-NTA column (Figure 3.2A). The final product revealed multiple bands. We also used the ELP-dependent aggregation property; after two rounds of temperature cycling above and below the inverse temperature of 35°C, a single band was observed (Figure 3.2B). The purified protein by inverse temperature cycling was stained with a monoclonal anti-SDF1 antibody, showing a clear band at ~31 kDa (Figure 3.2C), consistent with the predicted molecular mass of SDF1-ELP.

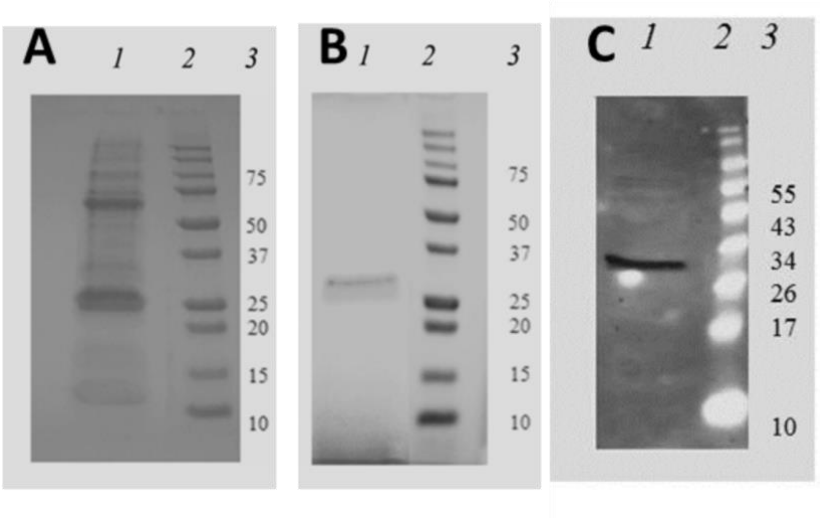

Figure. 3.2**:** Comparative purity assessment of SDF1-ELP by SDS-PAGE. (A)Representative gel image of protein purified using Nickel NTA Column. (B) Representative gel image of protein purified using inverse temperature cycling. Lane 1 is the profile of the purified protein; Lane 2 is the molecular weight (MW) ladder and lane 3 is the corresponding identification of the MW marker. (C) Representative gel image shown when the purified SDF1-ELP protein using the inverse temperature cycling is analyzed by Western blot. Lane 1 is the SDF1-ELP band at 31 kDA. Lane 2 is the molecular weight ladder, and Lane 3 is the corresponding identification of the MW marker.

3.3.2.2 Circular Dichroism (CD)

CD spectra were obtained for SDF1, ELP and SDF1-ELP to ascertain if secondary structure of SDF1 was retained in the fusion protein. Figure 3.3 shows representative CD spectra for the 3 molecules. The result with SDF1 is consistent with a mixture of α helices, β sheets and random coils as depicted by Ryu et al [30]. In the case of ELP, a highly disordered structure is observed based on the very negative dip in the spectrum at around 205nm. For the SDF1-ELP, the spectrum suggests the presence of α helices and appears to have less random coils, thus at least some aspects of the secondary structure of SDF1 is preserved when fused to ELP.

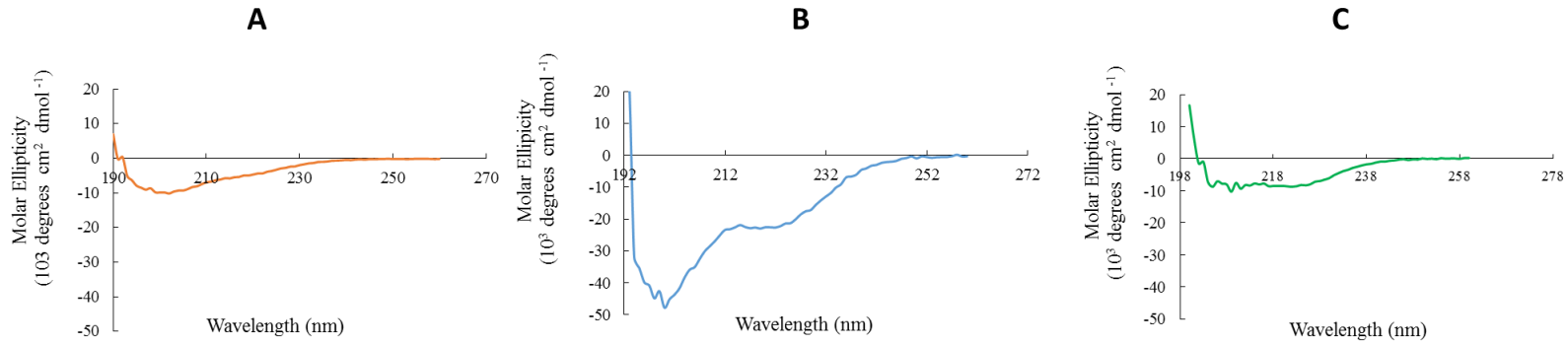

Figure. 3.3**:** CD spectra of (A) SDF1, (B) ELP and (C) SDF1-ELP. The raw CD spectra of the molecules were subtracted from their respective buffers, and normalized to the path length of the cuvette and their respective concentrations (SDF1-ELP: 15µM; SDF: 25µM; ELP: 4µM). CD signals with CD Dynodes above 700 were not included.

3.3.2.3 Particle Size and Charge

TEM images of the nanoparticles show a size of approximately 600 nm, which is corroborated with particle sizing data of 560 ± 28 nm obtained from the Zetasizer. The net charge on the protein surface was measured as approximately +3 mV.

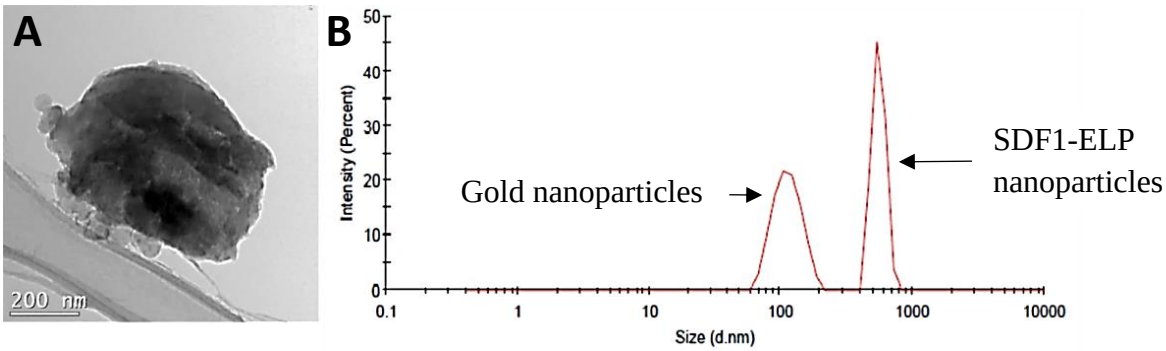

Figure. 3.4**:** Size of SDF1-ELP Nanoparticles. (A) TEM image of a single SDF1-ELP nanoparticle. Bar = 200 nm; (B) Chromatogram of SDF1-ELP nanoparticles (~600nm) and 100nm diameter gold nanoparticles run on the Zetasizer.

3.3.3 Binding and Biological Activity

3.3.3.1 CXCR4 Receptor Binding Studies using Surface Plasmon Resonance

Binding affinity of the fusion protein to CXCR4 was compared to that of free SDF1, as well as ELP alone by surface plasmon resonance. ELP alone exhibited very little to no binding to CXCR4 as compared to the blank reference channel, as would be expected (Figure 3.5A). SDF1-ELP bound to CXCR4 with a dissociation constant (K_D) estimated to 1.14 nM (Figure 3.5B). The binding of free SDF1 to CXCR4 yielded a K_D of 0.3 nM (Figure 3.5C). By way of comparison, values reported in the literature for SDF1 range from 1.32 to 6nM [34-36].

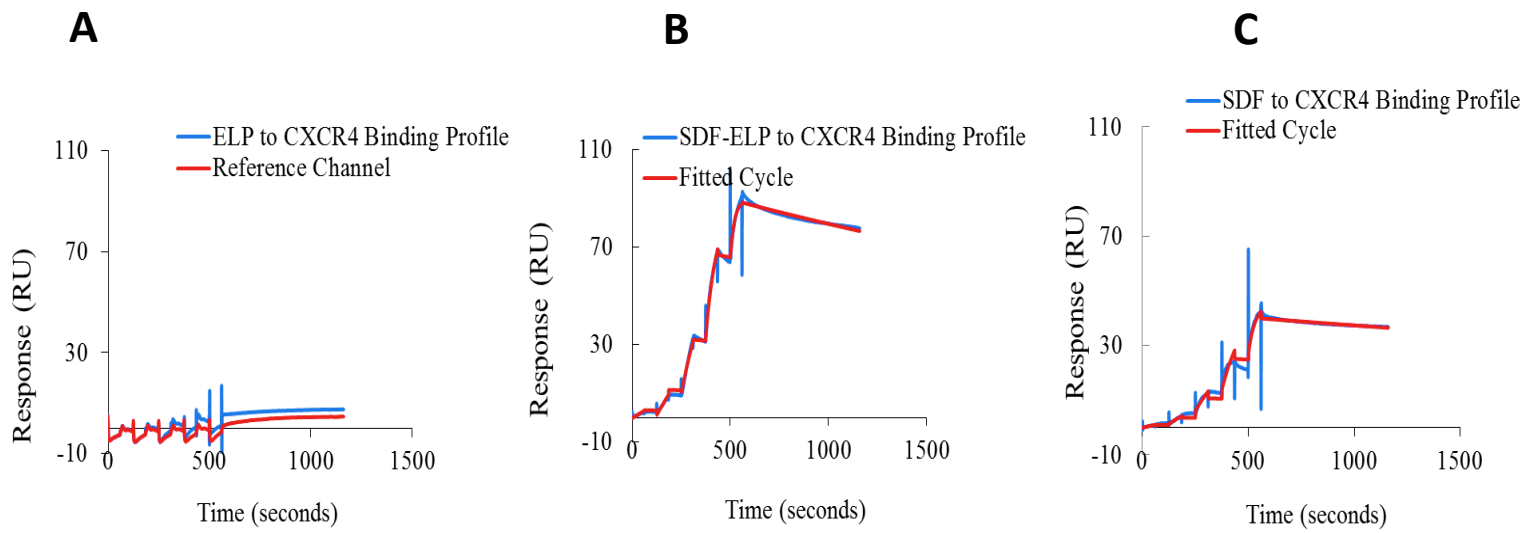

Figure. 3.5: Surface plasmon resonance analysis of CXCR4-SDF1 binding. SDF1-ELP, SDF1 and ELP were captured on different channels of a CM4 chip and the binding of different concentrations of CXCR4 (0.74 nM to 60 nM) to the individual proteins was measured in a single kinetic experiment. The first channel was left blank and used as reference channel. The reference channel subtracted binding curves were fitted to a one site interaction model. Each step on the sensogram represents binding to a specific concentration of CXCR4, starting from the smallest concentration (0.74 nM) and ending at the highest concentration (60 nM). (A) Sensogram for free ELP and the reference channel, where no binding is expected to occur. N=3. (B) SDF1-ELP binding to CXCR4 fitted sensogram. N=3. (C) Representative binding of free SDF1 to CXCR4 fitted sensogram.

3.3.3.2 Calcium Flux Study

To characterize the biological activity of SDF1-ELP, we measured its effect on intracellular calcium release in HL60 cells. A dose response of SDF1-ELP and free SDF1 in the range of 100 to 1000 nM for each was performed on HL60 cells preloaded with the cytosolic calcium ion sensitive dye Fluo 4. We noted that SDF1-ELP at 1000nM caused the highest intracellular calcium release (Figure 3.6). Furthermore, SDF1-ELP at 100nM and 1000nM exhibited slightly higher responses compared to free SDF1 at the same concentrations.

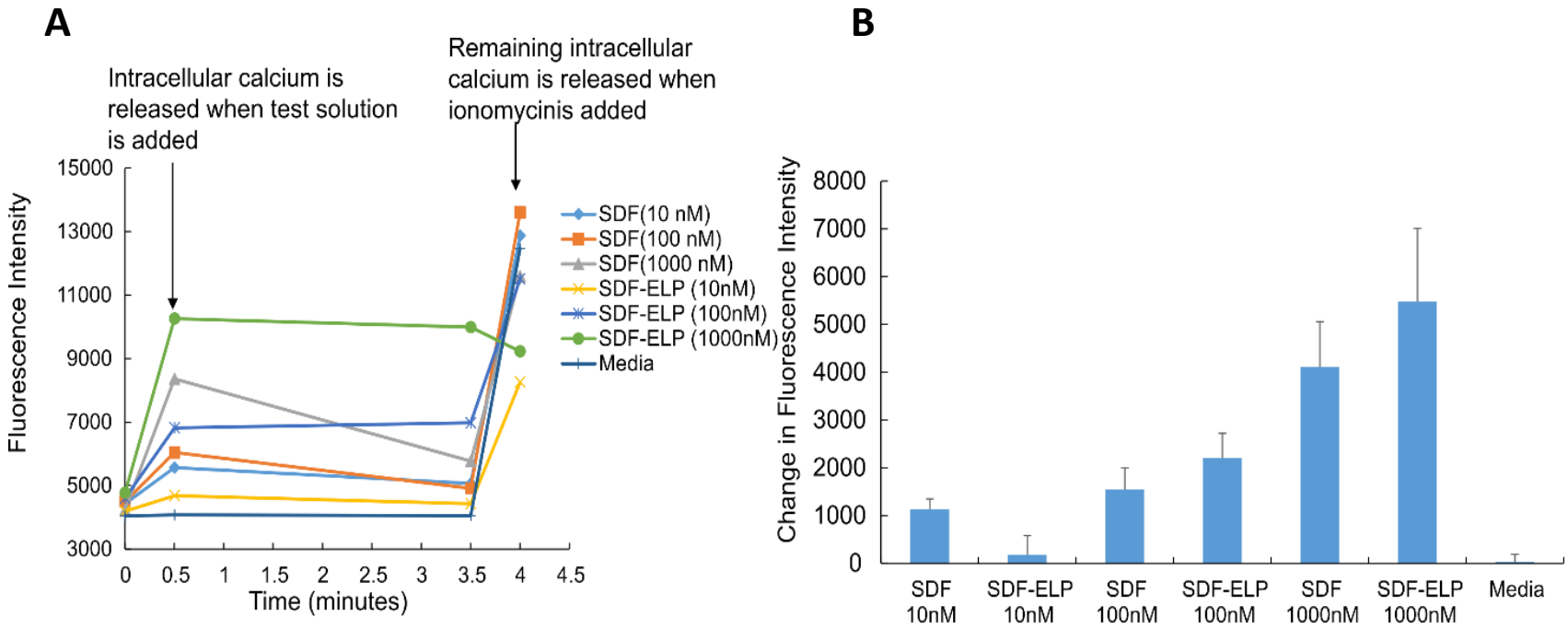

Figure. 3.6: Dose response using SDF1-ELP (and SDF1) on intracellular calcium release as measured by Fluo-4 in HL60 cells. (A) Time course of cell manipulations and Fluo-4 fluorescence intensity. (B) Fluo-4 fluorescence measured 30 s into the assay minus fluorescence measured at the starting point. N=6.

We then directly compared the effect of SDF1-ELP at two representative doses (the highest response of SDF1-ELP - 1000nM; a typical dose of SDF1 used in the literature [37] – 10 nM) to several negative controls, namely ELP alone, KGF-ELP, and plain medium. As shown in Figure 3.7, ELP and KGF-ELP triggered a small rise in calcium levels and plain medium had no effect at all. In addition, 1000nM SDF1-ELP caused a significantly higher intracellular calcium rise as compared to 10 nM SDF1 as well as any of the negative controls.

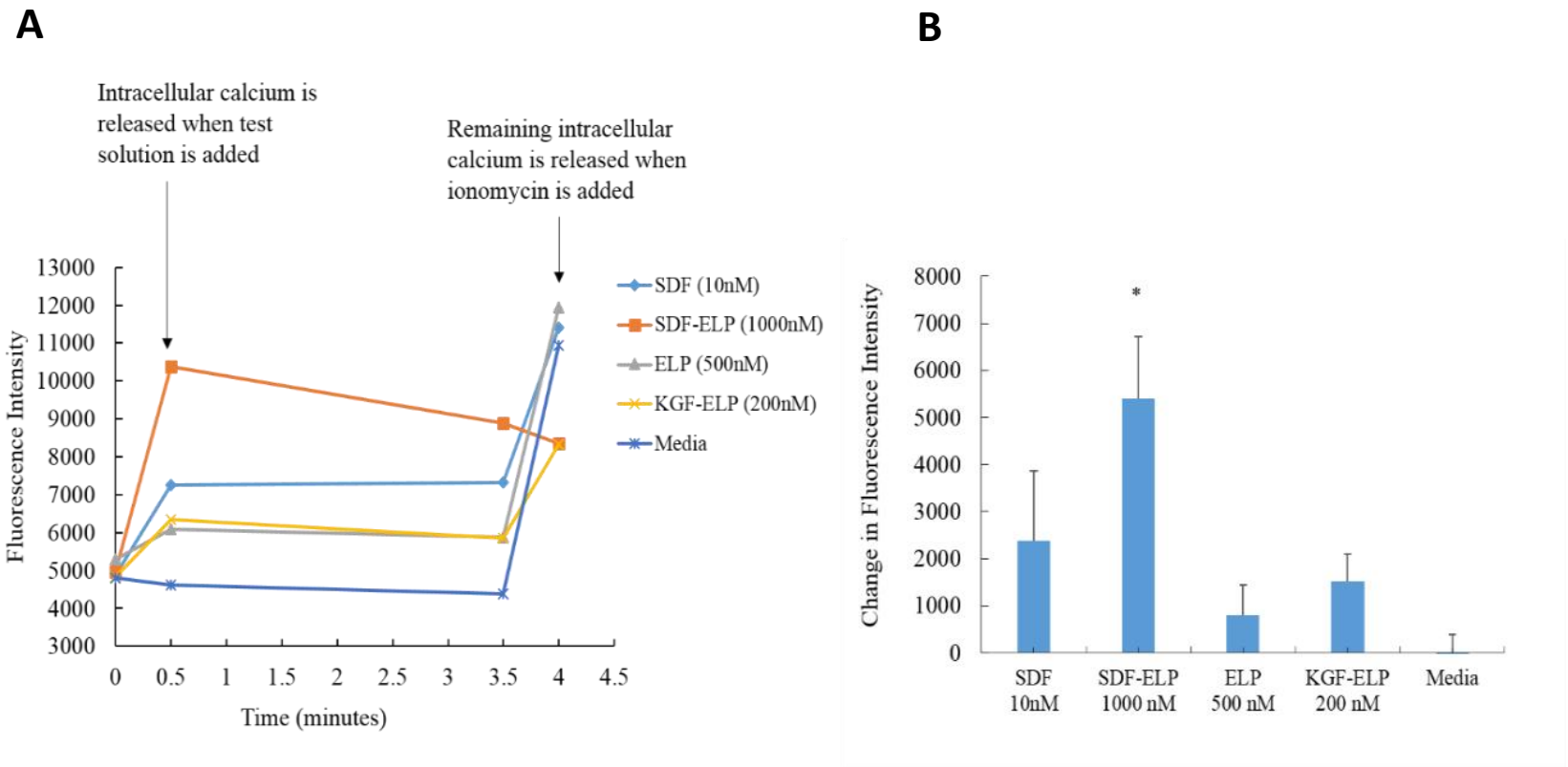

Figure. 3.7: Effect of SDF1-ELP, SDF1 and plain medium on intracellular calcium release as measured by Fluo-4 in HL60 cells. (A) Time course of cell manipulations and Fluo-4 fluorescence intensity. (B) Fluo-4 fluorescence measured 30 s into the assay minus fluorescence measured at the starting point. N=6. (*: $p < 0.05$, one way ANOVA, Fisher's LSD post-test).

SDF1-ELP preparations are expected to contain primarily SDF1-ELP nanoparticles that are at equilibrium with monomers. To attempt to determine whether biological activity was primarily in the monomeric vs. nanoparticle fractions, we separated freshly aggregated SDF1-ELP by filtration through a 10nm pore membrane, and compared the calcium rise triggered by the filtrate (assumed to mainly consist of SDF1-ELP monomers) vs. the material on top of the membrane (assumed to mainly consist of SDF1-ELP nanoparticles). A higher calcium release was obtained from the top fraction containing the SDF-ELP nanoparticles, as compared to the bottom fraction containing the SDF1-ELP monomers although the difference was not statistically significant. (Figure 3.8).

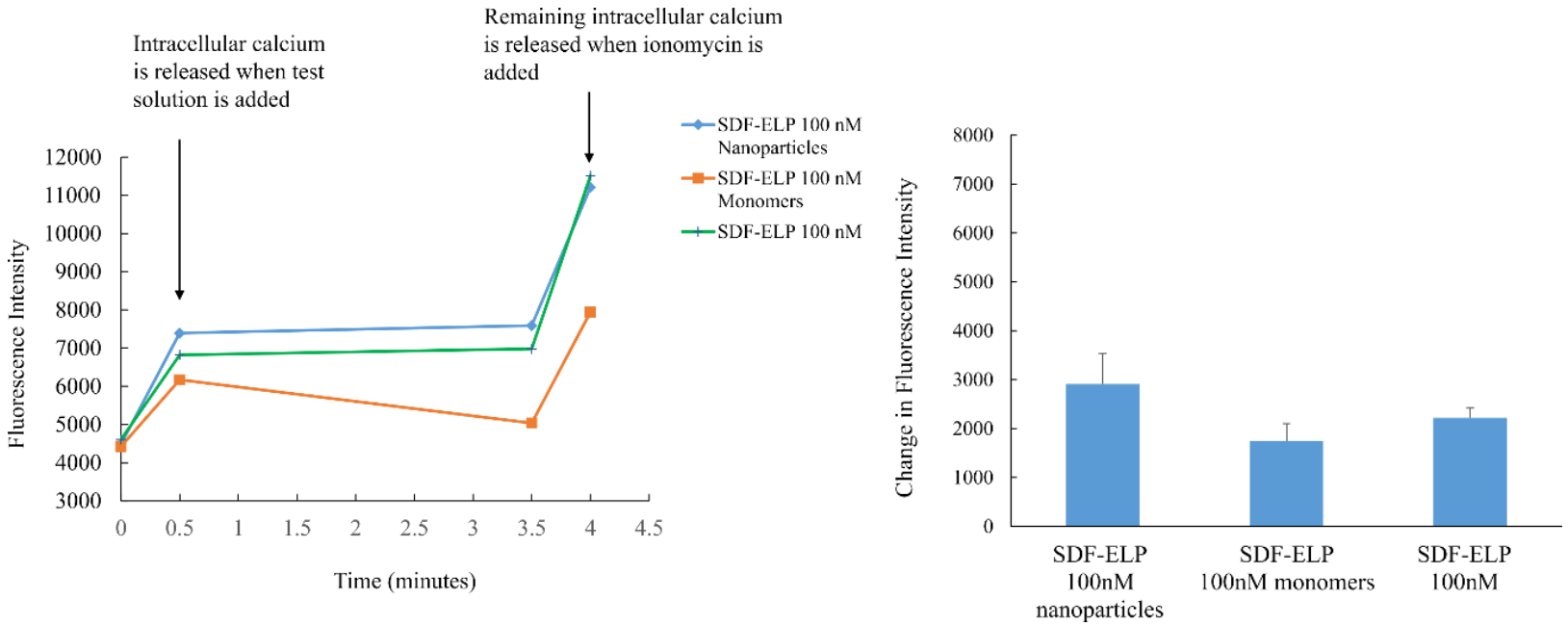

Figure. 3.8**:** Comparison of the effect of SDF1-ELP nanoparticles versus SDF1-ELP monomers on intracellular calcium release as measured by Fluo-4 in HL60 cells. (A) Time course of calcium concentration as measured by Fluo 4AM fluorescence. (B) Fluo-4 fluorescence measured 30 s into the assay minus fluorescence measured at the starting point. N=6.

3.3.4 Stability Studies in Elastase

To investigate the stability of SDF1-ELP in elastase, one of the proteases that are known to degrade SDF1 in vivo [38], we incubated SDF1-ELP and SDF1 in elastase over a period of 12 days. Samples collected at 4 day intervals were subjected to a Western blot analysis. We noted that SDF1-ELP remained intact throughout the incubation period (Figure 3.9A), while no positive bands were seen for the SDF1 samples (Figure 3.9C).

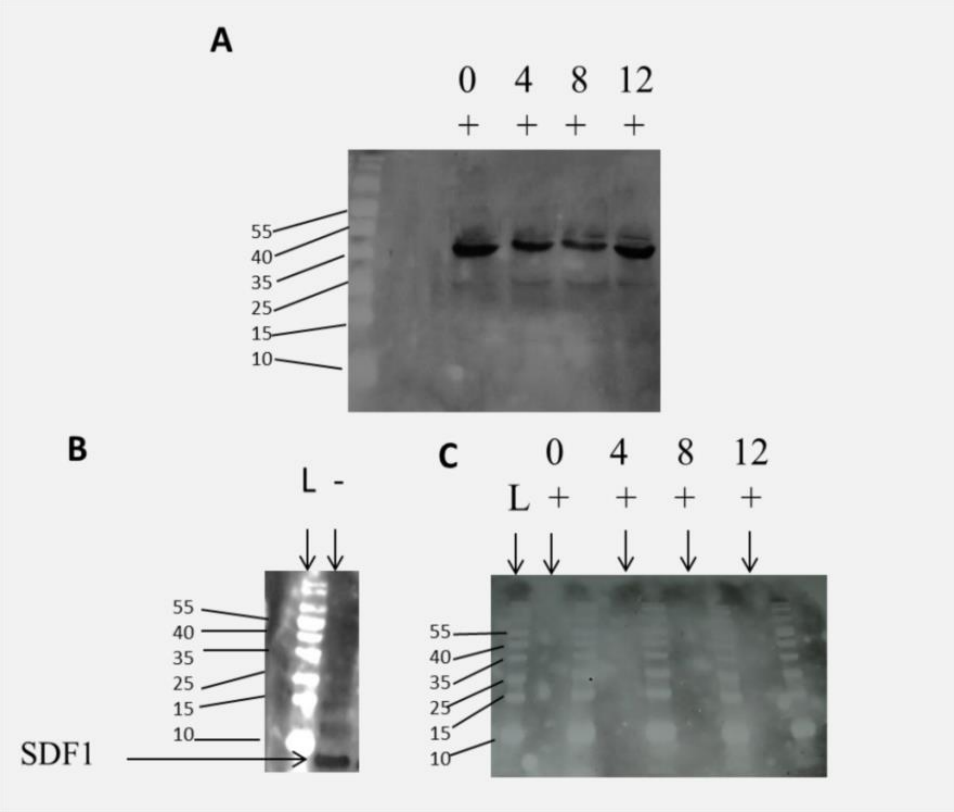

Figure. 3.9 Degradation of SDF-ELP or SDF by elastase. SDF1-ELP and SDF1 were incubated in elastase over a 12 day period. Samples were pulled at 4 day intervals and subjected to Western blot analysis. (A) Representative blot of SDF1-ELP samples after incubation in elastase. (B) Lane 1, labelled L is the molecular weight ladder. Lane 2,

labelled (-) is SDF1 with no elastase. (C) Representative blot of SDF1 samples in elastase. No SDF positive bands are seen in any of the lanes.

3.3.5 In Vivo Activity

The bioactivity of SDF1-ELP was tested in vivo using a diabetic mouse model. Excisional wounds (1 x 1 cm^2) were created on the back of diabetic mice and were treated with 1000nM SDF1-ELP nanoparticles in fibrin gels, 1000nM of free SDF1 in fibrin gels, 1000nM ELP nanoparticles in fibrin gels, or fibrin gels with plain medium (used as vehicle control). The closure of the wound was monitored over a period of 42 days. We noted that the wounds treated with SDF1-ELP were more closed than any other group at all time points of observation (Figure 3.10). In fact, by postwounding day 21, the SDF1-ELP treated wounds were about 95% closed, and 100% closed on day 28, while the mice in the remaining groups did not fully close until day 42. Although the SDF1 group exhibited a trend towards faster closure at postwounding day 14, this group was essentially the same as the ELP and vehicle control at days 21 and beyond. The ELP and vehicle control groups followed closely each other during the entire study. Wound tissues harvested and stained on day 42 exhibited a continuous epidermis, confirming wound closure in all groups. However, both the epidermis and dermis were significantly thicker in the SDF-ELP group (Figure 3.11).

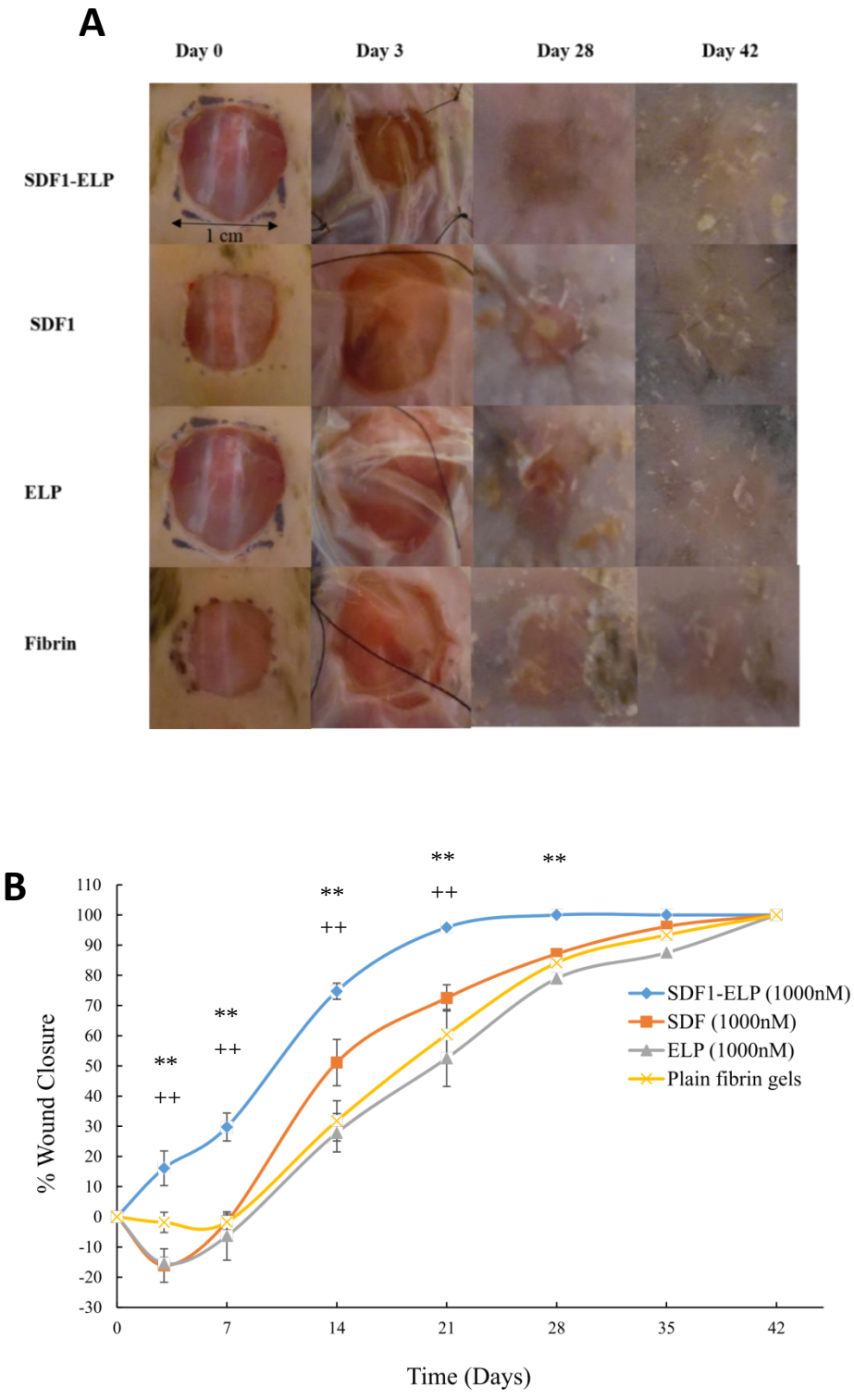

Figure. 3.10**:** Effect of SDF1-ELP on skin wound closure in diabetic mice**.** Full-thickness excisional wounds were treated with fibrin gel with SDF1-ELP particles, fibrin gel

containing free SDF1, fibrin gel containing ELP particles or plain fibrin gel (vehicle control). (A) Representative images of the wounds on different days. On postwounding day 28, the wound treated with SDF1-ELP was fully closed, while in the other groups it was still open, only fully closing by day 42. (B) Quantified wound closure as a function of time. N = 5. (** and ++: p <0.01, one way ANOVA, Fisher's LSD post-test; (++) = SDF1-ELP compared to SDF1, (**) = SDF1-ELP compared to ELP or plain fibrin)

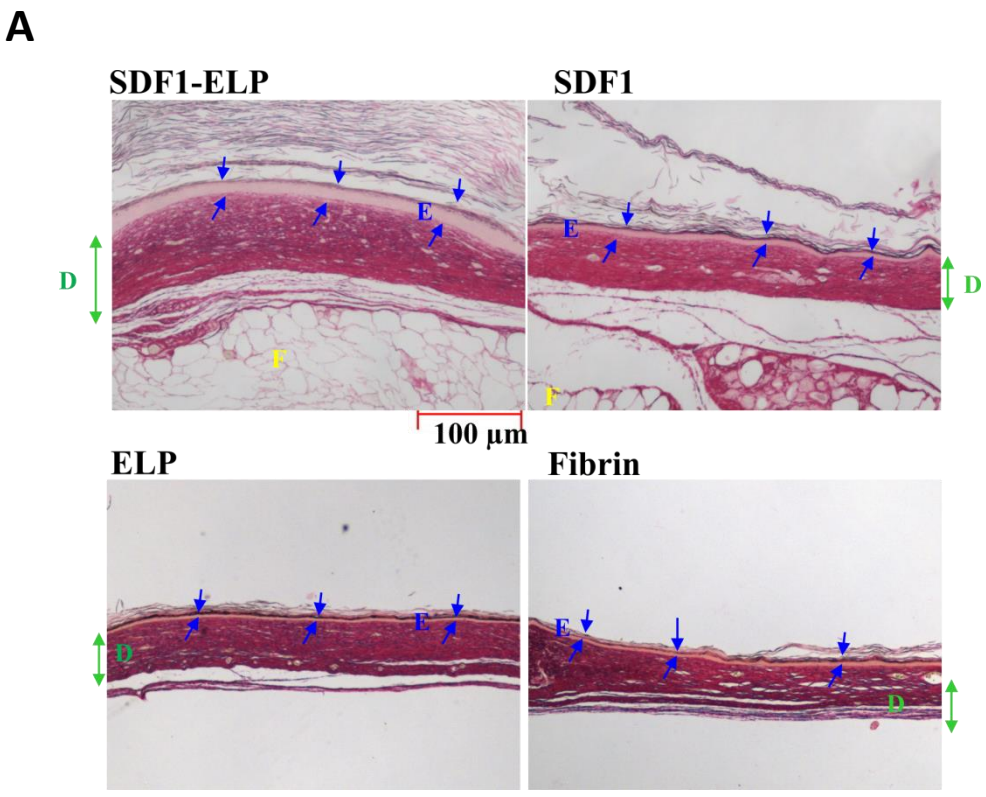

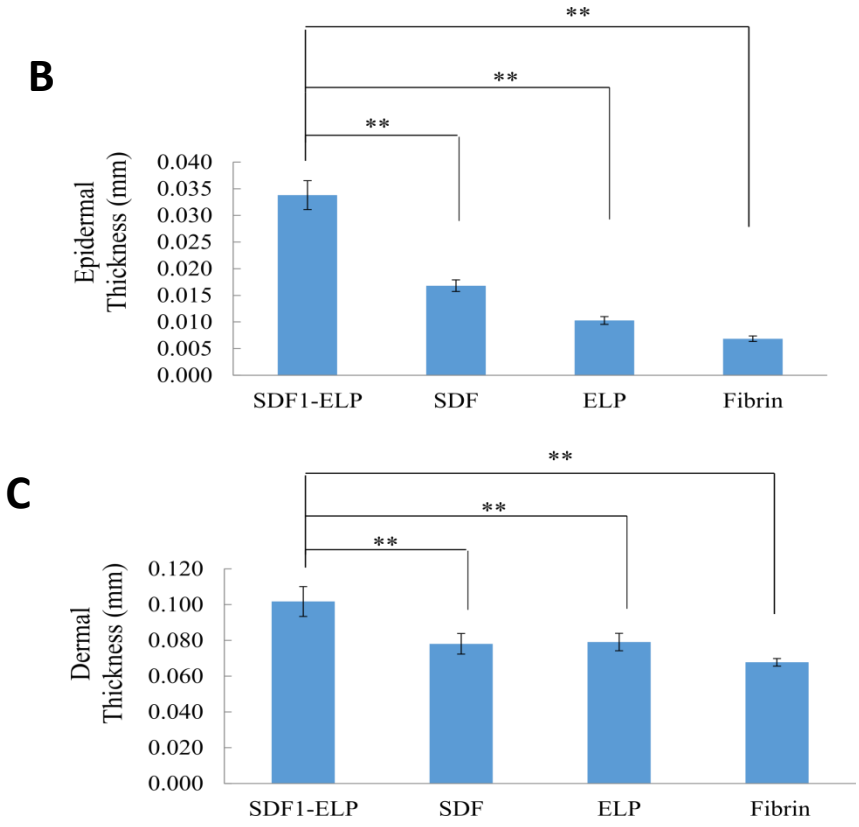

Figure. 3.11: Morphology of wounds excised on post-wounding day 42. (A) Wounds were stained with the collagen stain picosirius red, which also makes it easy to identify the main skin layers. Structures are labeled as: E= epidermis; D= dermis; F = fat. Representative images are shown. Blue arrows represent epidermal layer thickness. Green arrow represents dermal layer thickness. (B, C) Thickness of the epidermis and dermis, respectively, as quantified by ImageJ. Values shown are averages of two (2) different tissue sections per group, with three (3) 4x magnification fields evaluated per section (N = 10). (**: $p < 0.01$, one way ANOVA, Fisher's LSD post-test)

3.4 DISCUSSION

In this study, we generated a fusion protein with SDF1 and ELP domains that forms nanoparticles of ~600 nm in size above its inverse transition temperature. We verified

that SDF1-ELP binds the SDF1 receptor CXCR4 with similar affinity compared to free SDF1, and that the in vitro biological activity (intracellular calcium release) of SDF1-ELP is very similar to that of free SDF1 when using HL60 cells as responders, which express CXCR4 [39]. When applied to excisional wounds on the back of diabetic mice, the SDF1-ELP nanoparticles significantly accelerated wound closure as compared to free SDF1, ELP alone, or vehicle. Wounds treated with SDF1-ELP nanoparticles closed around 21 days post wounding, representing a 50% decrease compared to the other groups, which required up to 42 days to fully close. Furthermore, the SDF1-ELP treated wounds healed with a significantly thicker epidermal and dermal layer as compared to the other groups.

Previous work has demonstrated the ability of topically applied recombinant SDF1 to promote wound healing in experimental animals when used in high and repeated doses [12]. This is however impractical and very costly [40]. Our goal was to design an SDF1 derivative that would have similar activity compared to pure recombinant SDF1, but would also have a simpler purification process (thereby reducing manufacturing costs), and could be used as a substitute for SDF1 therapeutic applications. For this purpose, we used a fusion protein approach whereby ELP was chosen as the fusion partner because the ELP portion has a tendency to self-assemble above a transition temperature to form nanoparticles that can be separated by simple centrifugation [26], [28], [41],[42]. Thus, the SDF1-ELP fusion protein can be purified using a non-chromatographic, but thermally driven, method based on the phase transition property of ELP. We fused the ELP at the C-terminus of SDF1 with an intervening 15 amino acid residue linker to limit potential interference of the long ELP chain length on the activity

of the SDF1 binding domain which is known to be at the N-terminus [29]. We chose a 50 pentapeptide repeat for the ELP sequence motif based on previous work which showed that this elastin cassette has an inverse transition temperature which is lower than physiological [28]; in fact we measured an inverse temperature of about 35°C, thus ensuring that the majority of the protein is in nanoparticle form in the wound.

The SDF1-ELP nanoparticles bound the CXCR4 receptor with high affinity, with a K_D =1.14nM, which is close to the reported values for free SDF1 ranging from 1.32 to 6nM [34-36]. The biological activity of SDF1-ELP, as measured by intracellular calcium release in HL60 cells, was dose dependent and very similar to that of free SDF1. Furthermore, we noted that the system was not saturated and more calcium was released when the concentration of either SDF1 or SDF1-ELP was increased to 1000nM. Similar observations have been reported in calcium imaging studies of cardiomyocytes stimulated with SDF1, where a saturation of the response did not occur until SDF1 concentration reached 5000 nM [43]. Based on the low K_D for the binding to CXCR4, we would however expect the CXCR4 receptors to be about 99% bound in the presence of 100 nM SDF1 or SDF1-ELP. It is therefore likely that other processes besides ligand-receptor binding, such as endocytosis and further intracellular processing of the SDF1-CXCR4 complexes play a quantitative role in mediating the cellular response [44].

While the binding and cellular effects of SDF1-ELP were similar to that of SDF1 in vitro, SDF1-ELP significantly outperformed SDF1 in vivo. The wounds treated with SDF1-ELP were about 95% closed by postwounding day 21, while those treated with SDF1 were only about 70% closed. By day 28, the wounds treated with SDF1-ELP were 100% closed, while those treated with free SDF1 were only about 80% closed. Wound

treated with SDF1, ELP, or vehicle, took 42 days to fully close. It is noteworthy that wound cross-sections exhibited a significantly thicker epidermis and dermis compared to the other groups. This finding is similar to that previously reported by Koria et al [28], where KGF-ELP induced a higher proliferation of keratinocytes, which resulted significant increase in reepithelialization in full-thickness wounds made on diabetic mice as compared to the controls. While angiogenesis is the most commonly presumed mechanism of SDF1, a recent review suggests potentially many different cellular targets for SDF1 [11], making the role of SDF1-CXCR4 in the wound healing process more complicated. The mechanism of action of SDF1-ELP is therefore unclear.

Because SDF1-ELP had superior in vivo performance compared to SDF1, while both behaved almost identically in vitro, we hypothesized that SDF1-ELP nanoparticles are more stable in the diabetic wound environment compared to SDF1. Prior studies suggest that the ELP fusion proteins can serve as "drug depots" with a better stability profile and/or in vivo half-life than the free target protein [23]. For example, glucagon-like peptide-1 (GLP1; a potential type-2 diabetes drug) fused to ELP is more resistant to proteolysis by neutral endopeptidase, which is known to degrade GLP1 in vivo, as compared to free GLP1 [27]. The same study also shows that a single injection of the GLP1-ELP fusion protein was able to reduce blood glucose levels in mice for 5 days, which is about 120 times longer than what has been observed for the free GLP1. Similarly, we observed that SDF1-ELP was very stable in elastase which is known to degrade free SDF1 in vivo [38].

We used our in vitro intracellular calcium release assay to quantify the activity of SDF1-ELP monomers as compared to the nanoparticles. We noted that more activity

appeared to be in the nanoparticle versus the monomeric fractions, although the difference was not statistically significant. In fact, it seemed that bioactivity was contributed by both nanoparticle and monomeric forms. Based on this we cannot conclude that release from the nanoparticle was necessary for bioactivity.

In conclusion, we have developed an SDF1-ELP fusion protein that has comparable biological and binding activities to recombinant human SDF1, and also has the ability to self-assemble into nanoparticles below physiological temperatures, making it a potential drug depot for use in chronic wound treatment.

While our research focus is on skin wounds, our SDF1-ELP fusion protein nanoparticles may be useful for other wound healing applications, such as in myocardial infarction, where SDF1 has been reported to recruit stem cells to promote local tissue regeneration [14, 45].

3.5 REFERENCES

[1] C.K. Sen, G.M. Gordillo, S. Roy, R. Kirsner, L. Lambert, T.K. Hunt, F. Gottrup, G.C. Gurtner, M.T. Longaker, Human skin wounds: a major and snowballing threat to public health and the economy, Wound Repair Regen, 17 (2009) 763-771.

[2] A. Tellechea, E. Leal, A. Veves, E. Carvalho, Inflammatory and Angiogenic Abnormalities in Diabetic Wound Healing: Role of Neuropeptides and Therapeutic Perspectives, TOCVJ, 3 (2010) 43-55.

[3] R. Edwards, K.G. Harding, Bacteria and wound healing, Curr Opin Infect Dis, 17 (2004) 91-96.

[4] S.A. Eming, T. Krieg, J.M. Davidson, Inflammation in wound repair: molecular and cellular mechanisms, J Invest Dermatol, 127 (2007) 514-525.

[5] H. Brem, M. Tomic-Canic, Cellular and molecular basis of wound healing in diabetes, J Clin Invest, 117 (2007) 1219-1222.

[6] X. Xu, F. Zhu, M. Zhang, D. Zeng, D. Luo, G. Liu, W. Cui, S. Wang, W. Guo, W. Xing, H. Liang, L. Li, X. Fu, J. Jiang, H. Huang, Stromal cell-derived factor-1 enhances wound healing

through recruiting bone marrow-derived mesenchymal stem cells to the wound area and promoting neovascularization, Cells Tissues Organs, 197 (2013) 103-113.

[7] A.L. George, P. Bangalore-Prakash, S. Rajoria, R. Suriano, A. Shanmugam, A. Mittelman, R.K. Tiwari, Endothelial progenitor cell biology in disease and tissue regeneration, J Hematol Oncol, 4 (2011) 24.

[8] C. Kalka, H. Masuda, T. Takahashi, W.M. Kalka-Moll, M. Silver, M. Kearney, T. Li, J.M. Isner, T. Asahara, Transplantation of ex vivo expanded endothelial progenitor cells for therapeutic neovascularization, Proc Natl Acad Sci U S A, 97 (2000) 3422-3427.

[9] S.M. Majka, K.A. Jackson, K.A. Kienstra, M.W. Majesky, M.A. Goodell, K.K. Hirschi, Distinct progenitor populations in skeletal muscle are bone marrow derived and exhibit different cell fates during vascular regeneration, J Clin Invest, 111 (2003) 71-79.

[10] T. Takahashi, C. Kalka, H. Masuda, D. Chen, M. Silver, M. Kearney, M. Magner, J.M. Isner, T. Asahara, Ischemia- and cytokine-induced mobilization of bone marrow-derived endothelial progenitor cells for neovascularization, Nat Med, 5 (1999) 434-438.

[11] W.B. Bollag, W.D. Hill, CXCR4 in Epidermal Keratinocytes: Crosstalk within the Skin, Journal of Investigative Dermatology, 133 (2013) 2505-2508.

[12] A. Sarkar, S. Tatlidede, S.S. Scherer, D.P. Orgill, F. Berthiaume, Combination of stromal cell-derived factor-1 and collagen-glycosaminoglycan scaffold delays contraction and accelerates reepithelialization of dermal wounds in wild-type mice, Wound Repair Regen, 19 (2011) 71-79.

[13] M. Ziegler, M. Elvers, Y. Baumer, C. Leder, C. Ochmann, T. Schonberger, T. Jurgens, T. Geisler, B. Schlosshauer, O. Lunov, S. Engelhardt, T. Simmet, M. Gawaz, The bispecific SDF1-GPVI fusion protein preserves myocardial function after transient ischemia in mice, Circulation, 125 (2012) 685-696.

[14] V.F. Segers, T. Tokunou, L.J. Higgins, C. MacGillivray, J. Gannon, R.T. Lee, Local delivery of protease-resistant stromal cell derived factor-1 for stem cell recruitment after myocardial infarction, Circulation, 116 (2007) 1683-1692.

[15] O.O. Yang, S.L. Swanberg, Z. Lu, M. Dziejman, J. McCoy, A.D. Luster, B.D. Walker, S.H. Herrmann, Enhanced inhibition of human immunodeficiency virus type 1 by Met-stromal-derived factor 1beta correlates with down-modulation of CXCR4, J Virol, 73 (1999) 4582-4589.

[16] W. Hiesinger, J.M. Perez-Aguilar, P. Atluri, N.A. Marotta, J.R. Frederick, J.R. Fitzpatrick, 3rd, R.C. McCormick, J.R. Muenzer, E.C. Yang, R.D. Levit, L.J. Yuan, J.W. Macarthur, J.G. Saven, Y.J. Woo, Computational protein design to reengineer stromal cell-derived factor-1alpha generates an effective and translatable angiogenic polypeptide analog, Circulation, 124 (2011) S18-26.

[17] W. Hiesinger, A.B. Goldstone, Y.J. Woo, Re-engineered stromal cell-derived factor-1alpha and the future of translatable angiogenic polypeptide design, Trends Cardiovasc Med, 22 (2012) 139-144.

[18] L. Baumann, S. Prokoph, C. Gabriel, U. Freudenberg, C. Werner, A.G. Beck-Sickinger, A novel, biased-like SDF-1 derivative acts synergistically with starPEG-based heparin hydrogels and improves eEPC migration in vitro, J Control Release, 162 (2012) 68-75.

[19] S.Y. Rabbany, J. Pastore, M. Yamamoto, T. Miller, S. Rafii, R. Aras, M. Penn, Continuous delivery of stromal cell-derived factor-1 from alginate scaffolds accelerates wound healing, Cell Transplant, 19 (2010) 399-408.

[20] P.W. Henderson, S.P. Singh, D.D. Krijgh, M. Yamamoto, D.C. Rafii, J.J. Sung, S. Rafii, S.Y. Rabbany, J.A. Spector, Stromal-derived factor-1 delivered via hydrogel drug-delivery vehicle accelerates wound healing in vivo, Wound Repair Regen, 19 (2011) 420-425.

[21] F. Dalonneau, X.Q. Liu, R. Sadir, J. Almodovar, H.C. Mertani, F. Bruckert, C. Albiges-Rizo, M. Weidenhaupt, H. Lortat-Jacob, C. Picart, The effect of delivering the chemokine SDF-1alpha in a matrix-bound manner on myogenesis, Biomaterials, 35 (2014) 4525-4535.

[22] M.A. Olekson, R. Faulknor, A. Bandekar, M. Sempkowski, H.C. Hsia, F. Berthiaume, SDF-1 Liposomes Promote Sustained Cell Proliferation in Mouse Diabetic Wounds, Wound Repair Regen, (2015).

[23] M.F. Shamji, H. Betre, V.B. Kraus, J. Chen, A. Chilkoti, R. Pichika, K. Masuda, L.A. Setton, Development and characterization of a fusion protein between thermally responsive elastin-like polypeptide and interleukin-1 receptor antagonist: sustained release of a local antiinflammatory therapeutic, Arthritis Rheum, 56 (2007) 3650-3661.

[24] S.R. MacEwan, W. Hassouneh, A. Chilkoti, Non-chromatographic purification of recombinant elastin-like polypeptides and their fusions with peptides and proteins from Escherichia coli, J Vis Exp, (2014).

[25] W. Hassouneh, T. Christensen, A. Chilkoti, Elastin-like polypeptides as a purification tag for recombinant proteins, Curr Protoc Protein Sci, Chapter 6 (2010) Unit 6 11.

[26] D.E. Meyer, A. Chilkoti, Purification of recombinant proteins by fusion with thermally-responsive polypeptides, Nat Biotechnol, 17 (1999) 1112-1115.

[27] M. Amiram, K.M. Luginbuhl, X. Li, M.N. Feinglos, A. Chilkoti, A depot-forming glucagon-like peptide-1 fusion protein reduces blood glucose for five days with a single injection, J Control Release, 172 (2013) 144-151.

[28] P. Koria, H. Yagi, Y. Kitagawa, Z. Megeed, Y. Nahmias, R. Sheridan, M.L. Yarmush, Self-assembling elastin-like peptides growth factor chimeric nanoparticles for the treatment of chronic wounds, Proc Natl Acad Sci U S A, 108 (2011) 1034-1039.

[29] P. Loetscher, J.H. Gong, B. Dewald, M. Baggiolini, I. Clark-Lewis, N-terminal peptides of stromal cell-derived factor-1 with CXC chemokine receptor 4 agonist and antagonist activities, J Biol Chem, 273 (1998) 22279-22283.

[30] E.K. Ryu, T.G. Kim, T.H. Kwon, I.D. Jung, D. Ryu, Y.M. Park, J. Kim, K.H. Ahn, C. Ban, Crystal structure of recombinant human stromal cell-derived factor-1alpha, Proteins, 67 (2007) 1193-1197.

[31] J. Yang, R. Yan, A. Roy, D. Xu, J. Poisson, Y. Zhang, The I-TASSER Suite: protein structure and function prediction, Nature Methods, 12 (2015) 7-8.

[32] A. Roy, A. Kucukural, Y. Zhang, I-TASSER: a unified platform for automated protein structure and function prediction, Nature Protocols, 5 (2010) 725-738.

[33] Y. Zhang, I-TASSER server for protein 3D structure prediction, BMC Bioinformatics, 9 (2008) 40.

[34] R. Salcedo, K. Wasserman, H.A. Young, M.C. Grimm, O.M. Howard, M.R. Anver, H.K. Kleinman, W.J. Murphy, J.J. Oppenheim, Vascular endothelial growth factor and basic fibroblast growth factor induce expression of CXCR4 on human endothelial cells: In vivo neovascularization induced by stromal-derived factor-1alpha, Am J Pathol, 154 (1999) 1125-1135.

[35] M.P. Crump, J.H. Gong, P. Loetscher, K. Rajarathnam, A. Amara, F. Arenzana-Seisdedos, J.L. Virelizier, M. Baggiolini, B.D. Sykes, I. Clark-Lewis, Solution structure and basis for functional activity of stromal cell-derived factor-1; dissociation of CXCR4 activation from binding and inhibition of HIV-1, EMBO J, 16 (1997) 6996-7007.

[36] G.A. McQuibban, G.S. Butler, J.H. Gong, L. Bendall, C. Power, I. Clark-Lewis, C.M. Overall, Matrix metalloproteinase activity inactivates the CXC chemokine stromal cell-derived factor-1, J Biol Chem, 276 (2001) 43503-43508.

[37] A. Aiuti, The Chemokine SDF-1 Is a Chemoattractant for Human CD34+ Hematopoietic Progenitor Cells and Provides a New Mechanism to Explain the Mobilization of CD34+ Progenitors to Peripheral Blood, J Exp Med, 185 (1997) 111-120.

[38] A. Valenzuela-Fernández, T. Planchenault, F. Baleux, I. Staropoli, K. Le-Barillec, D. Leduc, T. Delaunay, F. Lazarini, J. Virelizier, M. Chignard, D. Pidard, F. Arenzana-Seisdedos, Leukocyte elastase negatively regulates stromal cell-derived factor-1 (SDF-1)/CXCR4 binding and functions by amino-terminal processing of SDF-1 and CXCR4, J Biol Chem, 277 (2002) 15677-15689.

[39] C. Bogani, V. Ponziani, P. Guglielmelli, C. Desterke, V. Rosti, A. Bosi, M.C. Le Bousse-Kerdiles, G. Barosi, A.M. Vannucchi, C. Myeloproliferative Disorders Research, Hypermethylation of CXCR4 promoter in CD34+ cells from patients with primary myelofibrosis, Stem Cells, 26 (2008) 1920-1930.

[40] W. Hiesinger, J.R. Frederick, P. Atluri, R.C. McCormick, N. Marotta, J.R. Muenzer, Y.J. Woo, Spliced stromal cell-derived factor-1alpha analog stimulates endothelial progenitor cell migration and improves cardiac function in a dose-dependent manner after myocardial infarction, J Thorac Cardiovasc Surg, 140 (2010) 1174-1180.

[41] H.J. Kang, J.H. Kim, W.J. Chang, E.S. Kim, Y.M. Koo, Heterologous expression and optimized one-step separation of levansucrase via elastin-like polypeptides tagging system, J Microbiol Biotechnol, 17 (2007) 1751-1757.

[42] F. Hu, T. Ke, X. Li, P.H. Mao, X. Jin, F.L. Hui, X.D. Ma, L.X. Ma, Expression and purification of an antimicrobial peptide by fusion with elastin-like polypeptides in Escherichia coli, Appl Biochem Biotechnol, 160 (2010) 2377-2387.

[43] I. Hadad, A. Veithen, J.Y. Springael, P.A. Sotiropoulou, A. Mendes Da Costa, F. Miot, R. Naeije, X. De Deken, K.M. Entee, Stroma cell-derived factor-1alpha signaling enhances calcium transients and beating frequency in rat neonatal cardiomyocytes, PLoS ONE, 8 (2013) e56007.

[44] L. Zhou, X. Guo, J. Ba, L. Zhao, CD44 is involved in CXCL-12 induced acute myeloid leukemia HL-60 cell polarity, Biocell, 34 (2010) 91-94.

[45] S. Prokoph, E. Chavakis, K.R. Levental, A. Zieris, U. Freudenberg, S. Dimmeler, C. Werner, Sustained delivery of SDF-1alpha from heparin-based hydrogels to attract circulating pro-angiogenic cells, Biomaterials, 33 (2012) 4792-4800.

4. CHAPTER 4: SDF1α-elastin-like-peptide fusion protein promotes cell migration and revascularization of experimental wounds in diabetic mice

Note: This chapter is partially reproduced from the following publication **written by Agnes Yeboah**:

Agnes Yeboah, Rene Schloss, Martin L. Yarmush, Francois Berthiaume. "SDF1α-elastin-like-peptide fusion protein promotes cell migration and revascularization of experimental wounds in diabetic mice" Advances in Wound Care (To be submitted, 2016)

4.1 INTRODUCTION

The management of wound healing and subsequent scarring remains a challenge for health care professionals. Chronic wounds are especially difficult to treat as the wound repair process is interrupted by underlying medical conditions such as diabetes and immunosuppression, leading to a prolonged and excessive inflammatory phase [1], and persistent infections [2] to wound. The high levels of inflammatory cells induce the production of serine proteases and matrix metalloproteinases (MMPs) that degrade and inactivate the components of the extra cellular matrix and growth factors needed for wound healing [3].

Studies have demonstrated that topical growth factors are promising therapeutics for non-healing wounds [4], and their effectiveness have been demonstrated in non-clinical animal models. Despite its therapeutic potential, one of the biggest challenges in the development of exogenous growth factors for clinical use is designing effective drug delivery platforms and technologies that ensure the safe and prolonged release of growth

factors at the wound site during the entire skin regeneration process. This is because the quantity and bioavailability of exogenous growth factors are usually impaired by the same proteolytic activities that degrade their endogenous counterparts. To date, the only topical growth factor that has received US Food and Drug Administration approval for wound healing is recombinant human platelet-derived growth factor PDGF (Regranex®) [5], which although has been shown to be effective at treating leg ulcers, needs to be used in multiple applications due to degradation by proteinases. However, an FDA instigated black box on the product label warns of an increased risk in cancer deaths in patients who used multiple application of the growth factor.

One growth factor which has been shown to enhance the closure of skin wounds is Stromal cell-Derived Growth Factor 1-alpha (SDF1) [6]. SDF1 is known to promote revascularization which is needed for re-epithelialization [7-9] by recruiting endothelial progenitor cells that differentiate into mature vascular endothelium [10, 11]. However, similar to Regranex®, repeated and high doses of topical SDF1 was needed to achieve therapeutic efficacy [6] in animal models, making its potential use commercially not only expensive and impractical, but its translation to the clinic likely to face significant regulatory hurdles as repeated application of SDF1 is also known to enhance tumor progression [12].

In the previous chapter, we showed the development of an SDF1 derivative, SDF1-elastin-like peptide (SDF1-ELP) with a similar in vitro bioactivity as SDF1, but a superior in vivo efficacy. In this chapter, we show that while SDF1-ELP promotes the migration of cells and induces vascularization similar to SDF1 in vitro, it is more stable in wound fluid. When applied to full thickness skin wounds in diabetic mice, wounds

treated with SDF1-ELP exhibited more endothelial cells (CD31 positive cells) as compared with SDF1 and vehicle controls, suggesting increased vascularization.

4.2 MATERIALS AND METHODS

4.2.1 Synthesis and characterization of SDF1-ELP

The design, development and characterization of SDF1-ELP were described in the previous chapter. Briefly, SDF1-ELP was made by juxtaposing human SDF1 to an elastin-like peptide (ELP) in a pET25B+ vector. The fusion protein was expressed in E.coli and purified using a unique property conferred by the ELP, which enables it to reversibly aggregate into nanoparticles above its inverse transition temperature. 2 cycles of temperature cycling and centrifugation were used to isolate SDF1-ELP. Purity and identity of SDF1-ELP were confirmed using SDS-PAGE and Western Blot, respectively. Particle size was confirmed using a Zetasizer (Malvern instrument) and transmission electron microscopy. The binding and biological activity of SDF1-ELP was determined using surface plasmon resonance technology (SPR) via a Biacore equipment (GE Health Care) and a calcium flux assay, respectively.

4.2.2 SDF1-ELP-Mediated HL-60 Chemotaxis Assay.

To evaluate chemotactic responses to SDF1-ELP, we used the Human Leukemia-60 (HL-60) cell line, which highly expresses the SDF1 receptor CXCR4 [13], in Boyden chambers. The HL60 cells were obtained from the American Type Culture Collection (ATCC, Manassas, Virginia) and were cultured in Iscove's Modified Dulbecco's Medium (ATCC) supplemented with 20% fetal bovine serum (Gibco by Life Technologies) and 1% penicillin-streptomycin (Life Technologies). HL-60 cells were cultured in this

medium until they reached a concentration of about 10^6 viable cells/mL. A total of 10^5 cells (in 100 µl) were placed on top of Transwells (Falcon™ Cell Culture Insert, Transparent PET Membrane 8.0µm pore size; Corning). The bottom of the Transwells was filled with 600 µL of SDF1-ELP, free SDF1, ELP alone, or another fusion protein, keratinocyte growth factor (KGF)-ELP [14] . Plates were incubated at 37°C for 1, 2 and 4 h. The number of cells that migrated to the bottom of the well was counted using a hemacytometer (Hausser). The results were normalized to the initial 10^5 added cells.

4.2.3 Separation of Chemotactic Activity in Monomeric and Nanoparticle Forms of SDF1-ELP.

The SDF1-ELP fusion protein forms nanoparticles above its inverse temperature, previously determined to be about 35ºC. We prepared SDF1-ELP at a concentration of 8µM in 500 µL PBS and warmed the solution up to 40°C to initiate nanoparticle formation and pipetted it into a 1.5mL Nanosep® and Nanosep MF centrifuge tube with a 10nm nominal pore size (Pall Corporation). The tube was centrifuged at 5000g for 5 min at 40°C to separate monomers (which end up in the filtrate) from nanoparticles (which remain on top of the membrane). We reran the cell migration studies with 600 µL of the filtered SDF1-ELP monomer, or SDF1-ELP nanoparticles, made to a concentration of 250nM in medium as the test solutions, with a control group using unfiltered SDF1-ELP (250nM), and additional groups using 10 nM recombinant SDF1, or plain medium.

4.2.4 Quantification of SDF1-ELP Monomer Release from Nanoparticles.

To investigate the release of SDF1-ELP monomers from nanoparticles over time, SDF1-ELP was prepared at a concentration of 1000nM in Iscove's Modified Dulbecco's Medium (ATCC) supplemented with 20% fetal bovine serum and 1% penicillin-streptomycin. The solution was incubated at 37ºC to initiate nanoparticle formation. After 0, 1, 2, 3 and 6 h of incubation, SDF1-ELP monomers were separated from nanoparticles by centrifugation in Nanosep tubes as described earlier. The filtrate (50 µL) containing the SDF1-ELP monomers was pipetted onto a nitrocellulose membrane placed inside a dot blot apparatus, along with recombinant human SDF1 (Peprotech) standards between 0 to 125 nM. The nitrocellulose membrane was allowed to air dry, after which it was blocked with blotting-grade blocker (Bio-Rad Laboratories), treated with an anti-human SDF1 (Peprotech) and incubated overnight at 4°C. After thorough washing with TBST, a secondary goat anti-rabbit IgG-horseradish peroxidase antibody (Abcam) was added. Once the nitrocellulose membrane was developed, the amount of SDF-ELP monomers shown on the dot blot membrane was quantified using SDF1 standards also on the same membrane.

4.2.5 In Vitro Angiogenesis Assay

The ability of SDF1-ELP to induce angiogenesis was measured using an in vitro vascularization assay. We cultured Human Umbilical Vascular Endothelial Cells (HUVECs; Life Technologies) in a 75cm^2 tissue culture flask in Medium 200 supplemented with Low Serum Growth Supplement (Life Technologies) until they were 80% confluent. 289µL of 10 mg/mL of Matrigel (Corning Lifesciences) was thawed on ice overnight and spread evenly over the wells of a 24 well plate. The plates were

incubated for 40 min at 37ºC to allow the Matrigel to gel. Trypsinized cells were transferred to a conical tube and centrifuged at 180 x g for 7 minutes until the cells were pelleted. Cells were resuspended to a concentration of 4 x 10^5 cells / mL using non-supplemented Medium 200PRF (Life Technologies). SDF1-ELP (1000nM), SDF1 (1000nM) and ELP (1000nM) were prepared in 300 µL of the cell suspension (total of 1.2 x 10^5 cells) and pipetted onto the Matrigel. The negative control was plain media, while the positive control was basic fibroblast growth factor (25nM). After about 20-22 hours of incubation of the plate at 37°C, the cells were removed and the plates were washed twice with HBSS. The final wash was replaced with calcein AM (Life Technologies) prepared to a concentration of 8 µg/mL in HBSS. The plates were incubated at 37°C for 30 minutes, after which they were washed twice with HBSS. Images were acquired at 10X magnification using an Olympus IX81® microscope.

4.2.6 Stability in Diabetic Wound Fluid

To investigate the persistence of SDF1-ELP protein nanoparticles in a wound site, 10µM of SDF1-ELP, SDF1 or ELP were incubated for 15 days in human diabetic wound fluid or in PBS vehicle. Wound fluid from the left abdomen of a diabetic patient was used for the studies. The use of the human wound fluid was approved by the Rutgers Institutional Review Board. Initially, we investigated background bioactivity in the diabetic fluid itself, as it may mask the effect of the test proteins. We diluted the wound fluid with Iscove Modified Dulbecco Medium (IMDM) from 1X (no dilution) to 1200X, and tested chemotactic activity of the resulting solution as described above.

Based on our previous experience with the cell migration assay, we diluted 10 µM SDF1, which had been incubated in wound fluid for 15 days, down to 10 nM (1000X wound

fluid dilution). Similarly, 10 µM SDF1-ELP were incubated in wound fluid for 15 days, and then diluted down to 250 nM using IMDM (40X wound fluid dilution). We then performed the migration assay to compare chemotactic activity of free SDF1 vs. SDF1-ELP after the 15 day incubation period. As negative controls, we used 10 µM ELP pre-incubated for 15 days in wound fluid, also diluted down to 250 nM ELP, plain media, and plain wound fluid diluted 40X with IMDM.

4.2.7 In Vivo Bioactivity of SDF-ELP vs. free SDF1.

4.2.7.1 Animals

All animal studies were approved by the Rutgers University Institutional Animal Care and Use Committee (IACUC). Ten-week old, genetically modified diabetic mice from Jackson Laboratory (BKS.Cg-Dock7^{m} +/+ Lepr^{db}/J) were used.

4.2.7.2 Wound Experiments

One day prior to the surgery, the hair on the back of the mice was completely removed and the shaved area was thoroughly washed with water. The next day (day of surgery), the mice were put under isoflurane anesthesia and their dorsal area sterilized for surgery with a sequential application of betadine scrub (Purdue Products) and 70% ethanol. 1 cm x 1 cm square excisional wounds were created on the back of the mice using a pre-made template. Test solutions consisting of SDF1-ELP, SDF, ELP and plain PBS, were prepared in fibrin gels as previously described and applied onto the wound area, after which the wounds were covered with Tegarderm™ (3M) and secured using sutures

(Henry Schein).

4.2.7.3 Histological Processing and analysis

After 7, 28 and 42 days post wounding, the animals were sacrificed and the wound area excised. The tissues were fixed in 10% formalin (VWR) for 24 hours, and then stored at 2 - 8°C in 70% ethanol. For histology, tissues were embedded in paraffin and thin sections were stained for CD31 positive cells using a primary rabbit polyclonal anti-CD31 antibody (Abcam). The number of CD31 positive cells in the stained sections was quantified using ImageJ (National Institutes of Health, Bethesda, MD). Values shown are averages of two different tissue sections per group, with about three different fields evaluated per section.

4.2.8 Statistical Analysis

Statistical analysis was performed using KaleidaGraph software. Data from two independent groups were analyzed using the Fisher Least Significant Difference, after performing a one way ANOVA. A p-value of <0.05 is represented by a star (*) on the graphs while a p-value of < 0.01 is represented by two stars (**) on the graphs; both are considered statistically significant.

4.3 RESULTS

4.3.1 Chemotactic Activity of SDF1-ELP vs. Free SDF1

The ability of SDF1-ELP to promote the migration of HL60 cells, which express CXCR4 [13], was evaluated in Transwells. As shown in Figure 4.1, SDF1-ELP caused a dose-dependent migratory response up to 1000 nM. A dose of 250nM SDF1-ELP achieved

approximately the same percent cell migration as 10nM free SDF1, which was used as positive control. This concentration of free SDF1 is reported to induce a robust migratory response [15]. Negative controls included vehicle consisting of plain medium with no peptide, ELP alone, or KGF-ELP, which is mitogenic for keratinocytes [16], but for which HL60 cells do not express the receptor. Very little migration was seen in all of the negative controls used.

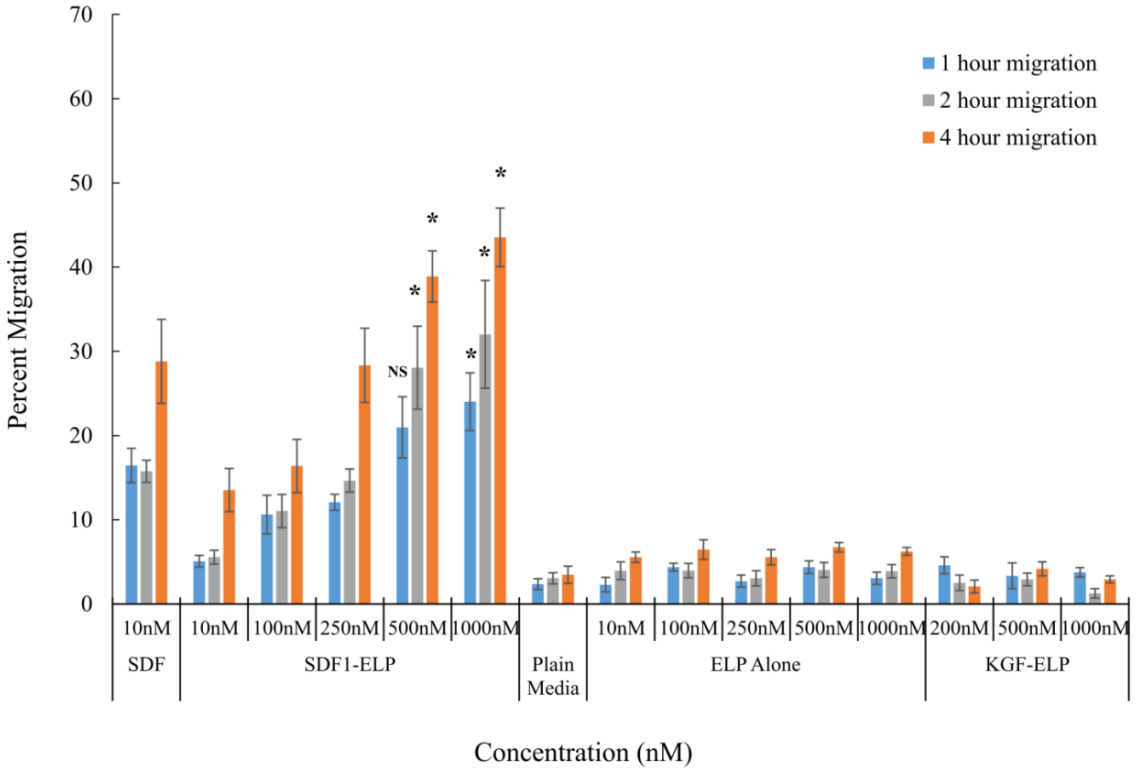

Figure 4.1: Chemotactic activity of SDF1-ELP towards HL60 cells. (A) HL60 cells were put on the top of 8 µm pore Transwells. The bottom of the wells was filled with 600 µL IMDM with SDF1-ELP, free SDF1, ELP alone, or KGF-ELP at the concentrations shown. The number of migrated cells was measured after 1, 2, and 4 h at 37°C. N=6 for each condition. SDF1-ELP migration results after 1, 2 and 4 h were statistically

compared with the corresponding SDF1 migration results (*: $p < 0.05$, one way ANOVA, Fisher's LSD post-test. NS=not statistically significant).

4.3.2 Chemotactic Activity of SDF-ELP Nanoparticles vs. Monomeric Form

Since chemotaxis was measured at physiological temperature (37°C), which is only slightly above the SDF1-ELP inversion temperature of about 35°C, both monomeric and nanoparticle forms of SDF-ELP may be present in this assay. We therefore probed to what extent the monomers and nanoparticles contributed to the observed migration response by separating them through a 10nm nominal pore size membrane. As a control, we also used free SDF1 on similar membranes. The HL-60 cell migration experiment was repeated using the monomers (which end up in the filtrate), nanoparticles (which remain on top of the membrane), as well as unfiltered SDF1-ELP. As shown in Figure 4.2, the chemotactic activity of the monomeric fraction was significantly greater than that of the nanoparticle fraction; however, a significant amount of migration occurred with the nanoparticle fraction as well. Thus, HL60 migration may be contributed by both forms of SDF1-ELP, with a predominant effect of the monomeric form.

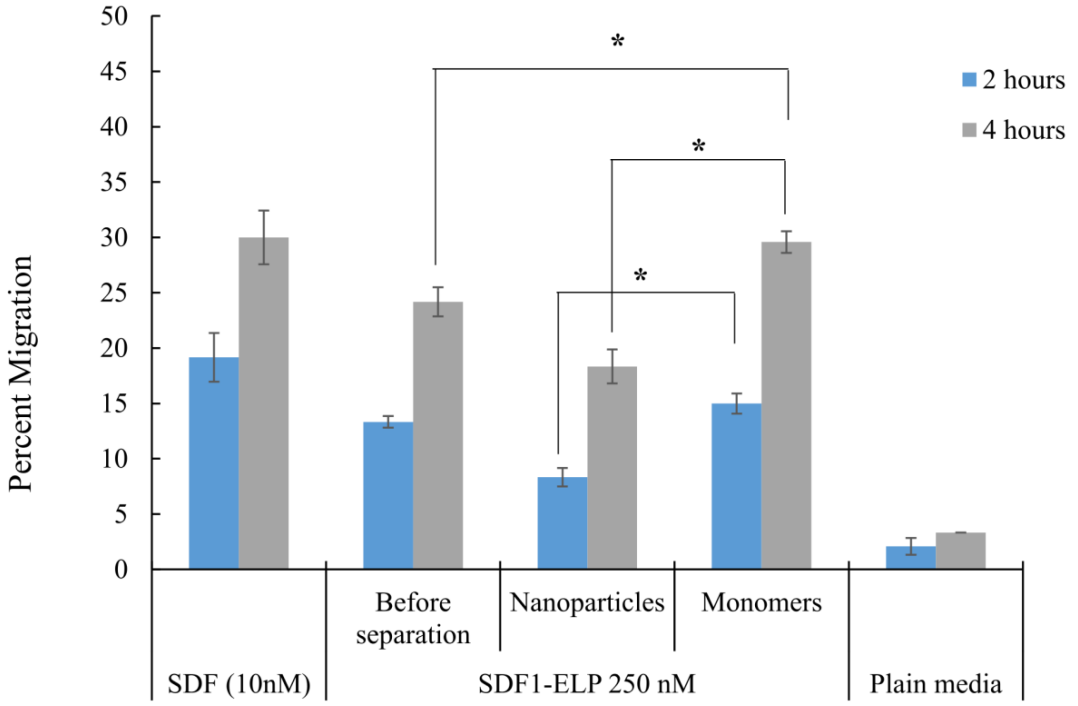

Figure 4.2: Chemotactic Activity of SDF-ELP Nanoparticles vs. Monomeric Form. SDF1-ELP nanoparticles were separated from monomers by centrifugation through a 10 nm pore size membrane. HL60 migration was measured using SDF1-ELP nanoparticles that remained on top of the membrane, as well as the SDF1-ELP monomers that passed through the membrane. N=6 for each condition. (*: $p < 0.05$, one way ANOVA, Fisher's LSD post-test).

4.3.3 Chemotactic Activity – Release of SDF1-ELP Monomers from Nanoparticles

We measured how much SDF-ELP monomer was released out of the nanoparticles over the time course of the migration study. Dot blot quantitation of the filtrate as a function of incubation time revealed a time-dependent increase after a lag of about 1 h, as shown in Figures 4.3A and B. The fraction of SDF1-ELP monomers released at the end of the

incubation time of 4 h can be estimated to be about 8%. Therefore, when using a total SDF-ELP concentration of 250 nM during the HL60 chemotaxis study, the concentration of SDF-ELP monomer can be estimated to be around 20 nM.

A

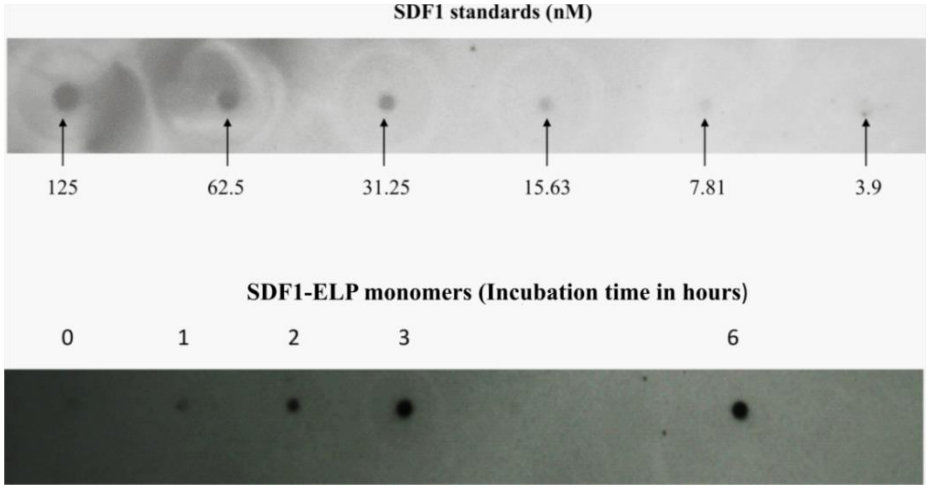

B

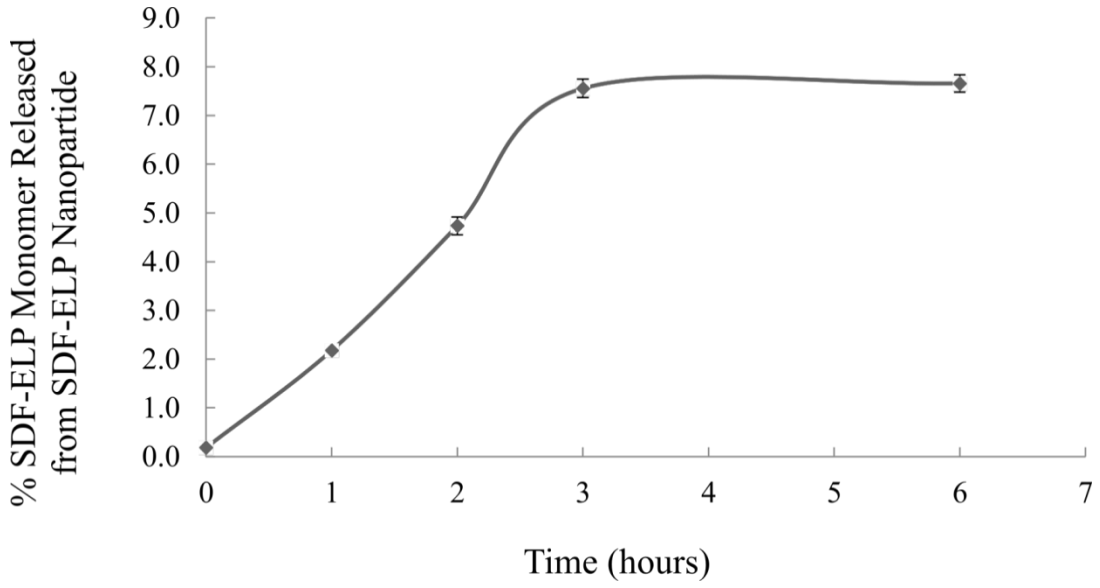

Figure 4.3: Release of SDF1-ELP monomers from nanoparticles. (A) SDF-ELP nanoparticles were incubated in medium at 37°C for up to 6 h. Samples retrieved at

different time points were analyzed by dot blot along with free SDF1 standards. B) The fraction of SDF-ELP monomers released at each time point was estimated by measuring using the pixel intensity of the dot blot images compared with the SDF1 standards using ImageJ. N = 3

4.3.4 In Vitro Endothelial Tube Formation

The ability of SDF1-ELP to promote angiogenesis was evaluated in a tube formation assay using HUVECs. SDF1-ELP, SDF1 and ELP were prepared to concentrations of 1000nM in HUVEC suspensions and pipetted onto Matrigel-coated plates. The test solutions were prepared to match the concentrations which we had been previously tested in animal studies. The angiogenic activities of the test solutions were compared with bFGF, used as positive control [17]. After a 22 hour incubation at 37°C, followed by staining with calcein AM, fluorescence images show the multicellular structures that formed in each condition. Similar to bFGF, Both SDF1-ELP and SDF1 promoted tube formation and capillary-like networks, while ELP and vehicle controls had no such effects (Figure 4.4).

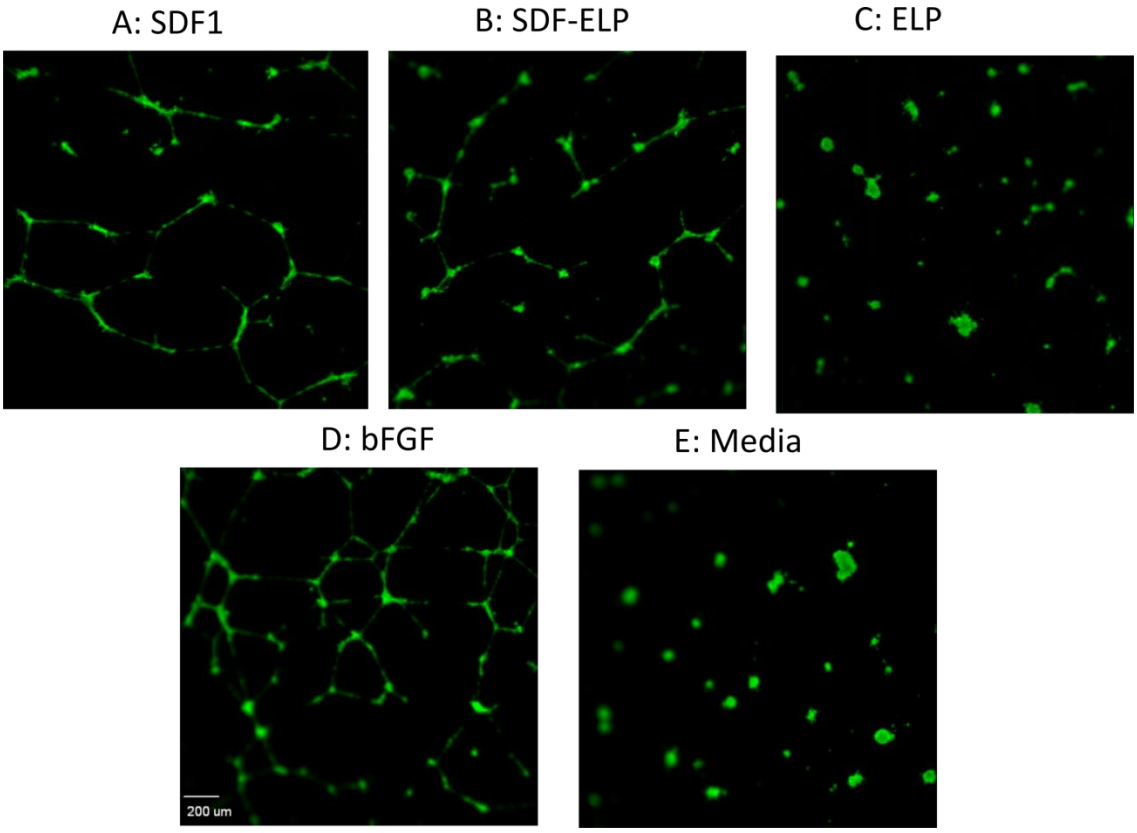

Figure 4.4: Tube formation assay. Representative fluorescent images of capillary-like structures formed by HUVECs plated on matrigel (N=3), in presence of (A) free SDF1; (B) SDF-ELP; (C) ELP alone; (D) bFGF used as positive control; (E) plain medium, used as negative control. Scale bar: 200 µm

4.3.5 In Vitro Stability in Human Diabetic Wound Fluid

To compare the stability of SDF1-ELP vs. SDF1 in a wound environment, we measured the bioactivity of each protein after prolonged incubation in human diabetic wound fluid. Because wound fluid by itself is chemotactic to HL60 cells, we tested the chemotactic activity of different dilutions of wound fluid on HL60 cells, and found that wound fluid diluted between a range of 40 to 1200X had a minimal chemotactic effect (Figure 4.5A).

After a 15 day incubation of 10 µM SDF1-ELP, SDF1 and ELP in 1X wound fluid, we diluted the solutions to concentrations that will allow us repeat our cell migration experiment (Figure 1), but with minimum interference from the wound fluid itself. As such. SDF1 was diluted down to 10 nM (1000X wound fluid dilution), whereas SDF1-ELP and ELP were diluted down to 250nM (40X wound fluid dilution). Additional negative controls for the experiment were wound fluid diluted 40X, and plain media. As shown in Figure 4.5B, the chemotactic activity of free SDF1 after incubation in wound fluid was significantly reduced, as compared to SDF1-ELP.

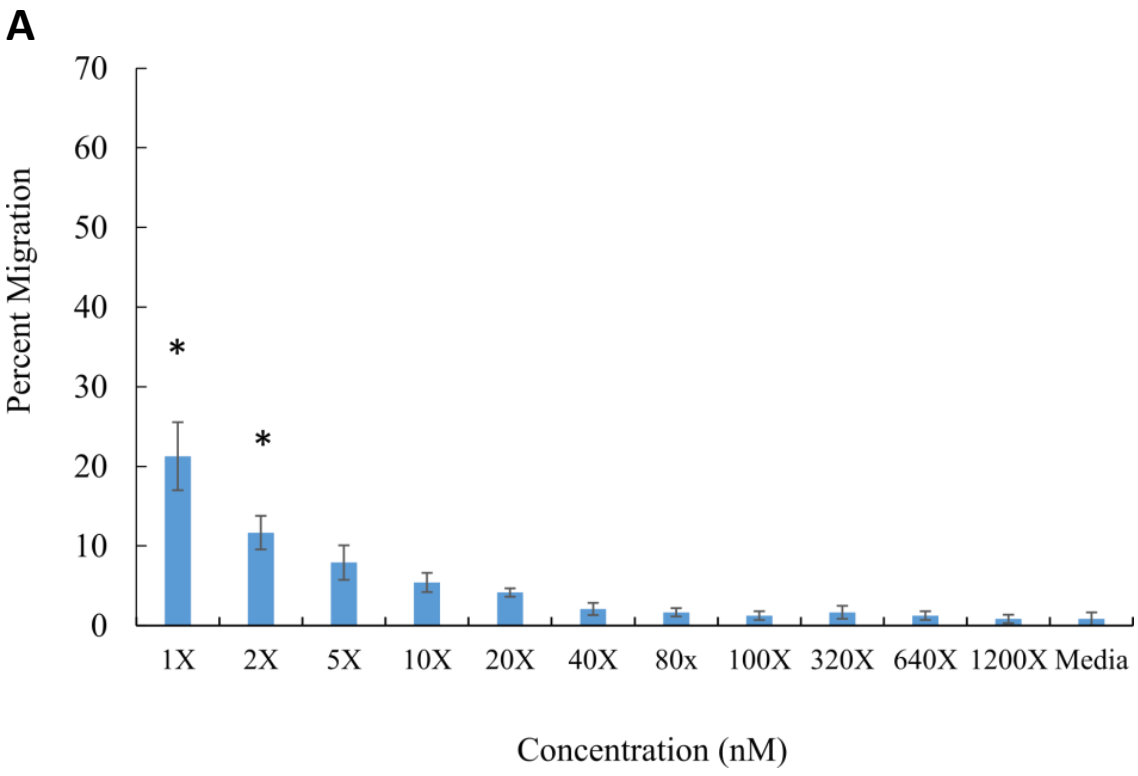

B

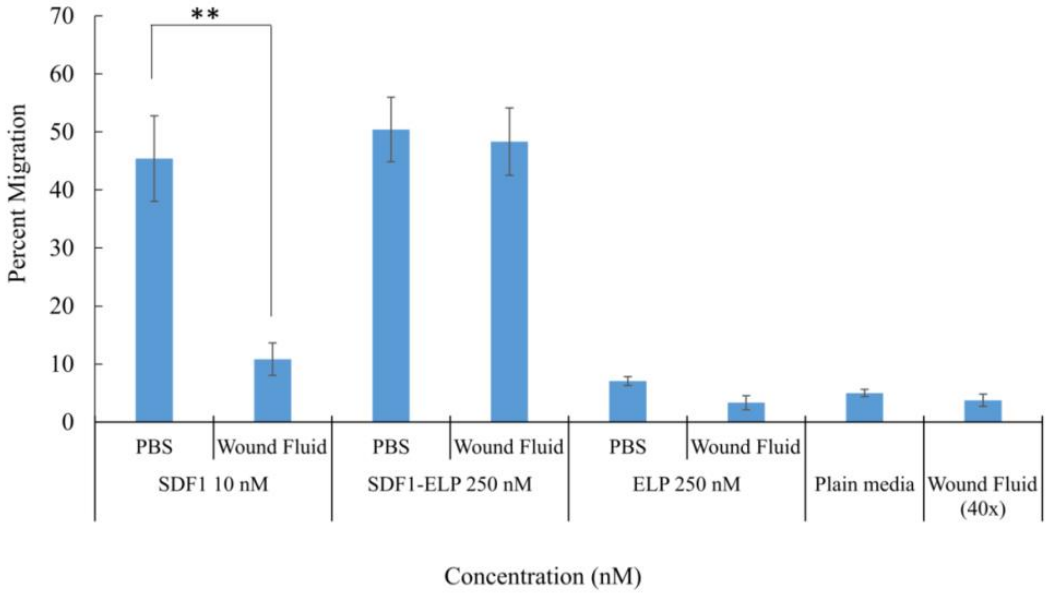

Figure 4.5: Chemotactic activity of SDF-ELP vs. SDF after incubation in wound fluid. (A) Wound fluid (WF) was diluted between ranges of 40 to 1200X with IMDM and used to perform an HL-60 cell migration assay, to understand the chemotactic effect of the wound fluid on the cells. (B) SDF1-ELP and SDF1 were incubated in wound fluid for 15 days and used to perform an HL-60 cell migration assay. N=6 for each condition. (*: $p < 0.05$, **: $p < 0.01$, one way ANOVA, Fisher's LSD post-test).

4.3.6 SDF-ELP vs. SDF1-mediated Wound Healing Response in Diabetic Mice

SDF1 is known to promote revascularization which is needed for re-epithelialization of chronic wounds [7-9]. SDF1-ELP was more stable during ex vivo wound fluid incubation than SDF1, under idealized in vitro conditions, they had similar angiogenic potential. To

determine whether SDF1-ELP was more effective in actual wounds, we treated excisional wounds in diabetic mice with a single dose of SDF-ELP, free SDF1, ELP alone, or plain fibrin (vehicle) control. Wound tissues were harvested after 7, 28 and 42 days post wounding and stained for CD31+ cells (Figure 4.6A). The total number of CD31+ positive cells per field was evaluated using ImageJ. The results indicated that SDF1-ELP promoted higher numbers of CD31+ cells as compared to free SDF1, ELP alone, or plain fibrin (vehicle) control (Figure 4.6B).

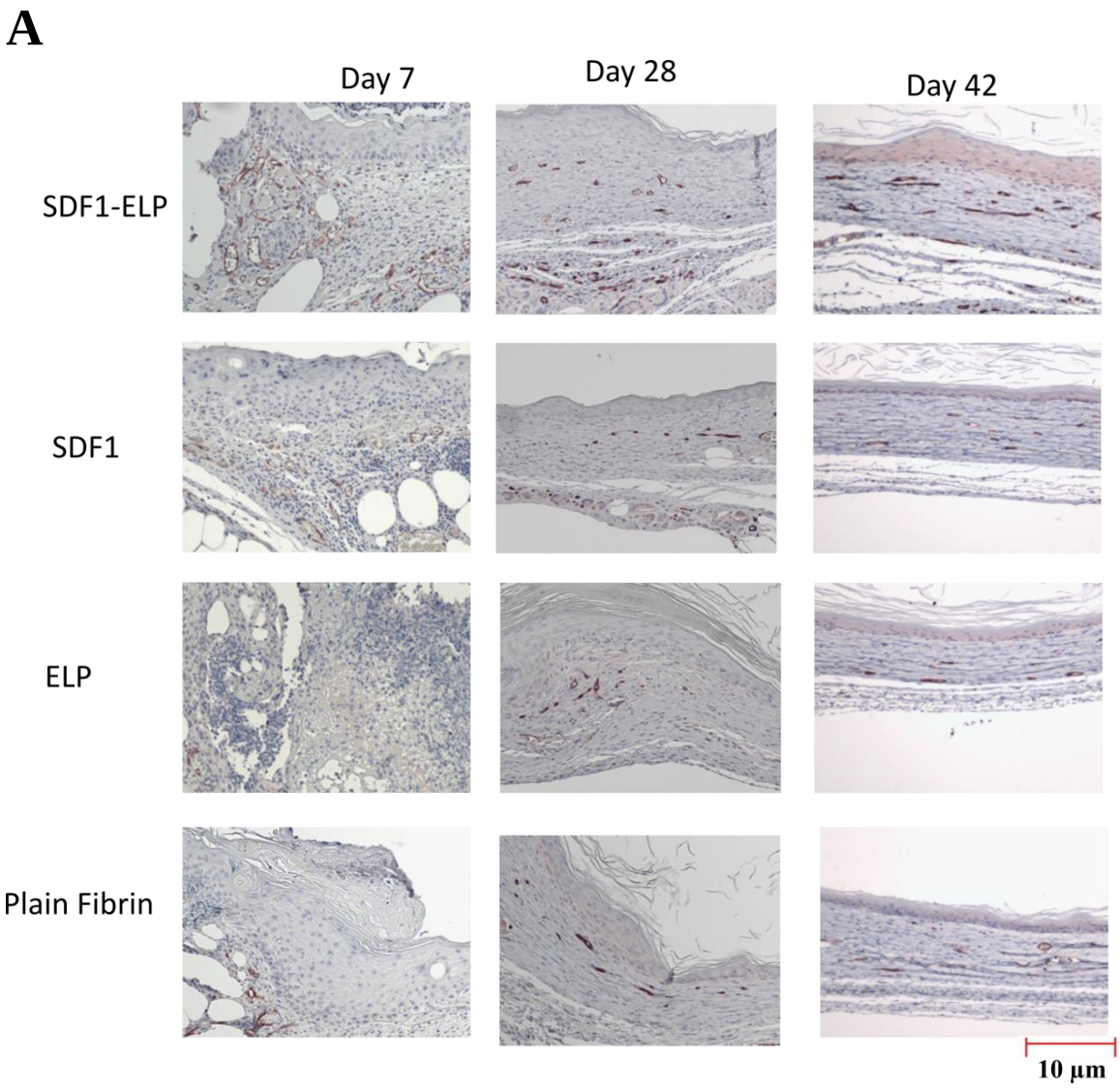

B

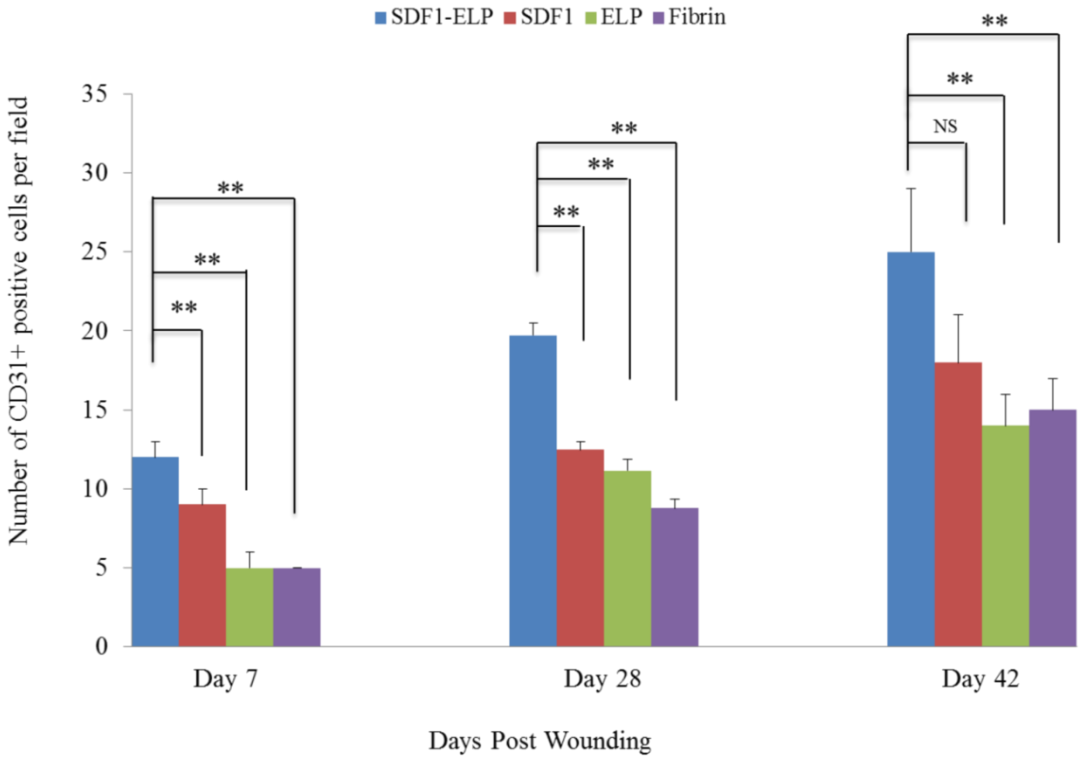

Figure 4.6: Distribution and quantification of CD31+ positive cells per field in wound tissues. Wound tissues were harvested after 7 and 42 days post wounding and stained for CD31+ cells. Histology slides were visualized using a 10x objective. Scale bar = 10 µm. Images shown are representative for wounds harvested on: (A) Day 7: pictures of histology slides were taken at the entrance of the wound. Day 28 and day 42: pictures were taken inside the wound area. Structures are labeled as: E= epidermis; D= dermis. (B) The number of CD31 positive cells at the different time points was quantified using ImageJ. Representative images are shown. A total of 3 animals per treatment group were used and 2 different tissue sections (N=6) were analyzed per group, with three (3) 10x magnification fields evaluated per section. (**: $p < 0.01$, one way ANOVA, Fisher's LSD post-test).

4.4 DISCUSSIONS AND CONCLUSIONS

In this study, we explored the mechanism of action of SDF1-ELP that may explain its superior in vivo performance to free SDF1 as discussed in our previous chapter. In vitro, SDF1-ELP promoted the migration of cells and induced vascularization, similar to SDF1. However, when both SDF1-ELP and SDF1 was incubated in wound fluid ex vivo for an extended period of time, SDF1-ELP fusion protein nanoparticles were stable while SDF1 lost its biological activity. When applied to an excisional wound made on the dorsal area of diabetic mice, SDF1-ELP instigated a higher amount of vascular endothelial cells as compared SDF1 and the remaining controls.

We modelled the chemotactic potential of SDF1-ELP with HL60 cells, which also expresses the CXCR4 receptor. We noted that a higher concentration of SDF-ELP nanoparticles (250nM or more) was needed to achieve the same migration effect as 10 nM of SDF because the migration effect mainly resulted from the monomer phase of the fusion protein. The nanoparticles acted as a depot which slowly released monomers causing a gradient in the transwell, which instigated the movement of cells from the top to the bottom of the transwell. About 8% of SDF-ELP monomers were released from the nanoparticles during the 4 hour migration experiment with the HL60 cells. We noted that this observation is positive and attractive for in vivo application because unlike recombinant free SDF1 that is immediately released for use and could be available for rapid degradation degraded by proteases, SDF1-ELP monomers, even if degraded by proteases is expected to be regenerated by the depot of nanoparticles that will reside at the wound site. Based on the particle size of our SDF1-ELP nanoparticles, approximately 150 SDF1-ELP monomers is available for use, estimated as follows:

Volume occupied by SDF1-ELP monomer = $(1.21 \times \text{MW})\ A^3 \approx 40\ nm^3$

Diameter of SDF1-ELP nanoparticle ≈ 600 nm

Approximate Volume of nanoparticle (assuming spherical shape) ≈ 3,202,560 nm^3

This implies there are about 3,202,560 /40 ≈ 80,064 molecules of SDF-ELP monomers in one particle

Several investigators have reported the ability of SDF1 not only to attract endothelial progenitor cells, but to also induce vascularization in endothelial cells. For example, Strasser et al [18] and Chen et al [19] reported angiogenesis induced by SDF1 in human umbilical vascular endothelial cells while Mirshahi et al [20] reported SDF1 induced vascularization in human microvasculature endothelial cells. We observed that SDF1-ELP (and SDF1) induced vascularization using HUVEC cells similar to what had been previously reported.

However, despite the similar in vitro bioactivity of SDF1-ELP to SDF1, we observed SDF1-ELP to be more stable in ex vivo wound fluid when compared to SDF1. SDF1-ELP was stable after 15 day incubation in wound fluid, while free SDF1 was biologically inactive. This is similar to Olekson et al's [21] report that SDF-1 was rendered biologically inactive, when incubated in wound fluid ex vivo.

As such, we used our animal studies to investigate if the better stability profile of SDF1-ELP in wound fluid will imply that it will enable a higher amount of endothelial cells in the wound area. As expected, SDF1-ELP promoted a higher amount of vascular endothelial cells throughout the wound healing timeline, as compared SDF1 and the remaining controls.

We therefore conclude that the stability of SDF1-ELP allows it to be retained in the chronic wound to promote a higher amount of revascularization which leads a higher rate of wound healing as compared to SDF1 and other controls. SDF1-ELP is a promising agent for the treatment of chronic skin wounds.

4.5 REFERENCES

[1] A. Tellechea, E. Leal, A. Veves, E. Carvalho, Inflammatory and Angiogenic Abnormalities in Diabetic Wound Healing: Role of Neuropeptides and Therapeutic Perspectives, The Open Circulation amd Vascular Journal, 3 (2010) 43-55.

[2] R. Edwards, K. Harding, Bacteria and Wound Healing, Curr Opin Infect Dis, 17 (2004) 91-96.

[3] S.A. Eming, T. Kreig, J.M. Davidson, Inflammation in Wound Repair: Molecular and Cellular Mechanisms, Journal of Investigative Dermatology, 127 (2007).

[4] A. Grazul-Bilska, Wound Healing: The role of growth factors, Drugs Today, 39 (2003) 787-800.

[5] P.S. Murphy, G.R.D. Evans, Advances in wound healing: a review of current wound healing products, Plastic Surgery International, 2012 (2012).

[6] A. Sarkar, S. Tatildede, S.S. Scherer, D.P. Orgill, F. Berthiaume, Combination of stromal cell derived factor-1 and collagen-glycosaminoglycan scaffold delays contraction and accelerates reepithilization of dermal wounds in wild-type mice, Wound Repair Regen., 19 (2011) 71-79.

[7] C. Kalka, H. Masuda, T. Takahashi, W.M. Kalka-Moll, M. Silver, M. Kearney, T. Li, J.M. Isner, T. Asahara, Transplantation of ex vivo expanded endothelial progenitor cells for therapeutic neovascularization, Proc Natl Acad Sci U S A, 97 (2000) 3422-3427.

[8] S.M. Majka, K.A. Jackson, K.A. Kienstra, M.W. Majesky, M.A. Goodell, K.K. Hirschi, Distinct progenitor populations in skelatal muscle are bone marrow derived and exhibit different cell fates during vascular regeneration, The Journal of Clinical Investigation, 111 (2003) 71-79.

[9] T. Takahashi, C. Kalka, H. Masuda, D. Chen, M. Silver, M. Kearney, M. Magner, J.M. Isner, T. Asahara, Ischemia- and cytokine-induced mobilization of bone marrow-derived endothelial progenitor cells for neovascularization, Nat Med, 5 (1999) 434-438.

[10] X. Xu, F.Q. Zhu, M. Zhang, D.F. Zeng, D.L. Luo, G.D. Liu, W.H. Cui, S.L. Wang, W. Guo, W. Xing, H.P. Liang, L. Li, X.B. Fu, J.X. Jiang, H. Huang, Stromal Cell-Derived Factor-1 Enhances Wound Healing through Recruiting Bone Marrow-Derived Mesenchymal Stem Cells to the Wound Area and Promoting Neovascularization, Cells Tissues Organs, 197 (2013) 103-113.

[11] A.L. George, P. Bangalore-Prakash, S. Rajoria, R. Suriano, A. Shanmugam, A. Mittelman, R.K. Tiwari, Endothelial progenitor cell biology in disease and tissue regeneration, J Hematol Oncol, 4 (2011) 24.

[12] B.A. Teicher, S.P. Fricker, CXCL12 (SDF-1)/CXCR4 Pathway in Cancer, Clinical Cancer Research, 16 2927-2931.

[13] C. Bogani, V. Ponziani, P. Guglielmelli, C. Desterke, V. Rosti, A. Bosi, M.C. Le Bousse-Kerdiles, G. Barosi, A.M. Vannucchi, C. Myeloproliferative Disorders Research, Hypermethylation of CXCR4 promoter in CD34+ cells from patients with primary myelofibrosis, Stem Cells, 26 (2008) 1920-1930.

[14] Koria, P. Koria, H. Yagi, Y. Kitagawa, Z. Megeed, Y. Nahmias, R. Sheridan, M.L. Yarmush, Self-assembling elastin-like peptides growth factor chimeric nanoparticles for the treatment of chronic wounds, PNAS, 108 (2011) 1034-1039.

[15] A. Aiuti, I.J. Webb, C. Bleulm, T. Springer, The Chemokine SDF-1 Is a Chemoattractant for Human CD34 Hematopoietic Progenitor Cells and Provides a New Mechanism to Explain the Mobilization of CD34 Progenitors to Peripheral Blood, The Journal of Experimental Medicine, 185 (1997) 111-120.

[16] P. Koria, H. Yagi, Y. Kitagawa, Z. Megeed, Y. Nahmias, R. Sheridan, M.L. Yarmush, Self-assembling elastin-like peptides growth factor chimeric nanoparticles for the treatment of chronic wounds, Publication of the National Academy of Sciences, 108 (2011) 1034-1039.

[17] M. Bastaki, E.E. Nelli, P. Dell'Era, M. Rusnati, M.P. Molinari-Tosatti, S. Parolini, R. Auerbach, L.P. Ruco, L. Possati, M. Presta, Basic fibroblast growth factor-induced angiogenic phenotype in mouse endothelium. A study of aortic and microvascular endothelial cell lines, Arterioscler Thromb Vasc Biol, 17 (1997) 454-464.

[18] G.A. Strasser, J.S. Kaminker, M. Tessier-Lavigne, Microarray analysis of retinal endothelial tip cells identifies CXCR4 as a mediator of tip cell morphology and branching, Blood, 115 (2010).

[19] T. Chen, H. Bai, Y. Shao, M. Arzigian, V. Janzen, E. Attar, Y. Xie, D.T. Scadden, Z.Z. Wang, Stromal cell-derived factor-1/CXCR4 signaling modifies the capillary-like organization of human embryonic stem cell-derived endothelium in vitro, Stem Cells, 25 (2007) 392-401.

[20] F. Mirshahi, J. Pourtau, H. Li, M. Muraine, V. Trochon, E. Legrand, J. Vannier, J. Soria, M. Vasse, C. Soria, SDF-1 activity on microvascular endothelial cells: consequences on angiogenesis in in vitro and in vivo models, Thromb Res, 99 (2000) 587-594.

[21] M.A. Olekson, R. Faulknor, A. Bandekar, M. Sempkowski, H.C. Hsia, F. Berthiaume, SDF-1 liposomes promote sustained cell proliferation in mouse diabetic wounds, Wound Repair Regen, 23 (2015) 711-723.

5 CHAPTER 5: CONCLUSIONS

5.1 KEY FINDINGS

5.1.1 Summary of dissertation findings

The goal of the dissertation was to investigate the therapeutic potential of a derivative of SDF1, SDF1-ELP in the treatment of skin wounds. This goal was broken down into specific aims as follows:

- develop SDF1-ELP fusion proteins and characterize the physical properties of the nanoparticles for use in wound healing;
- compare the in vitro and in vivo biological activity of SDF-ELP to free SDF1
- explore the mechanism of action of SDF1-ELP versus free SDF1

We found that the recombinant fusion protein comprised of SDF1 and an elastin-like peptide conferred the ability to self-assemble into nanoparticles. The fusion protein showed binding characteristics similar to that reported for free SDF1 to the CXCR4 receptor. The biological activity of SDF1-ELP, as measured by intracellular calcium release in HL60 cells was dose dependent, and also very similar to that of free SDF1. In contrast, the biological activity of SDF1-ELP in vivo was significantly superior to that of free SDF1. When applied to full thickness skin wounds in diabetic mice, wounds treated with SDF1-ELP nanoparticles were 95% closed by day 21, and fully closed by day 28, while wounds treated with free SDF1, ELP alone, or vehicle were only 80% closed by day 21, and took 42 days to fully close. In addition, the SDF1-ELP nanoparticles significantly increased the epidermal and dermal thickness of the healed wound, as

compared to the other groups. We investigated the mechanism of action and properties of SDF1-ELP that led to its superior in vivo performance than free SDF1. We noted that SDF1-ELP promoted the migration of cells and induced vascularization similar to SDF1, but was more stable in ex vivo wound fluid when compared to SDF1. When applied to an excisional wound created on the dorsal area of diabetic mice, SDF1-ELP promoted a higher amount of CD31+ (vascular endothelial) cells as compared SDF1 and the remaining controls.

5.1.1.1 SDF1-ELP forms nanoparticles above its inverse transition temperature

SDF1 was cloned into a plasmid backbone which contained 50 pentapeptide repeats of ELP. The inverse temperature for the ELP polypeptide had been previously been determined to be around 40°C [1] . The inverse transition temperature for the SDF1-ELP fusion protein was determined to be ~35°C. This aligns with Trabbic-Carlson et al's observation [2] that fusing a target molecule could change the inverse transition temperature of the ELP. Above its inverse transition temperature, SDF1-ELP formed nanoparticles with an approximate size of 600 nm.

5.1.1.2 SDF1-ELP has similar in vitro biological and binding activity as SDF1

We used the Surface Plasmon Resonance principle of a Biacore instrument to understand the binding activity of SDF1-ELP to its receptor, CXCR4. This technology was used as it eliminates the need to 'iodine-label' the SDF1-ELP (which has been the case for SDF1-CXCR4 binding data reported by other researchers [3],[4]). The use of the Biacore allowed for the real time, safe and robust collection of binding data. The SDF1-ELP fusion protein bound the CXCR4 receptor with high affinity, with a K_D =1.14nM, which is close to the reported values for free SDF1 ranging from 1.32 to 6 nM [3-5]. We used

the Human Leukemia-60 (HL-60) cell line which is known to highly and reliably express the SDF1 receptor CXCR4 [6] to evaluate the in vitro bioactivity of SDF1-ELP and noted that the intracellular calcium release of SDF1-ELP is very similar to that of free SDF1 when using HL60 cells as responders, confirming that SDF1-ELP and SDF1 have similar in vitro biological activity.

5.1.1.3 SDF1-ELP significantly accelerated wound closure as compared to free SDF1, ELP alone, or vehicle. The SDF1-ELP treated wounds healed with a significantly thicker epidermal and dermal layer as compared to the other groups

We evaluated the in-vivo efficacy of SDF1-ELP by delivering it to excisional wounds made on diabetic mice and observed for wound closure over a period of time. After wounds had healed, we harvested wound tissues for histology and analyzed the collagen deposition as well as morphological features of the skin. Wounds treated with SDF1-ELP nanoparticles closed around 21 days post wounding, representing a 50% decrease compared to the other groups, which required up to 42 days to fully close. In addition, the wounds treated with SDF1-ELP exhibited a significantly thicker epidermal and dermal layer as compared to the other groups.

5.1.1.4 SDF1-ELP promotes the migration of cells and induces vascularization similar to SDF1 in vitro

SDF1 is chemokine that is known to contribute to angiogenesis by recruiting endothelial progenitor cells (EPCs) from the bone marrow through a CXCR4 dependent mechanism [7]. Also, SDF-1 is known to have a neovascularization effect on endothelial cells by inducing cell proliferation, differentiation, sprouting and tube formation in vitro and preventing apoptosis of endothelial progenitor cells [8], [9]. We evaluated the

chemotactic ability of SDF1-ELP to investigate its potential to promote the migration of HL60 cells, which express CXCR4, in Transwells. SDF1-ELP caused a dose-dependent migratory response up to 1000 nM. A dose of 250nM SDF1-ELP achieved approximately the same percent cell migration as 10nM free SDF1, which is the concentration of free SDF1 reported to induce a robust migratory response [10]. We observed that the migration of cells was mainly instigated by SDF1-ELP monomers that were slowly released out of SDF1-ELP nanoparticles depot over the course of the migration assay.

We also evaluated the ability of SDF1-ELP to promote angiogenesis in a tube formation assay using HUVECs and noted that SDF1-ELP promoted tube formation and capillary-like networks similar to SDF1.

5.1.1.5 SDF1-ELP is more stable in elastase and in wound fluids as compared to SDF1

Other researchers have reported that ELP fusion proteins can serve as "drug depots" with a better stability profile and/or in vivo half-life than the free target protein [11]. For example, Amiram et al [12] showed that glucagon-like peptide-1 (GLP1; a potential type-2 diabetes drug) fused to ELP was more resistant to proteolysis by neutral endopeptidase, which is known to degrade GLP1 in vivo, as compared to free GLP1

To compare the stability of SDF1-ELP versus SDF1 we incubated the two proteins in elastase and wound fluid and evaluated their stability profile. For the elastase experiment, samples were collected at 4 day intervals and subjected to Western blot analysis. We noted that SDF1-ELP remained intact throughout the incubation period while no positive bands were seen for the SDF1 samples. For the wound fluid experiments, we measured the bioactivity of each protein after prolonged incubation in human diabetic wound fluid

and noted that the chemotactic activity of free SDF1 after incubation in wound fluid was significantly reduced, as compared to SDF1-ELP.

5.1.1.6 SDF1-ELP instigated a higher amount of vascular endothelial cells as compared SDF1 and the remaining controls.

As previously mentioned, SDF1-ELP was more stable after ex vivo wound fluid incubation than SDF1, and under idealized in vitro conditions, they had similar angiogenic potential. We were therefore interested in probing whether the combined observation of SDF1-ELP's stability in wound fluid and it's in vitro angiogenic potential wound help explain its superior in vivo performance than free SDF1. We treated excisional wounds in diabetic mice with a single dose of SDF-ELP, free SDF1, and other controls, harvested wound tissues after 7, 28 and 42 days post wounding and stained the sections for CD31+ cells. The results indicated that SDF1-ELP promoted higher numbers of CD31+ cells as compared to free SDF1 and other controls.

We therefore conclude that SDF1-ELP is sustained longer at the wound site, allowing it to promote a higher amount of revascularization which leads a higher rate of wound healing as compared to SDF1 and other controls. SDF1-ELP is a promising agent for the treatment of chronic skin wounds.

5.2 LIMITATIONS

5.2.1 Clinical Use of SDF1-ELP

While the SDF1-CXCR4 axis leads to positive outcomes for wound healing, it is also known to be involved in several aspects of tumor progression and metastasis [13]. The CXCR4 receptor is expressed on several tumors; SDF1 plays a crucial role in promoting

the proliferation, migration and invasion of these cancer cells [14], [15]. In this project, SDF1-ELP was topically and locally applied to the wound area as nanoparticles, and as such the potential for the delivered growth factor to trigger unwanted adverse cancerous effects should be minimal. However the safety profile of SDF1-ELP needs to be fully evaluated prior to use in the clinic. Additional in vivo studies need to be performed to confirm that there is no risk of cancer formation. Since the nanoparticles increase the availability and sustenance of SDF1 at the wound area, further preclinical studies needs to focus on understanding the effect of the sustained exposure of the growth factor to the surrounding tissues at the wound site.

5.2.2 Diabetic Mouse Wound Model

In this work, 1 cm x 1 cm square full thickness skin wounds were made on the back the mice, using a pre-made template. Treatments were applied on Day 0 (the day the wound was made) and the wound closure monitored over a period of time. While this mouse wounding model has been used by several researchers, it is not a perfect representation of wounds in patients with diabetes or chronic wounds. In fact, some researchers believe that a wound model comparable to chronic, non-healing human wounds does not exist [16]. One potential way to bridge this gap is to leave the wound untreated for a period of time prior to application of treatments. From example, a wound made on Day 0 can be covered with dressing to avoid infection, but left untreated till day 4, i.e. until the inflammation phase, prior to the application of the treatments. In addition, the laboratory species (mice) we used for our in vivo studies is not the best representation of humans. It is known that mice have a subcutaneous panniculus carnosus muscle, which contributes to the repair process (via contraction and collagen formation) [16]. However, this

structure is absent in humans. Although pigs are believed to have the closest skin structure to humans, it is known that their wounds heal rapidly and also heal through contraction.

5.2.3 The Use of Fibrin Gels as a Delivery Vehicle

We used fibrin gels as a delivery vehicle in our in vivo work to prevent SDF1-ELP and the other controls from leaking away when pipetted on the wound area. Prior to application to the wound, fibrinogen with the protein treatment solution was mixed with thrombin to form the fibrin gel treatments. The mixture was immediately pipetted to the wound and allowed to gel after which the wounds were covered with wound dressing.

While this approach was fine for exploratory studies, the methodology is not practical for future clinical use. A more robust means of delivering the treatments is needed. For example, the treatments can be pre-formulated in the fibrin gel and made into molds or patches for application to the wound.

5.3 FUTURE DIRECTIONS

5.3.1 Tracking nanoparticles in vitro and in vivo

While we understand that SDF1-ELP is very stable in elastase and in wound fluid, we do not fully know the fate of the nanoparticles in cells or in the wounds. To attempt to answer this question, one of our future works is to track the nanoparticles in cells, in ex-vivo wound fluid and also in the wound. Similar to work done by Sarangthem et al [17], we plan on conjugating a fluorophore to SDF1-ELP, incubating it with cells such as HL60 or HUVECs and monitoring the cellular localization and/or internalization of the

nanoparticles. To understand the stability of the SDF1-ELP nanoparticles in vivo, fluorescent labelled SDF1-ELP will be put into the animal wounds and the wound site imaged at different time points. Alternatively, skin tissues will be harvested at different time points and analyzed for the presence/sustenance of SDF1-ELP using an SDF1 antibody. This will help us evaluate the efficacy of the nanoparticles at different stages in the wound healing cascade.

5.3.2 Delivery of SDF1-ELP nanoparticles using other dermal scaffolds and skin substitutes

Dermal scaffolds, such as Integra™ and Alloderm™ are commercially available and have been developed to promote regeneration of the dermis. These products are applied onto the cleaned wound bed and provide a structure for blood vessels and other cells to migrate and grow into. Skin substitutes are also used on chronic wounds, but typically incorporate a source of growth factors; for example, Transcyte™ contains extracellular matrix bound with growth factors secreted by human fibroblasts during the manufacturing process. Since these scaffolds and skin substitutes have already proved successfully for wound healing treatments, we also plan to experiment the delivery of our SDF1-ELP nanoparticles to the wound area using these matrices. Since our nanoparticles are below 1 μm, they can easily be incorporated into these matrices which typically have pore sizes greater than 50 μm.

5.3.3 Combination of SDF1-ELP with other growth factor ELPs (such as KGF1-ELP)

Previous work has demonstrated that Keratinocyte Growth Factor-ELP induced a higher proliferation of keratinocytes, which resulted significant increase in reepithelialization in

full-thickness wounds made on diabetic mice as compared to the controls [1]. In this work, we have demonstrated that SDF1-ELP promotes the healing of wounds by increasing vascularization which leads to thicker epidermal and dermal regeneration. Ongoing work in the laboratory is to evaluate the anti-apoptotic peptide derived from erythropoietin, ARA290-ELP, which will help reduce inflammation at the wound site. Thus, we plan to investigate a combined strategy that utilizes these 3 bioactive peptides (KGF, SDF and ARA290) delivered using the ELP technology, and evaluate its profound effect on wound healing.

5.4 REFERENCES

[1] P. Koria, H. Yagi, Y. Kitagawa, Z. Megeed, Y. Nahmias, R. Sheridan, M.L. Yarmush, Self-assembling elastin-like peptides growth factor chimeric nanoparticles for the treatment of chronic wounds, Proc Natl Acad Sci U S A, 108 (2011) 1034-1039.

[2] K. Trabbic-Carlson, D.E. Meyer, L. Liu, R. Piervincenzi, N. Nath, T. LaBean, A. Chilkoti, Effect of protein fusion on the transition temperature of an environmentally responsive elastin-like polypeptide: a role for surface hydrophobicity, Protein Engineering, Design and Selection, 17 (2004) 57-66.

[3] M.P. Crump, J.H. Gong, P. Loetscher, K. Rajarathnam, A. Amara, F. Arenzana-Seisdedos, J.L. Virelizier, M. Baggiolini, B.D. Sykes, I. Clark-Lewis, Solution structure and basis for functional activity of stromal cell-derived factor-1; dissociation of CXCR4 activation from binding and inhibition of HIV-1, EMBO J, 16 (1997) 6996-7007.

[4] R. Salcedo, K. Wasserman, H.A. Young, M.C. Grimm, O.M. Howard, M.R. Anver, H.K. Kleinman, W.J. Murphy, J.J. Oppenheim, Vascular endothelial growth factor and basic fibroblast growth factor induce expression of CXCR4 on human endothelial cells: In vivo neovascularization induced by stromal-derived factor-1alpha, Am J Pathol, 154 (1999) 1125-1135.

[5] G.A. McQuibban, G.S. Butler, J.H. Gong, L. Bendall, C. Power, I. Clark-Lewis, C.M. Overall, Matrix metalloproteinase activity inactivates the CXC chemokine stromal cell-derived factor-1, J Biol Chem, 276 (2001) 43503-43508.

[6] C. Bogani, V. Ponziani, P. Guglielmelli, C. Desterke, V. Rosti, A. Bosi, M.C. Le Bousse-Kerdiles, G. Barosi, A.M. Vannucchi, C. Myeloproliferative Disorders Research, Hypermethylation of CXCR4 promoter in CD34+ cells from patients with primary myelofibrosis, Stem Cells, 26 (2008) 1920-1930.

[7] H. Zheng, G. Fu, T. Dai, H. Huang, Migration of endothelial progenitor cells mediated by stromal cell-derived factor-1alpha/CXCR4 via PI3K/Akt/eNOS signal transduction pathway, J Cardiovasc Pharmacol, 50 (2007) 274-280.

[8] O. Salvucci, L. Yao, S. Villalba, A. Sajewicz, S. Pittaluga, G. Tosato, Regulation of endothelial cell branching morphogenesis by endogenous chemokine stromal-derived factor-1, Blood, 99 (2002) 2703-2711.

[9] J. Yamaguchi, K.F. Kusano, O. Masuo, A. Kawamoto, M. Silver, S. Murasawa, M. Bosch-Marce, H. Masuda, D.W. Losordo, J.M. Isner, T. Asahara, Stromal cell-derived factor-1 effects on ex vivo expanded endothelial progenitor cell recruitment for ischemic neovascularization, Circulation, 107 (2003) 1322-1328.

[10] A. Aiuti, I.J. Webb, C. Bleulm, T. Springer, The Chemokine SDF-1 Is a Chemoattractant for Human CD34 Hematopoietic Progenitor Cells and Provides a New Mechanism to Explain the Mobilization of CD34 Progenitors to Peripheral Blood, The Journal of Experimental Medicine, 185 (1997) 111-120.

[11] M.F. Shamji, H. Betre, V.B. Kraus, J. Chen, A. Chilkoti, R. Pichika, K. Masuda, L.A. Setton, Development and characterization of a fusion protein between thermally responsive elastin-like polypeptide and interleukin-1 receptor antagonist: sustained release of a local antiinflammatory therapeutic, Arthritis Rheum, 56 (2007) 3650-3661.

[12] M. Amiram, K.M. Luginbuhl, X. Li, M.N. Feinglos, A. Chilkoti, A depot-forming glucagon-like peptide-1 fusion protein reduces blood glucose for five days with a single injection, J Control Release, 172 (2013) 144-151.

[13] B.A. Teicher, S.P. Fricker, CXCL12 (SDF-1)/CXCR4 Pathway in Cancer, Clinical Cancer Research, 16 2927-2931.

[14] A. Sutton, V. Friand, S. Brule-Donneger, T. Chaigneau, M. Ziol, O. Sainte-Catherine, A. Poire, L. Saffar, M. Kraemer, J. Vassy, P. Nahon, J.L. Salzmann, L. Gattegno, N. Charnaux, Stromal cell-derived factor-1/chemokine (C-X-C motif) ligand 12 stimulates human hepatoma cell growth, migration, and invasion, Mol Cancer Res, 5 (2007) 21-33.

[15] F. Marchesi, P. Monti, B.E. Leone, A. Zerbi, A. Vecchi, L. Piemonti, A. Mantovani, P. Allavena, Increased survival, proliferation, and migration in metastatic human pancreatic tumor cells expressing functional CXCR4, Cancer Res, 64 (2004) 8420-8427.

[16] F. Gottrup, M.S. Ågren, T. Karlsmark, Models for use in wound healing research: A survey focusing on in vitro and in vivo adult soft tissue, Wound Repair and Regeneration, 8 (2000) 83-96.

[17] V. Sarangthem, E.A. Cho, S.M. Bae, T.D. Singh, S.J. Kim, S. Kim, W.B. Jeon, B.H. Lee, R.W. Park, Construction and application of elastin like polypeptide containing IL-4 receptor targeting peptide, PLoS ONE, 8 (2013) e81891.